

Electronic Thesis and Dissertation Repository

8-14-2014 12:00 AM

Surfactant Assisted Dispersion of Single-Walled Carbon Nanotubes in Polyvinylpyrrolidone Solutions


Tennison Yu, *The University of Western Ontario*

Supervisor: Dr. Jose Herrera, *The University of Western Ontario*

A thesis submitted in partial fulfillment of the requirements for the Master of Engineering Science degree in Chemical and Biochemical Engineering

© Tennison Yu 2014

Follow this and additional works at: <https://ir.lib.uwo.ca/etd>

 Part of the [Nanoscience and Nanotechnology Commons](#), [Other Chemical Engineering Commons](#), and the [Other Materials Science and Engineering Commons](#)

Recommended Citation

Yu, Tennison, "Surfactant Assisted Dispersion of Single-Walled Carbon Nanotubes in Polyvinylpyrrolidone Solutions" (2014). *Electronic Thesis and Dissertation Repository*. 2362.
<https://ir.lib.uwo.ca/etd/2362>

This Dissertation/Thesis is brought to you for free and open access by Scholarship@Western. It has been accepted for inclusion in Electronic Thesis and Dissertation Repository by an authorized administrator of Scholarship@Western. For more information, please contact wlsadmin@uwo.ca.

SURFACTANT ASSISTED DISPERSION OF SINGLE-WALLED CARBON
NANOTUBES IN POLYVINYLPIRROLIDONE SOLUTIONS

(Thesis format: Monograph)

by

Tennison Yu

Graduate Program in Chemical and Biochemical Engineering

A thesis submitted in partial fulfillment
of the requirements for the degree of
Master of Engineering Science

The School of Graduate and Postdoctoral Studies
The University of Western Ontario
London, Ontario, Canada

© Tennison Yu 2014

Abstract

Obtaining stable aqueous dispersions is one of the main challenges hindering a widespread and effective use of single-walled carbon nanotubes (SWNT) in many applications. Although it has been recognized that their versatility makes them an extremely attractive material, the unique molecular structure that gives SWNTs their unmatched electronic, mechanical, and thermal properties is also responsible for strong attractive forces between the nanotubes themselves. These are the result of hydrophobically driven van der Waals interactions, which are an inherent consequence of their carbon sp^2 hybridization network. This, combined with extremely high aspect ratios and flexibility, causes SWNTs to adhere strongly into tightly bundled ropes. In these bundles, SWNTs are not as useful as their linearized unbundled equivalents. Thus, in order to fully take advantage of their properties effectively, SWNTs must be debundled into individual nanotubes. Although several strategies have been suggested as a means to overcome these challenges, non-covalently coated nanotubes using amphiphilic molecules such as surfactants and polymers have gained significant attention in recent years.

In this contribution we will report a characterization study on such a system containing the surfactant, cetyltrimethylammonium bromide (CTAB) and the polymer, polyvinylpyrrolidone (PVP) at different molecular weights. Initial tests using Vis-NIR spectroscopy showed that although individually these molecules are poor dispersers of SWNTs, they show a synergic effect when combined for all cases. We have probed the reasons for this observation using a battery of characterization techniques including atomic force microscopy (AFM) viscosity, dynamic light scattering (DLS), surface tension, electrophoretic mobility, and pH to unravel the system.

Our data suggests that the observed synergistic effect is linked to the formation of stable supramolecular structures: “a 2-dimensional dispersion” as opposed to “1-dimensional” dispersion systems, based on a single surfactant, traditionally used. Specifically, the polymer appears to add an additional layer of stability by sterically augmenting dispersions through two possible effects: 1) contact area between the polymer and nanotube and 2) viscosity-based effects. We propose our approach as a facile way of augmenting current nanotube dispersion techniques, potentially allowing for increased usage in the world today.

Keywords: Carbon nanotubes, dispersion augmentation, surfactant, polymers, rheology, cetyltrimethylammonium bromide (CTAB), polyvinylpyrrolidone (PVP),

Acknowledgments

I came to the University of Western Ontario looking to expand my skillset and knowledge, knowing that my interest not only laid in biological sciences but physical and material sciences as well. Being only a two year program, I had not expected it to be anything grand but my experience has been nothing but that.

First, I have to thank my parents (especially my mom), both of whom saw me at an indecisive position after completing my undergraduate and encouraging me to consider graduate studies. Without their guidance I would not be where I am today.

Second, I would like to acknowledge all the staff and faculty that I've had the opportunity to meet around the University of Western Ontario, particularly those in the Department of Chemical and Biochemical Engineering. Their approachability, and dedication towards student success and challenging research have made time go by especially fast. I would like to thank the following professors as their help has been instrumental to my research.

Dr. Jose Herrera

Dr. Amarjeet Bassi

Dr. John de Bruyn

Dr. Lars Rehmman

Lastly, I would like to thank all my friends whom have encouraged and helped me invaluablely. In particular, I'd like to thank all my lab mates – Dongmin Yun, Daoping Guo, Jorge Gabayet, Omneya El-Sharnouby, and Inusa Abdullahi – for their company on late nights at the lab, and fun in lab parties.

Table of Contents

Abstract.....	ii
Acknowledgments.....	iii
List of Figures	vi
List of Tables	ix
List of Abbreviations	x
1. Chapter 1: Background	1
1.1 Motivation.....	2
1.2 Thesis Outline.....	2
2. Chapter 2: Literature Review	4
2.1 Introduction	4
2.2 Nanotube Structure and Properties.....	4
2.2.1 Electrical Properties	6
2.2.2 Mechanical Properties	9
2.2.3 Thermal Properties	10
2.3 Nanotube Composite Challenges.....	11
2.3.1 Assessing Nanotube Dispersions	13
2.4 Methods of Improving Nanotube Dispersions.....	15
2.4.1 Physical Methods	15
2.4.2 Covalent vs Non-covalent Chemical Modifications	15
2.5 Other Methods to Characterize Suspensions	27
2.5.1 Surface Tension.....	27
2.5.2 Viscosity	28
2.5.3 Dynamic Light Scattering	30
2.6 Summary	33
3. Chapter 3: Materials and Methods.....	34
3.1 Materials	34
3.2 Methods.....	34
3.2.1 Solution Preparation	34
3.2.2 Gel Permeation Chromatography (GPC).....	34
3.2.3 Spectroscopic Characterization	35
3.2.4 Atomic Force Microscopy	35
3.2.5 Dynamic Light Scattering (DLS).....	36

3.2.6	Surface Tension Characterization	36
3.2.7	pH Measurements.....	37
3.2.8	Viscosity Characterization.....	37
4.	Chapter 4: Results	38
4.1	Characterization of Nanotube Dispersions.....	38
4.1.1	Vis-NIR of Nanotube Suspensions.....	38
4.1.2	Atomic Force Microscopy	46
4.1.3	Dynamic Light Scattering (DLS)	49
4.2	Surface Tension.....	56
4.3	pH Measurements	59
4.4	Viscosity	63
4.5	Discussion.....	68
4.6	Summary	75
5.	Chapter 5: Conclusion	77
5.1	Future Directions	79
	References	81
	Appendix 1	93
	GPC.....	93
	Vis-NIR Spectra.....	94
	Surface Tension.....	95
	Viscosity	96
	Surface Area Tables	96
	Electrophoretic Mobility	97
	Permissions	99

List of Figures

Figure 2.1: A) Diagram by Thostenson et al. (2001) illustrating the unit cell found in graphene and nanotubes. In addition, the unit vectors a_1 and a_2 are given along with magnitudes n and m , the chiral vector, and chiral angle. The path of an armchair and zig-zag nanotube are also given which are further shown in B) which was designed by Dresselhaus et al. (1995) gives a 3D representation of a) armchair b) zig-zag and c) chiral nanotubes. ^{18,19}	5
Figure 2.2: TEM images of different MWNT acquired by Iijima (1991). ¹⁵ A SWNT would be a tube with only one ring.	6
Figure 2.3: The different chiralities of nanotubes and whether they are metallic and semi-conducting as prepared by Dresselhaus <i>et al.</i> (1995). ¹⁹	8
Figure 2.4: Parallel nanotube-nanotube interaction potential per length as calculated by Nativ-Roth <i>et al.</i> (2007) ⁶⁰	12
Figure 2.5: A) An example of the electron band structure of nanotubes. B) Kataura plot representing the band gap energy as a function of nanotube diameter. Both figures were prepared by Weisman <i>et al.</i> (2003) ⁷⁰	13
Figure 2.6: The resonant band of nanotubes over its non-resonant background gives the resonance ratio. This method was proposed by Tan <i>et al.</i> (2005) as a method of characterizing dispersion quality of nanotubes. ⁷¹	14
Figure 2.7: Phase diagram of CTAB at different temperatures and concentrations by Brinker <i>et al.</i> (1999). ⁹¹	18
Figure 2.8: Sample of the surfactants used by Tan <i>et al.</i> (2005) to determine dispersion ability. Structures were acquired from Chemspider database and are as follows: A) SDS B) NaDDBS C) Triton X-100 D) SC. ⁷¹	19
Figure 2.9: Regimes of polymers at different concentration levels as drawn by Mutch <i>et al.</i> (2007). A) represents the dilute regime, B) represents the semi-dilute regime, and C) represents the concentrated regime. ¹⁰⁸	22
Figure 2.10: Proposed adsorption mechanism of PEO-PPO-PEO triblock polymer by Nativ-Roth <i>et al.</i> (2007). Red regions are PPO and blue regions are PEO. ⁶⁰	24
Figure 4.1: Absorption spectra of CTAB dispersed nanotubes	39
Figure 4.2: Absorption spectra of 6% PVP-dispersed nanotubes	41

Figure 4.3: A) The obtained spectra of 0.1 %wt/v CTAB, 0.2 g/L SWNT, and 6 %wt/v PVP at different molecular weights. B) Resonant area comparison between 0.1 %wt/v CTAB (green), 6 %wt/v PVP (blue), and 0.1% CTAB with 6% PVP (orange) as obtained in (A) at dispersing 0.2 g/L SWNT.	43
Figure 4.4: Resonant Area of PVP-CTAB-SWNT dispersions at a fixed CTAB concentration of 0.1 % wt/v and 0.2 g/L SWNT.....	44
Figure 4.5: Final concentration of dispersed nanotube solution (g/L) with respect to the PVP concentration.....	45
Figure 4.6: Sample AFM image of CTAB-suspended SWNT dried over a silicon wafer	46
Figure 4.7: Distributions of A) diameter B) length and C) Molecular Weight as gathered from AFM images.....	47
Figure 4.8: Example of bimodal distribution seen in the MSD analysis of PVP at different molecular weights. This particular example was obtained for 1.1% PVP10.....	51
Figure 4.9: Particle size distribution of 0.1% CTAB in solution.....	53
Figure 4.10: DLS of SWNT suspended with 0.25% A) PVP40, B) PVP360, and PVP1300	54
Figure 4.11: Surface tension behavior of CTAB	57
Figure 4.12: Different resonance structures of the pyrrolidone head group of PVP. The figure was designed by <i>Mishra et al. (2009)</i> . ¹⁷³	59
Figure 4.13: The pH value of standard control solutions such as 0.1% CTAB and 6% of the different molecular weights of the polymer.....	60
Figure 4.14: pH reading of A) PVP40 and B) PVP360 at different concentrations. The blue represents of samples with 0.1 %wt/v CTAB whereas the orange represents samples with both 0.1 %wt/v CTAB and 0.2g/L SWNT.	61
Figure 4.15: Possible Tautomerism of PVP as shown in <i>Nikiforova et al. (2012)</i> . ¹⁷⁷	61
Figure 4.16: A) Demonstrates the determination of the point of zero charge while B) gives the pH value of standard control solutions such as 0.1% CTAB and 6% of the different molecular weights of the polymer.....	62
Figure 4.17: Relationship between viscosity and the total area of dispersion acquired from UV data	63
Figure 4.18: Dynamic viscosity of CTAB+PVP system with and without SWNT at a PVP molecular weight of A) 3500 g/mol B)10 000 g/mol C) 360 000 g/mol.....	65

Figure 4.19: Hypothesized interaction of polymer with nanotube. The nanotube is illustrated here as the black-gray cylinder with an outer covering of surfactant (red glow). The spheres on top represent the PVP polymers..... 70

Figure 4.20: Percent increase in dispersion over the total projectable area by PVP 71

Figure 4.21: Potential energy of polystyrene nanoparticles stabilized with different molecular weights of PVP. A) PVP10, B) PVP40, C) PVP360, and D) PVP2500 as produced by Smith et al. (1996).¹⁹⁵ 72

Figure 4.22: Percent increase in dispersion versus the total possible contact area by PVP 74

List of Tables

Table 2.1: Tabulated Young's Modulus and Strength of different materials	10
Table 4.1: Nanotube species observable through peaks of CTAB-assisted dispersion of nanotubes. The measured and predicted van Hove wavelengths from research by Bachilo <i>et al.</i> (2002) and Weisman <i>et al.</i> (2003) are included. ^{69,70}	40
Table 4.2: Ratio of Absorbances for 6% PVP dispersion systems for 0.2 g/L SWNT calculated as described by Haggemueller <i>et al.</i> (2008).....	42
Table 4.3: Reported lengths and radii from various research groups after sonication. The italicized results are the results obtained in our experiments	48
Table 4.4: Summary table of DLS results for the analysis of the different molecular weights of PVP	50
Table 4.5: Values of the small and large forms of PVP under the MSD analysis option.	52
Table 4.6: Estimated CMC values of CTAB with different molecular weights of PVP at different concentrations with the 95% interval that the true CMC value lies between.	58
Table 4.7: Overlap Concentration and the corresponding overlap viscosity of PVP as estimated using GPC and equation (2.10) ^{108,110}	64
Table 4.8: Ratio of total surface area projectable by the polymer to total surface area available of nanotubes	71

List of Abbreviations

AFM – Atomic Force Microscopy

CI – Confidence Interval

CMC – Critical Micelle Concentration

CNT – Carbon Nanotube

CTAB – Centrimonium Bromide

DLS – Dynamic Light Scattering

GA – Gum Arabic

GPC – Gel Permeation Chromatography

MSD – Multimodal Size Distribution

MWNT – Multi walled nanotube

NaDDBS – Sodium dodecylbenzene sulfonate

NNLS - Non-Negative Least Square

PABS – Polyamino benzene sulfonic acid

PEO – Polyethylene oxide

PMMA – Polymethylacrylate

PNVC – Poly-*N*-vinylcarbazole

PPO – Polypropylene oxide

PS – Polystyrene

PSSty – Polystyrene and sodium maleate

PVP - Polyvinylpyrrolidone

SANS - Small Angle Neutron Scattering

SC – Sodium Cholate

SDS – Sodium Dodecylsulfate

SWNT – Single walled nanotube

Chapter 1: Background

Part of the fullerene class of nanomaterials, carbon nanotubes possess superior mechanical, electrical, and thermal properties when compared to other materials commonly used.^{1,2} This makes them extremely attractive for applications in many different fields across science and engineering. Their potential applications include nano-electrical systems,^{3,4} reinforcement for composites,⁵ insulators for high heat systems,⁶ hydrogen storage,^{7,8} and catalysis.⁹ However, one of the primary challenges in the development of carbon nanotube-based technology is the inherent difficulty to properly disperse them in hydrophilic environments due to the hydrophobicity of carbon and the subsequent strong van der Waals interactions in close proximity. This is significant because it negates the ability to fully take advantage of a nanotubes high aspect ratio and surface area – a virtue critical to main of the applications above.

Several research groups have worked to develop ways to disperse nanotubes in aqueous solution. Methods that have been developed include mechanically shearing the structures apart using ultrasonication followed by either covalent or non-covalent modifications. Covalent modifications involve the use of chemical reactions to attach a functional group to the wall of the nanotube. This results in alteration of the carbon nanotube wall which can potentially affect its surface and even electronic properties or even fragment them. Non covalent modifications normally take advantage of surfactants (cationic, anionic, or neutral) and polymers to disperse the nanotubes.¹⁰ The surfactant and polymer molecules used for this purpose possess both hydrophobic and hydrophilic domains making them amphiphilic. As compared to other methods, the use of amphiphiles preserves the many important properties of nanotubes making this a better strategy for dispersion. Thus, there has been a substantial amount of work exploring the uses of both types of molecules for carbon nanotube dispersion in aqueous systems. Such work has created an unlisted but generally agreed upon set of criteria in the literature for which different dispersing agents are effective. This includes the necessity of specific molecular features such as hydrophobic tails, aromatic moieties and charged groups in surfactants and polymers allowing them to effectively adsorb onto the surface of nanotubes and lower its surface energy. Currently, much of the research investigating the effectiveness of different dispersing agents focus on the comparison of these agents one at a time. However, recent applications involving carbon nanotubes are multi-component systems involving the dispersing agent plus other elements. Sometimes this other element can be an additional surfactant or polymer while other times it can be even be ceramics. For example, both a sodium cholate (SC) - sodium dodecylsulfate (SDS)

and a SDS-carboxymethylcellulose system, have both been used to firstly disperse nanotubes and then purify them via density gradient ultracentrifugation.^{11,12} Additionally, surfactants and polymers such as hexadecyltrimethylammonium bromide, polyacrylic acid, and polyethylene oxide have been used to disperse nanotubes for the incorporation into a SiO₂ ceramic matrix.¹³

1.1 Motivation

Early research by our group led to the development of a polyvinylpyrrolidone/centrimonium bromide (PVP/CTAB) system for the dispersion of carbon nanotubes (CNTs) into a chitosan matrix. Incorporation of the nanotube system in the chitosan scaffold led to a dramatic 20 fold increase in Young's modulus of the composite, compared to that of the unmodified chitosan matrix.¹⁴ As a result of this significant improvement, the CTAB-PVP system was further explored here to determine its mechanism and how it could be exploited and improved for an even greater enhancement in dispersion. In addition, any results generated would be beneficial towards fillings the gap in knowledge for multi-component dispersing systems as remarked on above. Therefore, this thesis focuses on the specific determination of the mechanism of the CTAB and PVP system as a tandem dispersing method. The system is characterized using colloidal analysis techniques including viscosity, surface tension, atomic force microscopy and dynamic light scattering. The quality of nanotube dispersion is evaluated using Vis-NIR spectroscopy. By probing this system more deeply, we aim to obtain a better understanding on how surfactants and polymers can be used together to disperse nanotubes. This will undoubtedly allow for the tailoring of multi-component composite systems more effectively for the integration of CNTs in a multitude of electrical, thermal, mechanical motivated applications.¹⁵

1.2 Thesis Outline

This thesis presents work aimed at describing the mechanism of the CTAB/PVP surfactant polymer system to disperse nanotubes. Chapter 1 provides a general scope of the thesis including the background, motivation and research goals. Chapter 2 is a literature review of the field with the intent of broadening and also deepening the general background and motivation presented in Chapter 1. The topics that will be presented include the attractive features of nanotubes, and the challenges and strategies used for dispersing them into hydrophilic environments. With regards to the latter section, properties of surfactants and polymers will also be presented along with general theory on different techniques used to analyze these systems. Chapter 3 will further elaborate on these experimental

methods - the theory behind each technique and the rationale behind each specific procedure used. The results will then be presented and discussed in Chapter 4 and lastly, the thesis will close off with a conclusion of the findings and future recommendations in Chapter 5 to further flesh out the true potential of this research.

Chapter 2: Literature Review

2.1 Introduction

The development and quality of materials for the creation of different goods has been at the forefront of human research since the dawn of human invention and construction. Indeed, components such as glasses, metals, and polymers can be seen instantly in every direction throughout the world today. However, a large amount of objects seen in our daily lives are also a product of several materials combined. These composites are generally designed to have greater performance with a reduced cost compared to their individual make-up components alone. How a composite is designed and what materials will be used is of course dependent on the purpose of the product, e.g. strength in construction cement and electrical conductivity in wiring. Sometimes more than one particular property needs to be enhanced in order for the product to be attractive such as flexibility and weight in sports equipment; and heat resistance, hardness, and chemical stability in automotive parts. Unfortunately, the more properties that need to be optimized, the harder it is to find a suitable material such that all requirements are met. Truthfully, there will always be tradeoffs in the design of a product. A prime example is the use of hard plates in body armor which is effective in preventing ballistic injury but limits movement significantly. Thus, a truly captivating primary component would be one that has long lasting, high, and diverse performance properties that are tunable and have relatively low trade-off with one another. Such a material may seem hard to imagine, but modern research has paved the way for the development of several exemplary materials which are becoming increasingly promising. In 1991 Sumio Iijima discovered one of these new materials - a graphitic coaxial cylindrical carbon structure formed from arc-discharge evaporation of graphite electrodes. These came to be known as carbon nanotubes (CNTs) and they possess prominent and theoretically tunable mechanical, thermal, electrical, and optical properties which can be easily exploited for detection purposes.¹⁶ Because of this potential, research soon followed investigating their incorporation into different composites¹⁷ and subsequent studies have only reinforced their prospective role as filler material among other applications.

2.2 Nanotube Structure and Properties

Nanotubes are a type of nanomaterial comprised completely of carbon, making them part of the carbonaceous classification together with graphite and diamond. The basic unit of the nanotube structure can be likened to that of a honeycomb where each vertex of the hexagon contains a carbon

atom. By extending the basic hexagonal unit repeatedly in 2D, the resulting object is a planar graphene sheet filled with hexagonal carbons interconnected with each other (Figure 2.1). A nanotube is subsequently formed by rolling up the sheet into a cylindrical form. Because of this base molecular patterning, nanotubes also fall under the fullerene class of nanomaterials as well, fullerenes (or buckyballs) being the first carbonaceous nanomaterial discovered by Kroto *et al.* (1985).¹⁸

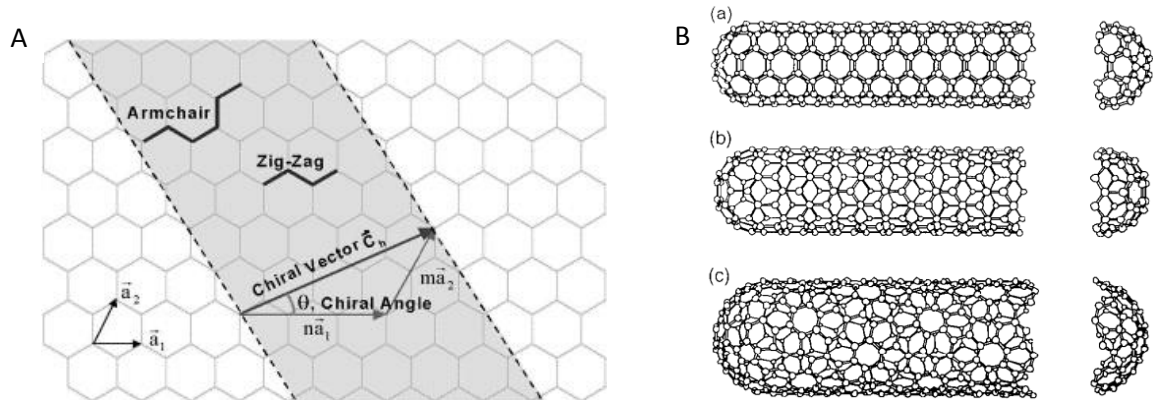


Figure 2.1: A) Diagram by Thostenson *et al.* (2001) illustrating the unit cell found in graphene and nanotubes. In addition, the unit vectors \vec{a}_1 and \vec{a}_2 are given along with magnitudes n and m , the chiral vector, and chiral angle. The path of an armchair and zig-zag nanotube are also given which are further shown in B) which was designed by Dresselhaus *et al.* (1995) gives a 3D representation of a) armchair b) zig-zag and c) chiral nanotubes.^{19,20}

The direction in which a graphene sheet is rolled up is significant however, because it can generate many different chiralities which are directly linked to the nanotubes optical and electrical properties. Different chiralities are denoted by (n, m) where both values are indices indicating the magnitude of two unit vectors, commonly denoted \vec{a}_1 and \vec{a}_2 . These vectors are placed at an arbitrary vertex to serve as the origin of “rolling up” on the graphene sheet. From these unit vectors, their sum, the chiral vector, C_h can be defined as below:

$$C_h = n\vec{a}_1 + m\vec{a}_2 \quad (2.1)$$

This vector becomes significant in describing the electrical and optical properties which will be described shortly. Other basic parameters such as the diameter (d) of the nanotube and its chiral angle (θ) between the two unit vectors can also be derived from n and m by using equations (2.2) and (2.3).

$$d = \frac{L}{\pi} = \frac{a\sqrt{n^2 + nm + m^2}}{\pi} \quad (2.2)$$

$$\sin \theta = \frac{\sqrt{3}m}{2\sqrt{n^2 + nm + m^2}} \quad (2.3)$$

where a in equation (2.2) describes the length of the unit lattice vector and is often approximated as 0.246nm. In terms of the angle, it can reach a maximum of 30° when $n = m$ and nanotubes that have this configuration are commonly known as armchairs. An angular minima is reached at 0° when either n or m is equal 0 in which case nanotubes are commonly referred to as zig-zag. These extreme classifications and other species in between can be seen in Figure 2.1B above.

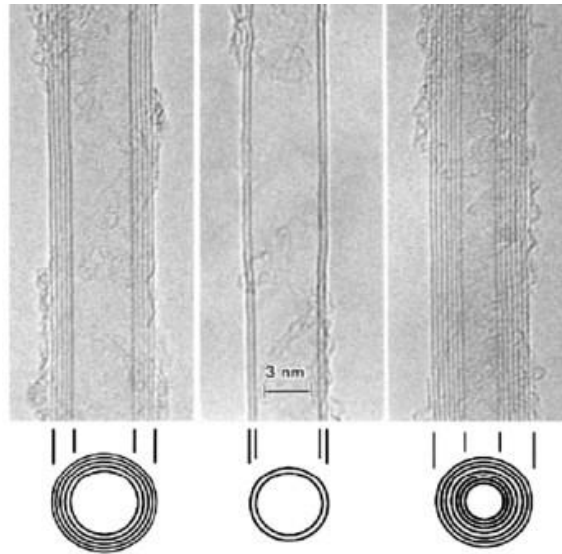


Figure 2.2: TEM images of different MWNT acquired by Iijima (1991).¹⁶ A SWNT would be a tube with only one ring.

There are primarily also two types of nanotubes, single-walled nanotubes (SWNT) and multi-walled nanotubes (MWNT). As the name implies, MWNT are essentially like SWNT except they possess multiple walls wrapping around each other like the concentric rings of a tree (Figure 2.2). Because of this they can have diameters from 5nm-50nm whereas SWNT usually have diameters below 5nm. However, because MWNT can have multiple layers, their structure related properties are not well understood. They are however cheaper to produce but SWNTs, because of their more pristine and genuine structure, show generally better performance when incorporated into composites.^{21,22}

2.2.1 Electrical Properties

One of the primary driving qualities of nanotubes that makes them so desirable in composites is their electrical properties. The unique band gap structure of nanotubes makes their ability to carry electrons very high.²³ In fact, early predictions using functions to model atomic orbitals and theories of electron movement in a solid lattice predicted CNT conductivity to be higher than that of metals at

room temperature. Yao *et al.* (2000) experimentally demonstrated this by showing that some SWNTs possessed a high current carrying density of 10^9 A/cm², 1000 times that of copper and aluminum.^{4,24} When nanotubes are incorporated into composites, is when their electrical prowess become very evident. For example, Kim *et al.* (2004) achieved a polymethylacrylate (PMMA)/MWNT composite that had a conductivity of 3000 S/m with only 0.4 %wt/v of nanotube.²⁵ Furthermore, Potschke *et al.* (2004) incorporated MWNT into a polyester composite and found a 16 fold increase in the conductivity. They achieved this with approximately 1000 S/m with 15 %wt/v of nanotubes.²⁶ In 2009, Spitalski *et al.* reviewed and tabulated much of these prior achievements and have all shown to be in the range of the studies mentioned.² Also, automotive companies such as Hyperion have successfully incorporated nanotubes into many of their different composite products such as fuel lines, O-rings, and pump modules as a means to dissipate charge build-up in engines.²¹ In these materials, nanotubes can offer 1 – 10 S/m conductivities without hindering other performance requirements of the automotive part such as low melting viscosity and high mechanical strength. Noticeably, it can be seen within these examples that conductivity varies with filler material. This opinion is also reflected in a review by Bauhofer *et al.* (2009) whom additionally showed that there is no clear consistency in using either SWNT or MWNT nor the treatment method (oxidation, purification) when seeking to obtain maximum conductance.²⁷ They also remarked that exfoliated nanotubes can be 50 times more conductive than bundled forms.²⁷ Lastly, worth mentioning is perhaps the most recent and enticing bit of electrical innovation which comes from Shulaker *et al.* (2013) whom exploited the fact that CNTs can possess a carrier mobility of approximately 10 000 cm²/V·s, 200 times that of silicon, to develop a faster type of computer processor.^{24,28} Overall, nanotubes hold a lot of promise in delivering almost futuristic electrical applications.

These electrical properties of nanotubes can be tied to their chirality which as stated above is linked to the unit vector magnitudes, n and m . Generally, if $n - m = 3l$ where l is an integer then a tube is considered to have metallic-like properties. Given this parameter, all armchair nanotubes are metallic and in general, metallic nanotubes represent about a third of all possible tube structures. The remaining two-thirds of nanotubes are semiconducting (when the above condition is not satisfied).^{29,30} Figure 2.3 below shows some of the different nanotube chiralities that are either metallic or semiconducting.

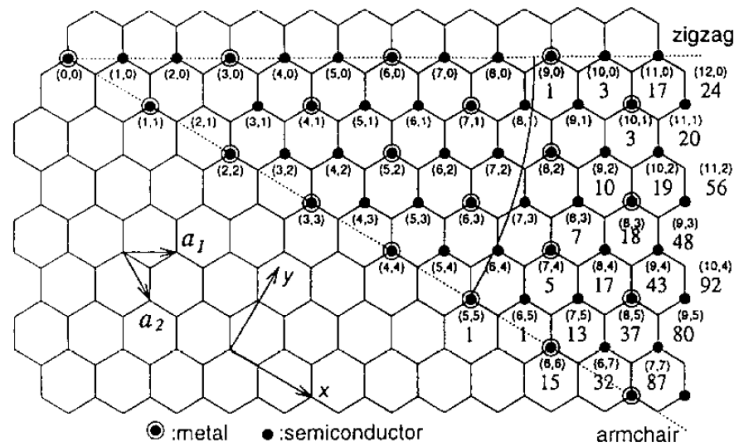


Figure 2.3: The different chiralities of nanotubes and whether they are metallic and semi-conducting as prepared by Dresselhaus *et al.* (1995).²⁰

The stated general condition above comes from the analysis of a nanotube's band structure which can be revealed by studying the electronic π system of two adjacent carbon atoms within the hexagonal lattice of graphene. In graphene, the bonding and antibonding bands of the π orbitals cross at the corners of the unit hexagonal cell (Brillouin zone) whereas the σ bonding and antibonding bands are too far from the Fermi level to affect electrical conductivity.³¹ The band crossing means the Fermi surface is concentrated at the 6 corners of the cell. Because nanotubes are bounded cylindrical and not endlessly propagating like graphene, it is necessary to apply a constraint onto the graphene electronic states in the circumferential direction. By applying this restriction onto a Bloch wavefunction, which describes the energy states of an electron in a crystal and can be used because a graphene lattice is also Bravais lattice, the states of a nanotube can be reduced to:

$$kC_h = 2\pi n \quad (2.4)$$

where n is the principal quantum number, k is the wavenumber (magnitude of wavevector) and C_h remains as defined before. Whether the quantized wavevector crosses the graphene Fermi level at the first Brillouin zone the nanotube is metallic. If the wavevectors do not cross the Fermi points, then the nanotube is semiconducting. The rule $n - m = 3l$ as stated above is a generalization of this phenomenon. The energy systems are linked to the diameters of the nanotube as well through C_h and therefore there are several effects worth noting with changes in diameter. Firstly, the band gap of semiconducting nanotubes decreases logarithmically with diameter. Secondly, with metallic nanotubes, small curvatures can induce minor pseudo-band gaps thereby leading to the production of small semi-metallic properties. Armchair nanotubes are exempt from this however because of their symmetry.³² Curvature strain can also lead to exceptions which can be seen, for example, in the (5,0) nanotube which shows metallic properties instead of semiconducting.³³ This is because small

diameters can lead to σ - π band overlaps.³⁰ Despite these dependences on curvature, it's interesting to note that nanotube electrical properties are almost independent on length.³⁴

2.2.2 Mechanical Properties

Length is however significant in terms of a nanotubes mechanical properties. Nanotubes have a large aspect ratio, are highly flexible and very strong especially in the axial direction.^{20,35,36} Among the many types of measurements to characterize mechanical strength, the two that arguably stand out the most are Young's Modulus and the tensile strength. The Young's Modulus describes the ratio of stress applied to the amount of resulting strain on the material. The tensile strength describes the maximum amount of stress a material can be subjected to before it breaks. Some of the first studies on nanotubes' mechanical ability in terms of these values were performed by Treacy *et al.* (1996) whom studied MWNT from a large bundle synthesized by the carbon arc method and used TEM to relate the amplitude of a nanotubes thermal vibration to the Young's modulus. They obtained an average value of 1800 GPa.³⁷ This result was confirmed by Wong *et al.* (1997) whom pinned one end of a MWNT to molybdenum disulfide surface and measured the bending force against displacement along the unpinned length. They found that the modulus was 1300 GPa and additionally found the average strength to be 14.2 GPa.³⁸ In 1998, Krishnan *et al.* were able to isolate SWNT and used a similar method to Treacy *et al.* (1996) to measure the Young's modulus and obtained a value of 1250 GPa.³⁹ Uniquely, Li *et al.* (2000) used modeling to predict the modulus and strength of a nanotube and found values of 790 GPa and 0.4-22.2 GPa, respectively.⁴⁰ Perhaps the most direct experiment of measuring these properties were described in separate publications by Yu *et al.* (2000). In these articles they attached both MWNT and SWNT to the ends of atomic force microscopy (AFM) tips and used them as force sensors to read out the applied load. In their experiments they found that MWNTs possessed a tensile strength of 11-63 GPa and a Young's modulus of 270-950 GPa.⁴¹ In comparison SWNTs possessed a tensile strength ranging from 13-52 GPa and a Young's modulus of 320-1470 GPa.⁴² A comparison, shown in Table 2.1 which also lists the Young's Modulus of other materials and reveals the mechanical properties of nanotubes far exceeds those of other common materials.⁴³

Material	Young's Modulus (GPa)	Strength (GPa)
Stainless Steel	180	0.860
Copper	117	0.220
Titanium Alloy	105-120	0.900
Polystyrene	3.00-3.50	0.03 – 0.10
Polypropylene	1.50-2.00	0.028 – 0.036

SWNT	320-1470 ⁴¹ , 790 ³⁸	13-52 ⁴² , 0.4-22.2 ⁴⁰
MWNT	270-950 ⁴¹ , 1300 ³⁸	11-63 ⁴² , 14.2 ⁴⁰

Table 2.1: Tabulated Young's Modulus and Strength of different materials

Often materials can appear stronger given an increased quantity. Thus, another comparison can be carried using the density-normalized modulus and strength. For SWNTs it has been observed that the density normalized modulus and strength is 19 and 56 times that of steel wire and 2.4 and 1.7 times that of silicon carbide.²¹ Steel wire can often be found in electrical wires and silicon carbide is a high endurance ceramic found in car brakes. Additionally, SWNT can withstand pressures up to 25GPa at which point it has been observed to adapt into a superhard phase which can withstand pressures up to 55GPa without collapse. In this new phase, the bulk modulus is greater than that of a diamond crystal (420 GPa), standing at 462-546 GPa.⁴⁴

Akin to research targeted towards enhancing the electrical potential of nanotubes, there has been just as much targeting mechanical properties.² Examples of products that have seen high mechanical benefits from nanotube incorporation include thin films, cements and gel composites. Di *et al.* (2012) formed pure nanotube films by drawing on a 40 μ m thick polytetrafluoroethylene layer. After peeling from the layer the films had a tensile strength of approximately 2 GPa and a Young's modulus of approximately 90 GPa,⁴⁵ which Wang *et al.* (2013), using a similar method, subsequently incorporated into a Bis-Maleimide polymer composite to yield a tensile strength of 3.8 GPa, a Young's modulus of 293 GPa and a conductivity of 1230 S/cm.⁴⁶ In cements, Sobolkina *et al.* (2012) saw a 40% increase in compressive strength and a moderate increase in tensile strength as well in their calcium silicate hydrate cement paste,⁴⁷ while for gels, recent groups such as Huang *et al.* (2011) developed a MWNT-PVP/PVA composites and found a maximum improvement of 133% in tensile strength with 1% loadings of MWNT.⁴⁸ Davis *et al.* (2011) successfully incorporated SWNTs into a chitosan matrix crosslinked with glutaraldehyde and reported a 20 fold increase in Young's modulus with the incorporation of 0.8 g/L nanotubes.¹⁴ Indeed, successfully dispersing nanotubes can lead to dramatic increases in composite mechanical properties. In 2006, Coleman *et al.* stated that is perhaps the most fundamental issue and is imperative for equal load transfer and the reduction of stress point. With poor dispersion, when the loading level is increased beyond the point where aggregation begins, this can lead to decreases in strength and modulus.⁴⁹

2.2.3 Thermal Properties

Due to their long-range crystallinity (ie. repeatability of the hexagonal unit) and the possible long

propagation of phonons (lattice vibrational states) along a relatively long mean free path, nanotubes were theoretically predicted to have greater thermal conductivity than other carbon allotropes such as graphite and diamond. Tests from both Kim *et al.* (2001) and Pop *et al.* (2005) on suspended MWNTs and SWNTs have shown that the two types yielded thermal conductivities of 3500 W/(m·K) and over 3000 W/(m·K), respectively at room temperature.^{50,51} To put this in context, silver has a thermal conductivity of 400-430 W/(m·K) and natural diamond has a thermal conductivity of about 2000 W/(m·K).⁵²⁻⁵⁴ In 2000, Berber *et al.* predicted through modeling the conductivity of (10, 10) armchair nanotubes to be 6600 W/(m·K) at room temperature which is two-fold greater than that of isotopically enriched diamond (3320 m·K). As temperature is decreased, the conductivity of both nanotubes and diamonds increased however nanotubes increased at a slightly higher rate.⁵⁵ In 2002, Biercuk *et al.* used 1% wt/v of nanotubes as filler for epoxy resin composites and successfully doubled the thermal conductivity compared to their sample without the nanotubes. Comparatively, a quality control of carbon fibers only showed a 40% improvement in conductivity when incorporated at the same amount. It should be noted that Gojny *et al.* (2006) investigated the potential for thermal advancement through nanotube incorporation into epoxy composites. This listed the overall size of the interface, aspect ratio, and interfacial adhesion as the contributing factors. A low interfacial area, weak interfacial adhesion and the existence of shielded internal layers is desired because it promotes conduction of phonons and minimizes coupling loss. Most composites seen had large interfaces which lead to increased phonon boundary scattering meaning lower than expected conductivity due to a reduction in mean free path. However, the authors noted at the end that a higher dispersion of nanotubes could reduce the distance between CNTs, facilitating phonon conduction through reduced scattering.⁵⁶ The necessity of high dispersion has also been stressed by several authors as reviewed by Han *et al.* (2011).⁵⁷

2.3 Nanotube Composite Challenges

Overall, nanotubes possess a variety of properties that make them attractable to be used as filler material. However, a repeatedly cited problem is that the hydrophobicity of a nanotube can lead to its aggregation upon synthesis and poor dispersions in solution.⁵⁸ Truly, in this state their industrial and academic value is greatly restricted because many of their inherent properties are limited. In terms of composites in particular, if nanotubes are not dispersed, they can act as focal points for stress and hinder both electrical and thermal conductivity. To better understand nanotube aggregation in composite design, Kyrylyuk *et al.* (2008) used the continuum model to investigate how bending

flexibility, length, polydispersity, and attractive interactions between nanotubes played a role. They found that not only did all these make a difference but special consideration must be given to the degree of nanotube aggregation, the presence of longer species, and the attractive interactions between them.⁵⁹ Indeed, the intrinsic aggregation of nanotube is a significant obstacle. Girifalco *et al.* (2000) also used the continuum model to assess the interaction between two parallel tubes and found that the driving force for aggregation is also linked to the CNTs radius.⁶⁰

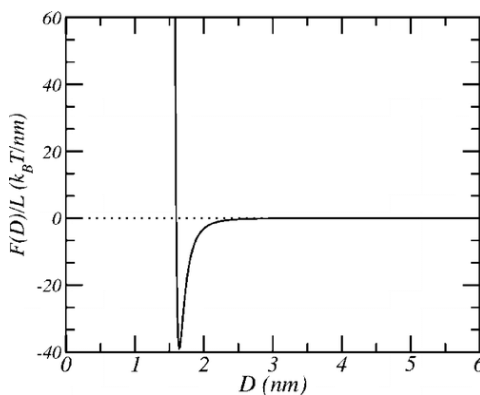


Figure 2.4: Parallel nanotube-nanotube interaction potential per length as calculated by Nativ-Roth *et al.* (2007)⁶¹

Observing Figure 2.4, a large attractive force (maximum of 40kT/nm or 1.644×10^{-19} J/nm at 25°C) can be seen at an inter-tube distance below 2nm. This quickly rebounds and stabilizes to 0 kT/nm around an inter-tube distance of 2.5nm onward. Note that kT is the product of the Boltzmann constant and temperature, a unit for energy. From this observation, we can gather that two 1 μm tubes bound in parallel would have an attractive energy of 1.644×10^{-16} J.^{60,62,63} Additionally, separating nanotubes also seems to be an anisotropic in terms of the energy barrier. Using (10,10) nanotubes, Angelikopoulos *et al.* (2012) observed through simulation that separating nanotubes through parallel shearing and “ripping” a tube perpendicular to the plane require different amounts of energy : 9.864×10^{-19} J/nm and 4.932×10^{-19} J/nm, respectively at room temperature. Putting these values into perspective, the energy between C-C single bonds under the same temperature condition is about 7.809×10^{-19} J/nm. Additionally, there also needs to be a consideration for static friction which has been estimated to be 0.066nN overall.⁶⁴ In all, these barriers are quite substantial and the authors remark vehemently on the challenges and needs of dispersion research. Indeed, in terms of ongoing investigations of dispersion mechanisms, many groups have looked into covalently and non-covalently chemical modifications of nanotubes to improve its interactions with its surrounding solvent whereas other groups have even looked into modifying the solvent system itself i.e. using chloroform, dimethylformamide, toluene, alcohols, etc instead of water.^{65–68} To promote the initial separation of

nanotubes, other methodologies involving physical separation using aggressive shearing techniques such as sonication before the chemical modifications have also been explored. With so many options, how to quantify and assess the quality of a nanotube dispersion is extremely important.

2.3.1 Assessing Nanotube Dispersions

Optical absorption is one of the most efficient ways to evaluate nanotube dispersion. However this is possible only for SWNT because of the unique and distinct electronic band structure which present spikes in the density of states termed van Hove singularities (Figure 2.5A). In MWNTs the density of states can be significantly more complex due to π - π interactions between the different coaxial layers present in a MWNT. Bandaru (2007) reports that generally, the resulting density of states comes from the summation of the different chiralities of the MWNT but other phenomena can arise depending on whether the layers of MWNT are metallic, semiconducting, or both in which case pseudo band gaps can occur.³ Understandably this would make interpreting absorption spectra difficult which is why SWNT will be the main focus of our work.

For SWNT, when light of wavelengths usually in the visible-near infrared red is sent onto the nanotube, it is absorbed causing electrons to be promoted through an interband transition E_{ij} between states in the valence (occupied) and conduction (empty) bands. The theoretical calculations presented in section 2.2.1 concerning electrical properties of nanotubes can also be used to predicting electronic states and thus the energy required for these electronic transitions. These calculations show a clear link between nanotube diameter and its band gap (transition energy). These quantized correlations are best demonstrated through a Kataura plot of SWNT (Figure 2.5B).⁶⁹ Indeed, because of this predictability, there has been much work done into tying a particular nanotube chirality to its absorption spectra.^{70,71}

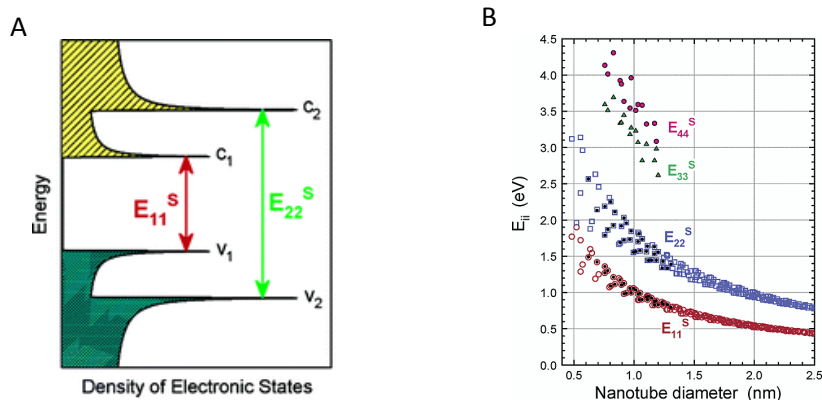


Figure 2.5: A) An example of the electron band structure of nanotubes. B) Kataura plot representing the band gap energy as a function of nanotube diameter. Both figures were prepared by Weisman *et al.* (2003)⁷¹

Once a spectra is generated, the dispersion quality of a particular nanotube chirality or the solution overall can be assessed by inspecting the sharpness or resolution of the peak(s) of interest. The sharpness is related to the quality of the dispersion because nanotubes in a more dispersed sample are more efficient in absorbing light, as bundling and agglomeration are known to quench that ability increasing light scattering instead. The sharpness of the spectra can be quantified using several different methods to gain information about nanotube dispersion. Several groups use the total area above a baseline designated to account for Rayleigh scattering (Figure 2.6):

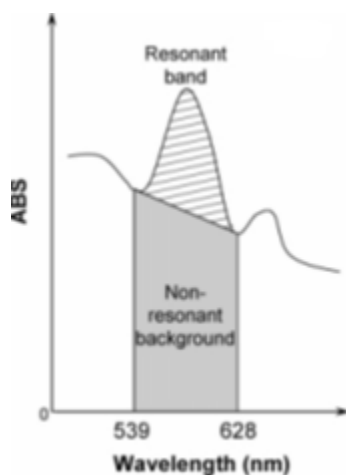


Figure 2.6: The resonant band of nanotubes over its non-resonant background gives the resonance ratio. This method was proposed by Tan *et al.* (2005) as a method of characterizing dispersion quality of nanotubes.⁷²

It's important to notice that the baseline is slanted and this is done to reflect the Rayleigh scattering which can lead to misleadingly higher amounts of absorbance. The relationship between scattering and the particular wavelength is given in equation (2.5) below.

$$A_{scattering} \propto \frac{1}{\lambda^4} \quad (2.5)$$

Other groups have also divided the total area above the absorption baseline by the respective scattering background under the baseline. The resulting value is termed the resonance ratio.⁷²⁻⁷⁴ A similar method that has also been proposed includes taking the ratio between the maximum absorbance of a peak at a certain wavelength and the corresponding background absorbance value at the same wavelength.⁷⁵

To measure the amount of nanotubes retained in solution after sample preparation, one can simply compare absorbance values at a set wavelength as was done by Wenseleers *et al.* (2004).⁷⁶ However, other groups have also used the Beer-Lambert Law to quantitatively find the final concentration of

nanotubes after sample preparation and compared it to the initial starting concentration (i.e. the efficiency).^{47,75,77}

Thus, in such a way, optical absorption offers a fast and reliable way to predict SWNT dispersion. In terms of other spectroscopic methodologies to assess dispersion, Raman and fluorescence spectroscopy can also be used. However, in comparison with other techniques, absorption spectroscopy is advantageous as Raman is limited by nanotube resonance with the laser used for the measurement. This means that the technique is insensitive to those nanotubes not in resonance with the laser. Fluorescence can also be used but can only analyze semiconducting nanotubes because of the longer decay time of the excited states, compared to that of metallic nanotubes.

2.4 Methods of Improving Nanotube Dispersions

As stated, there have many methods to improve the dispersion of carbon nanotubes. The following section will describe such methods in detail.

2.4.1 Physical Methods

To provide sufficient energy to physically separate nanotubes, the use of ultrasonicators has become one of the more accepted methods for nanotube dispersion. Horn sonicators produce a tunable oscillating conical field of high energy (surrounding temperatures that can instantly rise to 5000K) in the fluid which has been proposed to provide high local shear to the ends of the nanotube.^{78,79} Many groups such as Qian *et al.* (2000) used ultrasonication to disperse nanotubes when making MWNT/polystyrene (PS) composites, obtaining homogenous dispersions.⁸⁰ It should be noted though that sonication can severely affect a nanotube initial structure. For instance, in the case of SWNT, fragmentation and introduction of structural defects have been reported while in MWNT, the removal of walls is also possible.^{79,81} However, while other methods exist including aggressive mixing (2000 rpm) they are less efficient than ultrasonication.^{82,83} Because of the potential cutting effect and the fact that sonication is a very system dependent method, optimizing sonication requires significant trial and error.⁸³ Tan *et al.* (2005) explored the effects of sonication by obtaining absorption spectra of nanotubes at different sonication times. They found that at 2 hours of sonication which was also the highest time tried gave the highest resonance ratio value and therefore best dispersions. They also observed that after sonication, undispersed nanotubes (whether fragmented or still aggregated) can be removed by ultracentrifugation leading to a more homogeneous sample.⁷²

2.4.2 Covalent vs Non-covalent Chemical Modifications

Covalently bonding different functional groups to the surface of nanotubes with the aim to improve dispersion has been extensively reported in the literature.⁸⁴ This methodology is widely used because it can increase grafting potential between the nanotube and polymer matrix.^{79,85} The first step usually requires the introduction of hydrophilic chemical functionalities in the nanotube walls. This is usually done through acid treatments which can also help remove catalytic metals and amorphous carbon that would otherwise be present after nanotube synthesis.⁷⁹ Strong acids such as sulfuric and/or nitric are used typically as the starting point. Interestingly using the acid in liquid phase generates carboxylic moieties mostly whereas using them in gas phase leads to the generation of carbonyl and ether groups.⁷⁹ Regardless, once the electrophilic carbon site is created, other molecules can be attached via nucleophilic substitution forming more complex structures.⁸⁴ Many variants of this general methodology exist such as using 30% hydrogen peroxide together with the acid⁸⁶ or using F₂ gas to introduce fluorinated sites.⁷⁹ These can then be substituted nucleophilically followed by a reduction using a metal hydride to remove any remaining fluorine atoms attached.⁷⁹ One last variant worth mentioning is cycloaddition whereby a terminal dipolar oxide (usually nitrile oxide) group attaches to the surface of the nanotube in non-polar solvent such as triethylamine.⁸⁷ With the variety of approaches one can take with covalent modifications however, there is a significant drawback to this approach. Like sonication, over oxidation can also fragment nanotubes in places with structural defects resulting in nanotubes of reduced length in solution.^{79,88} Because of the shortening effect, the aspect ratio of nanotubes decreases significantly affecting thermal, electrical, and mechanical properties. An example of the latter includes a 15% reduction in buckling strength of SWNT as compared to pristine nanotubes when an sp³ bond is introduced.²² Covalent modifications protocols also disproportionately affect nanotubes with higher curvature. Experiments by Zhou *et al.* (2001) and Rinzler *et al.* (1998) have observed that oxidation from air and ozone occur more readily for nanotubes with higher curvature strain and larger amount of defects.⁸⁸⁻⁹⁰

In contrast to these methodologies, non-covalent modifications involve using amphiphatic molecules to stabilize the nanotube by adsorbing to its surface within the aqueous environment. Since the nanotubes walls are not chemically modified, this type of modification preserves the nanotubes inherent mechanical, thermal and electrical properties making this technique more attractive than covalent modifications.⁹¹ In this regard, molecules such as surfactants and different long-chain polymers are fairly attractive.^{36,75} In the subsequent subsections, different relevant concepts of surfactants and polymers will be introduced along with the progress of research in determining how these molecules aid in dispersing nanotubes.

2.4.2.1 Surfactants

Surfactant molecules offer one of the highest potential, when considering non-covalent approaches to nanotube dispersion. Surfactants are amphiphilic molecules meaning they possess molecular regions that enable them to readily interact with polar and nonpolar systems. There are four types of surfactants: anionic, cationic, zwitterionic, and non-ionic. In all cases, the hydrophobicity comes from a non-polar region of the molecule i.e. a long alkyl chain or cyclic rings. In cationic, anionic, and zwitterionic surfactants, the hydrophilic region comes from charged head groups which forms ion-dipole interactions with the water. Whereas cationic and anionic surfactants are stabilized through their counter-ion in addition to water, a zwitterionic surfactant is considered to be neutral overall due to the presence of opposing charges, however it still interacts with water in the same way. With a non-ionic surfactant interactions occur with water through hydrogen bonding. These molecules can also exist as individual molecules or form different macrostructures depending on the nature and thermodynamic stability of the molecule as well as the environment around it. At extremely low concentrations, surfactants are primarily found on the surface of the aqueous phase with their hydrophilic ends facing into the water and the hydrophobic tails facing away from it. As concentration increases the surface of the aqueous environment becomes saturated eventually and molecules have to start existing within the solution. This point is known as the critical micelle concentration (CMC) and immediately at this point, surfactant molecules are in the form of spherical micelles. A micelle in general is a structure that amphiphatic molecules can form to achieve thermodynamic stability in which the shell of the sphere are the hydrophilic head groups of the surfactant and the core consist of the hydrophobic regions. Again, the profile of micelle structures varies depending on the molecule used and the environment around it but generally if the concentration is increased, spherical micelles can approach a cubic phase in which a “crystal” like system can be formed. This phase is known as the isotropic phase. Beyond this, worm-like micelles can develop in the nematic phase and as the name implies, micelles become tube-like, analogous to the shape of a nanotube in general. When these rod-like micelles cluster, then the solution is said to be in its hexagonal phase. Lastly, at extremely high concentrations, micelles can enter the lamellar phase and become bilayer sheets similar to those found on the outer layers of cells. Between the hexagonal and lamellar phase, some surfactant systems can generate a bicontinuous cubic phase where the micelle tubes can branch off forming a 2D network of tubes instead of the 1D singular tube system. Figure 2.7 illustrates all these possible phases for the cationic surfactant, centrimonium bromide (CTAB).

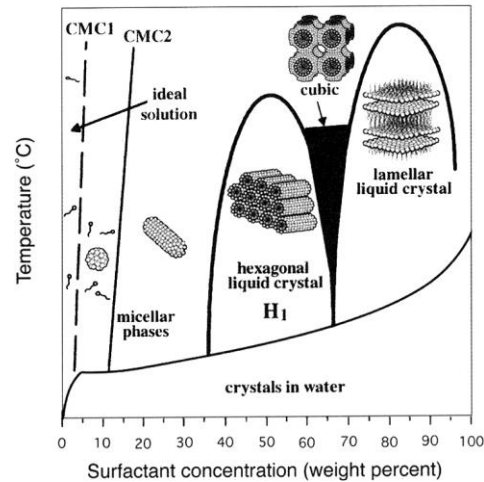


Figure 2.7: Phase diagram of CTAB at different temperatures and concentrations by Brinker *et al.* (1999).⁹²

The actual thermodynamic drive to form these structures can be illustrated by the equation:

$$\mu = \gamma a + \frac{K}{a} \quad (2.6)$$

where μ is the chemical potential at the micelle-water interface, γ is the interfacial energy between hydrocarbon tails and the aqueous phase, a is the surface area occupied per headgroup, and K is the proportionality constant for repulsion of head groups. Deriving this equation with respect to a then setting it to 0 reveals the presence of an optimal surface area per head group (a_0), which can be used to generate the packing parameter:

$$\frac{v_c}{a_0 l_c} \quad (2.7)$$

which is essentially a ratio comparing the chain volume (v_c) to the volume projected by the optimal head group ($a_0 l_c$). A small value indicates a small tail attached to a big head leading to high curvature and vice versa. An analysis of this parameter with the surface area and volume of spheres and cylinders shows that if the parameter is:

- Between $0 - \frac{1}{3}$ then spherical micelles are favored
- Between $\frac{1}{3} - \frac{1}{2}$ then cylindrical micelles are formed
- Between $\frac{1}{2} - 1$ then vesicles are formed
- Equal to 1 then bilayers are formed

Anything larger than 1 indicates unfavorable structures, specifically inverted micelles where tails are pointing into solution and heads are at the core. These structures are not possible in aqueous solutions and would form instead in non-polar environments. From the above equations it can be

seen that parameters such as length and volume of the alkyl chain of surfactants as well as the environment they're in are largely influential in micelle formation dynamics. Repulsion of head groups is another parameter that determines micelle form. This is influenced by the counter-ion in solution and the stability it can provide. However, the exact mechanism of this is still debated. Feitosa *et al.* (2006) reported higher counter-ion binding strength to micelle head groups as the mechanism for which micelle size decreased.⁹³ However, in 2002, both Joshi *et al.* and Aswal *et al.* reported that the hydrophilicity/size of hydrated ion is the real driving force as they saw that micelle size decrease with increasing ion hydrophilicity to water.^{94,95}

2.4.2.2 Surfactants for Nanotube Dispersions

As stated, because of a surfactants ambiphilic nature they are extremely attractive for nanotube dispersions. Of the much available literature it seems there is a common observation on the criteria that a surfactant has to have in order for it to be an efficient nanotube dispersant agent. These include the presence of charges, size of hydrophobic region, and the presence of aromatic groups. These criteria were well established by Tan *et al.* (2005) whom evaluated the degree of nanotube dispersions using several surfactants at their optimal concentration. Among the surfactants used were sodium dodecylsulfate (SDS), sodium dodecylbenzene sulfonate (NaDDBS), Triton-X100 and sodium cholate (SC).^{96,97} Based on the calculated resonance ratio values, it seemed that SC had the highest dispersive ability ratio followed by NaDDBS then Triton X-100 and lastly SDS.

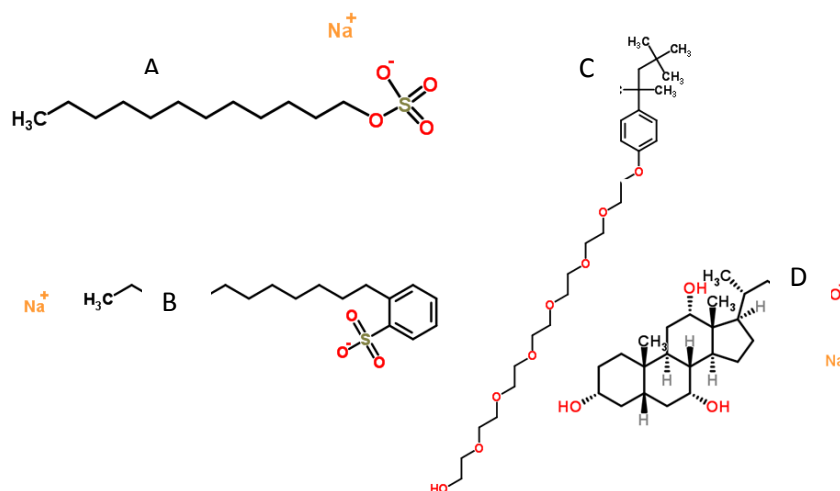


Figure 2.8: Sample of the surfactants used by Tan *et al.* (2005) to determine dispersion ability. Structures were acquired from Chemspider database and are as follows: A) SDS B) NaDDBS C) Triton X-100 D) SC.⁷²

Figure 2.8 shows the structures for these surfactants and it can be seen how the presence/absence of the different functional groups affects their respective dispersion ability. Compounds containing

aromatic moieties seem to consistently lead to better dispersions of SWNTs. This is primarily thought to be due to π - π stacking interactions which is the interaction of π -orbitals between the nanotube and the aromatic ring of the surfactant.⁹⁸ This type of interaction was seen by Lu *et al.* (2004) to dominate over the natural hydrophobic interaction of nanotubes by using fluorescence-based experiments.⁹⁹ Different from this are the interactions of alkyl chain surfactants on the surface of nanotubes which are typically accepted to promote dispersion through electrostatic repulsion,¹⁰⁰ however their binding to the surface of nanotubes is still somewhat contested. Though it was initially thought that micelles formed on the nanotube surface there is gaining evidence that random adsorption of monomers takes place on the nanotube surface instead especially for alkyl chain based surfactants.^{96,101,102} Of alkyl chain surfactants, Sahoo *et al.* (2010) proposed that NaDDBS was the best because it possessed a relatively longer alkyl chain, and is both aromatic and ionic. Comparatively, Triton X-100 lacks a charge but is still aromatic, enabling it to interact via π - π stacking, and therefore making it a decent stabilizer.¹⁰³ SDS, while having a long anionic charge, doesn't possess aromaticity making it one of the worst dispersing agents studied.⁶² Interestingly, the claim of longer alkyl chains by Sahoo *et al.* (2008) may be somewhat misplaced as Tan *et al.* (2005) reasoned that long chain surfactants would have a harder time penetrating the intertube region making its efficiency lower.⁷² Additionally, Sun *et al.* (2008) also evaluated the role of chain length on dispersions. Their results showed that a shorter chain would ultimately be better for nanotube dispersion especially with charged surfactants as it would allow for more adsorption onto the nanotube surface. This in turn would mean electrostatic repulsion between nanotubes would be higher, thus aiding in nanotube dispersion. In this regard, surfactant concentration is also important as there would be different points of surfactant saturation on the nanotubes surface. Research by Blanch *et al.* (2010) determined the concentrations at which different surfactants dispersed best using the resonance ratio as the quantification technique. As predicted, each surfactant had a different optimal concentration however they also noticed that for some surfactants such as Triton X-405 and sodium deoxycholate (dehydroxylated SC) adding more surfactant resulted in a decrease in dispersion. This contrasted the results obtained for sodium dodecylbenzene sulfonate (NaDDBS) for which nanotube dispersion remained relatively constant with increasing surfactant concentration. They explained this phenomenon using attractive depletion interactions where pressure exerted by micelles would force nanotubes to reaggregate to reduce the osmotic pressure. This effect would be more pronounced with longer nanotubes and larger micelles due to the higher number of potential contacts between the two species. They noted though that this reaggregation is not initially noticeable and depending on the surfactant can take weeks to months until clear differences are observed.¹⁰⁴ Lastly, it's worth mentioning that the most effective dispersing

agents observed by Tan and Resasco (2005), SC doesn't contain any aromatic group but rather a gonane core of which all steroid compounds are based on. In these compounds, the mechanism is an apparent adsorption like other alkyl moieties however the planar aspect of the molecule likely increases its adsorption ability.^{105,106} The pronounced dispersion ability of SC was also seen by Haggemueller *et al.* (2008) whom have added that the retention efficiency of SC is quite pronounced as well. In addition, they also observed that long alkyl chain surfactants (anionic and cationic) lead to poor nanotube dispersions, however they also noted that their efficiency in retaining nanotubes in solution (determined using Beers-Lambert law) is relatively high. This means that these surfactants seem to bind to aggregates as well as to dispersed nanotubes. Clearly then, by comparing the abilities of SC and alkyl chain surfactants, it can further be seen that every surfactant behaves in its own unique way. Overall, such observations only further drive research for better and better surfactants for nanotube dispersions.^{98,107,75}

2.4.2.3 Polymers

Another class of molecules, polymers have also been explored for nanotube dispersion. Polymers are large molecules comprised of repeating chemical units called monomers. The chemical and physical properties of a polymer are therefore very dependent on the monomer identity. For example, if a monomeric unit is hydrophilic then likely, the entire polymer would be readily soluble in water. In aqueous solution, polymers can exist in several regimes depending on the concentration. At very low concentrations, they can be described as free floating chains with very little contact with each other. This is known as the "dilute" region. However, as concentration increases polymers eventually reach the semi-dilute region. In this region, polymer chains are very close together and chains overlap with one another and entanglement occurs. The critical concentration in which this occurs is called the overlap concentration usually denoted by c^* . Beyond that, there also exists a region termed the concentrated regime (c^{**}) where the polymer has no space to freely move in solution, however this term is not well defined.¹⁰⁸ These regimes can be seen in Figure 2.9.



Figure 2.9: Regimes of polymers at different concentration levels as drawn by Mutch *et al.* (2007). A) represents the dilute regime, B) represents the semi-dilute regime, and C) represents the concentrated regime.¹⁰⁹

In determining when these phenomena occur for different polymers, there have been many theoretical formulas that have been proposed, some of which are based on geometry (assuming random walk of a real chain system) while others are based on experimental results. The random walk model is used to show that the direction of orientation of a bond in a polymer backbone is completely random. It should be noted though that there doesn't seem to be a generality within the literature as many different formulas have been proposed based on polymers with different head group sizes and backbone flexibility.^{108,110,111} Below are some example equations that are used to predict the transition from dilute to a semi-dilute regime for random polymeric coils:

$$C^* = \frac{3M_w}{4\pi R_g^3 N_A} \quad (2.8)^{111,112}$$

$$C^* = \frac{M_w}{N_A \left(\frac{h_o}{2}\right)^3} \quad (2.9)^{110}$$

$$C^* = \frac{0.77}{[\eta]} \quad (2.10)^{111,113}$$

where M_w is the molecular weight, R_g is the radius of gyration, $[\eta]$ is the intrinsic viscosity which will be described later and h_o is the root-mean-square-end-to-end distance of the polymer.¹¹⁰ Because of the potential chemical diversity and grand size of the molecules, polymers are also a very popular dispersing agent.

2.4.2.4 Polymers as Nanotube Dispersants

In understanding and optimizing for polymer dispersing agents, many types of polymers have been used to evaluate a mechanism in nanotube dispersion as will be seen. There are currently two main theories on the mechanism of nanotube dispersion by polymers: wrapping and non-wrapping. The two models differ in the strength of adsorption between the polymer and nanotube. Wrapping occurs when a strong monolayer of polymer helically wraps a nanotube. This is considered a very strong interaction since it affects the nanotubes electronic properties. In non-wrapping, polymers are weakly interacting with the nanotube through Van der Waals interactions, therefore they typically do not disrupt any electronic behaviour.⁶¹ Wrapping was once considered the only mechanism by which polymers interact with nanotubes. It was first postulated by O'Connell *et al.* (2001) who used atomic force microscopy (AFM) images to show that any aqueous monolayer of polymer (polyvinylpyrrolidone, polystyrene, etc) would be wrapping the surface of the nanotube.¹¹⁴ They

deduced this by observing changes in the length and height distributions of the AFM images and remarking that there was also a decreased presence of bundled ropes as well. They also argued that this was thermodynamically driven to eliminate the hydrophobicity between the nanotube and the solvent. The authors however initially dispersed their samples with SDS surfactant and made no reference to potential interactions between the two which can occur.^{115,116} Nevertheless, the model was one of the first that prompted the use of polymers as dispersing agents.^{68,117–120} Maity *et al.* (2008) demonstrated wrapping was indeed possible by using poly-*N*-vinylcarbazole (PNVC) to form nanocomposites with SWNT and MWNT. PNVC monomers contain two aromatic rings giving the polymer a strong affinity for the nanotube surface for the same reason as aromatic surfactants. To assess the interaction between the polymer and the nanotubes, the authors used Raman spectroscopy. In the case of MWNTs, they observed a decrease in the intensity of the D (defect) and G (graphitic) bands with the presence of polymer which the authors noted could only be caused by two things: either more energy was needed to vibrate the nanotubes or the tubes themselves have somehow become larger. Clearly the latter could not be true and since there was no shift in the position of the Raman bands, PNVC was likely not forming covalent bonds with the MWNT and instead was just adsorbed through wrapping. In contrast, when the authors used SWNTs they observed a band shift in the G and D bands which would suggest that some grafting had occurred. Most prominently, the results were supported by FE-SEM images which showed that the polymer was homogeneously covering the surface of MWNT and was forming complex entangled networks in the case of SWNT. Authors attributed the different results to a more reactive surface on SWNT. Another polymer that has been shown to wrap nanotubes is single-stranded DNA (ssDNA). Zheng *et al.* (2003) found that polythymine (T) wrapping was an enthalpically driven spontaneous process with energies favoring the interaction of polymer-nanotube instead of nanotube-nanotube binding. Using modeling, the adsorption mechanism was again thought to originate from π - π interactions between the nanotube and the nucleic acid, which was further promoted by the extreme solvability between the phosphate backbone and the aqueous solution.¹²¹ With regards to the effectiveness though, there has been some conflicting reports on which DNA based system would be better. Haggenueller *et al.* (2008) obtained better dispersion using polyadenine (A) and even better results when using ssDNA using alternating purine-pyrimidine bases.⁷⁵ From these examples, parallels can be drawn on polymer interactions and surfactant interactions. If the monomeric unit is capable of interaction, such as through π - π interactions then wrapping will likely occur and while these this is indeed a possible mechanism, weak non-wrapping mechanisms have also been seen for polymer-nanotube interactions. Nativ-Roth *et al.* (2007) used the block copolymer, polyethylene oxide-polypropylene oxide-polyethylene oxide (PEO-

PPO-PEO) to disperse nanotubes in aqueous solution. Briefly, initial tests using molecular dynamic modeling showed that PPO was the only block that had ability to bind to the nanotube with PEO blocks projecting outward randomly from the surface of the nanotube in a random manner as seen in Figure 2.10.

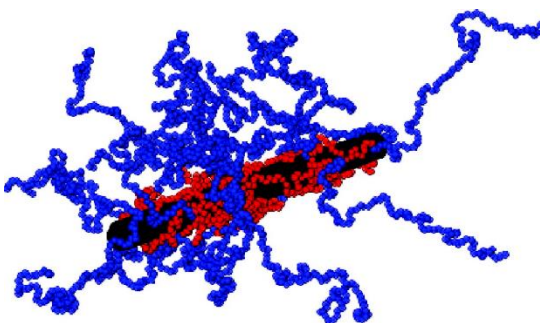


Figure 2.10: Proposed adsorption mechanism of PEO-PPO-PEO triblock polymer by Nativ-Roth *et al.* (2007). Red regions are PPO and blue regions are PEO. ⁶¹

No shift in the electronic structure of the nanotube was detected by both UV and Raman spectroscopy. Instead, small angle neutron scattering (SANS) was used to evaluate the system. SANS measures the interaction of neutrons with the nuclei of a sample where the resulting scattering intensity of a sample (differs per nuclei) is proportional to the negative power of the scattering vector. The value of this exponent can reveal information on the shape of the molecules within the system. For example, a thin and long cylindrical molecule with an extremely high aspect ratio and large persistence length like a nanotube or a wrapped nanotube would ideally have an exponent of -1 however this was not the case for the PEO-PPO-PEO nanotube system. In fact, the data could not be fitted to such a relation leading to the authors to conclude that the polymer retained their loose coil morphology. Interestingly, through modeling the authors noted that increasing the PPO length or the PEO length while keeping the other fixed will increase the dispersive potential of the block copolymer. In particular, they noted 20 monomeric units of PEO is sufficient in driving apart nanotubes apart at a separation distance of 2.5nm. It's important to also note that these effects were more pronounced for SWNT as opposed to MWNT because of the large differences in geometry. Dror *et al.* (2005) also performed a similar series of experiments in which they used cryo-TEM as well as SANS as described above to analyze the ability of two different polymers: Gum Arabic (GA) and alternating copolymer of styrene and sodium maleate (PSSty) to disperse nanotubes. In addition to both being amphiphilic and charged, the latter of which provides electrostatic repulsion, the polymers differed in two ways. GA is a highly branched polysaccharide while PSSty is a linear copolymer of alternating hydrophobic and hydrophilic units. They applied a modification of Pedersen's model for spherical amphiphilic block copolymers and

adapted it for cylindrical geometry.¹²² This model essentially describes a cylindrical core formed by a nanotube or a thin bundle decorated with polymer coils loosely adsorbed onto the nanotubes' surface.¹²³ They found that this model fitted well their experimental data for both polymers despite their physical differences. PSSSty for example, surrounded a 2nm radius core of a nanotube, with a radius of gyration of about 15nm. Interestingly, although the radius of gyration of GA is larger than that of PSSSty, more than double GA polymers can fit onto a nanotube compared to PSSSty and this was attributed to GA being a more compact molecule. Granite *et al.* (2012) also confirmed these observations by again running SANS on the polymers PEO-PPO-PEO and PVP. They additionally noted that surrounding the polymers was higher water density as compared to bulk solution. Also noteworthy was Dror *et al.* (2005) using cryo-TEM, which was able to reinforce the non-wrapping theory by showing what appeared to be spherical polymers in both aggregated and non-aggregated form.¹²³ Indeed, these type of aggregates have also been seen by Cotiuga *et al.* (2006) in which TEM was performed on dried dispersions where they used the copolymer PS-PEO. In their images, they saw that nanotubes were protruding from the polymer aggregates after drying had formed them.¹²⁴ Clearly then, if the polymer cannot interact strongly with the nanotube, it is most likely stabilizing through a steric mechanism. Overall, with the presented studies, it's evident that polymers can disperse nanotubes by either wrapping or non-wrapping and like surfactants, there has been significant research on elucidating different polymer-nanotube dispersion mechanisms. Polymers ranging from synthetics like PVP, PEO, and PPO, to biologically relevant polymers like purine-based DNA are only some of the few that have been tested.^{75,125,67}

2.4.2.5 Surfactant and Polymers as Nanotube Dispersants

In presenting both types of molecules, surfactants and polymers have shown great promise on their own however, the use of both together have also been explored but to a lesser extent. Many of the studies have long focused on using surfactants to disperse and stabilize nanotubes for the incorporation into a polymer matrix. For example, Gong *et al.* (2000) used polyoxyethylene 8- lauryl as a dispersing agent then added epoxy resin and a hardener to form their composite. Expectedly, this elevated the electrothermal properties of their composites compared to the sample in which the surfactant was absent. At the end of their study however, they remarked that one of the ways to improve their system required an understanding of the mechanism between surfactant, polymer, and nanotube.¹²⁶ In 2001, O'Connell *et al.* proposed a mechanism when they were determining how polymers interacted with nanotubes as stated above. Again, there unaccounted analysis of potential polymer-surfactant interaction casts doubt on the mechanism proposed. However, in 2002 O'Connell

et al. did present UV spectroscopic evidence of the SDS-PVP system showing peaks that were red shifted and broadened compared to pure SDS dispersed systems. Although they explained the broadening of peaks by proposing a more polarizable and inhomogeneous environment around the nanotubes through interactions between bundled tubes in side-by-side van der Waals contact,¹⁰¹ there was no explanation for the increase in intensity and the red-shifting bands as well. Typically, a band shift would indicate a change in nanotube binding preference for the surfactant but again, this was not discussed. Fukushima *et al.* (2003) and Bellayer *et al.* (2005) used imidazolium as a dispersing agent for the creation of composites through melt mixing with polystyrene and low-temperature crosslinking of ionic liquids, respectively,^{127,128} they proposed a π -cationic interaction primarily between imidazolium and the nanotube with the polymer playing a minor role in dispersion. Generally, this interaction can be rationalized in terms of cationic species associating with an electron rich environment such as the π system of a benzene ring or carbon nanotube. Surfactant polymer-assisted dispersion of nanotubes has also been used in the industry. Ma *et al.* (2010) reports their use in the latex industry where nanotubes are firstly aqueously dispersed with surfactant and then mixed in with the polymer latex solution and repeatedly freeze-dried and melted. Because the process is essentially mixing of two solutions, the process is versatile, cheap, and reproducible.¹²⁹

Recently, the use of polymers and surfactants tandem system has recently gained attention in purification of nanotubes through gradient centrifugation as well. Indeed, Qiu *et al.* (2011) used the dualistic system of CTAB and PVP in the purification of nanoparticles¹³⁰ and last year Tsuchiya *et al.* (2013) explored an SDS-carboxymethylcellulose system for nanotube dispersion and purification of different nanotube chiralities which is likely based on a co-surfactant system developed by Weisman and collaborators for the same purpose.^{11,131} They proposed that when SDS is incorporated, it preferentially binds metallic nanotubes, and as it passes through the gradient layers, the absence of SDS caused a decrease in nanotube adsorption thereby accelerating their precipitation out of solution. In contrast, carboxymethylcellulose stabilizes the semi-conducting nanotubes throughout the gradient thereby allowing them to remain in solution and be separated.¹² This type of phenomenon seems to indicate that surfactants and polymers can in fact have preferential binding to a nanotube, however in addition to the ones described above, it can largely be seen that a clear mechanism on how a surfactant, polymer, and nanotube system is still absent. This is understandable as a multi-component system can be difficult to probe thoroughly. It was observed throughout so far that although nanotube dispersion can be easily assessed by spectroscopy, the behavior and role the surfactant and polymer are much harder to probe due to their less diverse chemical and physical properties.

2.5 Other Methods to Characterize Suspensions

Again, the analysis of a multi-component system can be rather difficult since the interactions among surfactant micelles, polymers, and/or nanotubes are difficult to predict, due to their diverse chemical and physical properties. However, in analyzing different suspensions there are a variety of techniques available such as surface tension, viscosity, electrophoretic mobility and dynamic light scattering. Each of these techniques can be extremely useful in elucidating the behavior of a surfactant, polymer, and nanotubes in suspension. Beyond this point, a brief overview of how each technique has contributed to the analysis of either surfactants, polymers, and/or nanotubes will be presented.

2.5.1 Surface Tension

A natural phenomenon of liquids, surface tension results from intermolecular interactions of the molecules within the solution. However, not all molecules in the liquid experience the same level of interaction. Inner molecules, which are defined as molecules surrounded from all sides by the same molecule (i.e. Water molecules surrounded by more water molecules) will have a lower energy because there is a cohesive force stabilizing from all sides. However, at the outer regions of the liquid, where the liquid contacts the air, some molecules are devoid of that cohesive force from some directions. This lack of exposure is unfavorable to the molecules because of high energy and so to reduce the energy as much as possible to reach a stable form, the overall surface area of the liquid is minimized.

To define the surface tension using physical principles, it is formally described as half the force per unit length of a thin film liquid required to keep that film of liquid from being displaced. The half originates from the fact that the force contributes equally from both sides of the film. However, the surface tension can also be described in relation to energy as a force required to keep a liquid moving at constant speed and with constant deformation of the surface area. Therefore, the relationship of force to length can be converted to a relationship of work over area as shown below:

$$\gamma = \frac{F \Delta x}{2L \Delta x} = \frac{W}{\Delta A} \quad (2.11)$$

where γ is the surface tension F is the force, L is the length, Δx is the change in length, W is the potential energy, and ΔA is the change in area. Given this relationship, common units for surface tension are N/m or dyn/cm.

As previously mentioned a surfactant in aqueous solution below its CMC exists at the air-liquid interface with its hydrophilic head pointing into solution and its hydrophobic tail pointing out of it. The presence of these molecules can therefore alter the interactions of the different water molecules. When the surface of the water becomes saturated with surfactant, micelles form in solution. This saturation effect is most easily seen in the size and shape of the droplets within the solution. Therefore by analyzing the changes in droplet size respect to changes in the concentration of a surfactant, the CMC can be determined. There are many methods to do this such as the capillary rise method, maximum bubble pressure method, Du Nuoy Ring method, and the pendant drop method, however the pendant drop method is one of the easiest to use.¹³² Under the assumption that the drop is about a central vertical axis and that only surface tension and gravity are the forces acting on it, it minimizes the amount of factors that could be in play such as the cleanliness of a surface which is found in many other techniques. Once drops are formed, the shape of it can be related to the surface tension using a Young-Laplace fitting.¹³³ This technique is widely used in the literature to characterize surfactant systems. Aguila-Hernández *et al.* (2001) used it to determine how alkanolamines affected the CMC of nonionic surfactants. Chang *et al.* (1998) used it to determine how the CMC of SDS changes in the presence of styrene, dodecylmethacrylate, and or sodium bicarbonate with regards to different emulsion systems for emulsion polymerization techniques. Lastly Nahrungbauer (1997) used it to determine the interaction between SDS and ethyl (hydroxyethyl) cellulose, a hydrophobic polymer at the air-liquid interface. Indeed, using the technique to measure the CMC has been well established however, surface tension can only reveal interactions at the air-liquid interface. Other techniques are needed to reveal interactions within solutions.

2.5.2 Viscosity

Viscosity is another inherent property of fluids that can better reveal the interactions of different species within solution. It can be thought of as the resistance to flow when a shearing force is applied or the restoring force to any deformation. Mathematically, it is formally the proportionality constant between the stress (σ) applied and the resulting strain (ϵ) of a liquid as seen below:

$$\sigma = \eta\epsilon \quad (2.12)$$

In defining the stress and strain, the basic model of a liquid in between two planar surfaces is used. Then, the terms are defined as:

$$\sigma = \frac{F}{A} \quad (2.13)$$

$$\epsilon = \frac{\delta V}{\delta H} \quad (2.14)$$

where F is the resisting force applied to a plate with area, A , and V is the deformation velocity of the plate at a height, H , where the height is from a point of little deformation. Collectively, $\frac{\delta V}{\delta H}$, is known as the local shear velocity. Thus, the units are Pa·s which is equivalent to 10 poise (P).

Viscosity is the result of the molecules within the solution interacting together. Typically, those that are large molecules or have strong intermolecular interactions with either each other or the solvent will lead to high viscosities because of greater resistance to external shearing forces. Depending on the molecule dissolved, there can also be a response to such forces such as alignment with respect to the shearing force. If there is such a dependence then the solution is said to be Non-Newtonian as opposed to the case of a Newtonian fluid where there is no such dependency. Non-Newtonian fluids can further be broken down into shear-thickening and shear-thinning, where an increase in shear rate will lead to solutions to thicken in the former and thin in the latter. An example of a Newtonian fluid, shear-thickening, and shear-thinning fluid include water, oobleck, and latex paint. Some liquids can behave as Newtonian at one shear rate and then as non-Newtonian in other. An example of this includes long-chain polymers which in addition to being extremely large can also be extremely flexible, therefore they can be coiled into an almost particle like form. When they are subjected to shear however, the force causes them to strengthen and align in the direction of shear.¹³⁴ At maximum alignment, the system reaches a Newtonian state. This was demonstrated for polyvinylpyrrolidone by Ahmad *et al.* (1991) measuring changes in viscosity with increasing shear in water and ethanol.¹³⁵

Worth mentioning as well is that there are also different classifications of viscosity. Up to this point, the use of the term viscosity is referring to dynamic viscosity which follows the definition as stated by equation (2.15). Other useful variants of viscosity include the specific viscosity (η_{sp}) which compares the absolute viscosity (η) and the solvent viscosity (η_0) and is defined as

$$\eta_{sp} = \frac{\eta - \eta_0}{\eta_0} \quad (2.15)$$

By dividing the specific viscosity by the concentration and taking the limit, we can get the intrinsic viscosity as below:

$$[\eta] = \lim_{c \rightarrow 0} \frac{\eta - \eta_0}{\eta_0 c} \quad (2.16)$$

The intrinsic viscosity has units of mL/g and describes the solutes contribution to viscosity i.e. an increase in the solution viscosity when the concentration is raised to a critical level. The intrinsic viscosity can be used mathematically to predict the overlap concentration using the formulas as stated previously in *section 2.4.2.3*.

For nanotube-polymer solutions, the use of viscosity to characterize suspensions has been fairly diverse. Grady (2006) and Cotiuga *et al.* (2006) specifically used it to assess the degree and type of sonication that would be optimal for nanotubes. They looked at the intrinsic viscosity profiles of nanotubes dispersed in polymethylacrylate(PMMA)-block polyethylene oxide (b-PEO) using a probe and bath sonicator and found trends in which the viscosity increased indicating exfoliation and then a decrease indicating destruction and damage of the tubes. This makes sense as smaller particles would generate a lower viscosity.^{124,136} Using epoxy as a dispersing agent for nanotubes, Fan *et al.* (2007) evaluated the changes in steady-shear viscosity as a means of detecting improvements to dispersion. They used different types of dispersion techniques seeking to test suspensions in which the aspect ratios were different. Overall, they found that a higher aspect ratio and a higher concentration made a substantial increase in their suspensions viscosity and overall storage modulus.¹³⁷ Another interesting observation was also made by Ben-David *et al.* (2009). They compared the profile of viscosities with increasing shear rates to characterize the effects of SWNT on CTAB and found that the presence of nanotubes induced Non-Newtonian behavior in CTAB. As the concentration of CTAB increased, the profiles of CTAB solutions with and without nanotube became more and more similar indicating the transition to wormlike micelles in solution. Strangely, this phenomenon was only seen for SWNT and not MWNT nor carbon black and the authors suggested it may be because wormlike micelles and SWNT have similar dimensions. Lastly, Camponeschi *et al.* (2006) used viscosity as a means of characterizing the effects of adding carboxymethylcellulose to their NaDDBS nanotube suspensions. Their goal was to align the nanotubes and they found that not only did carboxymethylcellulose aid in dispersion by introducing a large steric hindrance to the system but it provided a molecular template that promoted nanotube alignment under lower shear stresses.

2.5.3 Dynamic Light Scattering

Lastly, dynamic light scattering also known as quasi-light scattering is a technique used to observe the size distribution of particles in solution. Light at a particular wavelength is emitted through a sample where particles are undergoing Brownian motion. Because of this, there will be constant small frequency shifts of the scattered light compared to the frequency of the incident radiation due to constructive or destructive interference (Doppler Effect).¹³⁸ The magnitude and frequency of the

intensity fluctuations are at a maximum when light is scattered from a single point in suspension and then decreases with increasing solution complexity. The number of photons and the pattern at which they enter the detector are detected with a digital correlator. The time between each photon counting is known as the sample time (Δt) and the time in between two particular photon counts is the correlation time (τ). If τ is only a few multiples greater than Δt then the photon counts are said to be correlated. If they're several times greater then the photon counts are said to be not correlated. This link between data is given by an autocorrelation function:

$$G^{(2)}(\tau) = \lim_{T \rightarrow \infty} \frac{1}{T} \int_0^T i_\theta(t) i_\theta(t + \tau) dt \quad (2.17)$$

Where i is the intensity reading at a particular time point with angle, θ . This function can be further normalized to:

$$g^2(t) = \frac{G^{(2)}(\tau)}{G^{(2)}(0)} \quad (2.18)$$

This normalized function carries information relating to the rate of movement of the particle molecules which can be accessed through the Siegert relationship as shown below between $g^{(2)}(t)$ and $g^{(1)}(t)$, the normalized electric field autocorrelation function.

$$g^{(2)}(\tau) = A + B |g^{(1)}(\tau)|^2 \quad (2.19)$$

When the solute is a single species of unique molar mass,

$$|g^{(1)}(\tau)| = \exp(-\Gamma\tau) \quad (2.20)$$

whereas if the solution is polydispersed (ie. containing many species or the same species at different sizes) then the magnitude is equated to $\sum C_p - \Gamma_p C_p$

$$|g^{(1)}(\tau)| = \sum C_p e^{-\Gamma_p \tau} \quad (2.21)$$

where the terms C_p and $-\Gamma_p$ are the weighting factors and decay rate of species p in a polydispersed solution. Thus, it can be seen that the autocorrelation function can be approximated by an exponential fitting. Notice that if the solution is monodispersed then $C_p = 1$ and the fitting becomes equation (2.20) again. It should be noted however that if the solution is polydispersed then equation (2.21) can become difficult to solve due to transformations being ill-conditioned, measurement noise, baseline drifts, and dust.¹³⁹ Because of this, developing different algorithms is a large part of light scattering research, as described below. Nevertheless, once the fitting parameters are acquired, Γ can be equated to Dq^2 where q is the scattering vector and D is the diffusion coefficient which can be used

to calculate the hydrodynamic radius (R_h) of the particle using the Einstein-Stokes equation and the molecular weight of the polymer using the Mark-Houwink equation. These formulas are given below:

$$q = \frac{4\pi n_0 \sin(\theta/2)}{4} \quad (2.22)$$

$$D = \frac{kT}{6\pi n_0 R_h} \quad (2.23)$$

$$D = KM^a \quad (2.24)$$

where n_0 is the refractive index of the solvent, θ is the scattering angle, while K , a , and kT remain as defined before. In using DLS for non-spherical particles such as nanotubes, there are two major assumptions that need to be taken into consideration. One is that the Einstein-Stokes assumes that the measured species are spherical. For non-spherical particles, the rate of settling is not that predicted by Stokes law so the measured particle sizes are only approximations. Secondly, the Lorenz-Mie theory which predicts how spherical particles scatter light cannot be directly translated to non-spherical systems. However, DLS is still an option for comparative evaluations when dealing with non-spherical dispersed systems since the particle shape, and size, and relative density shouldn't change between samples.¹⁴⁰ Because, non-spherical particles are also known to undergo anisotropic translation, this leads to a coupling between translational and rotational modes of diffusion which manifests itself in additional characteristic decay rates as mentioned above.¹⁴¹ This is especially true for flexible rods like particles such as nanotubes. Many groups have tried to decouple this problem by generating new algorithms for scattering data analysis.¹⁴² Badaire *et al.* (2004) and Shetty *et al.* (2009) have created algorithms involving multi-angle analysis to decouple readings from the length and diameter of carbon nanotubes. Badaire *et al.* (2004) sought to determine the effects of sonication on nanotubes and found that higher powers and long times can reduce the length of SWNT from approximately 2000 nm to 800 nm and the diameter from 40nm to 10nm.⁸¹ Shetty *et al.* (2009) sought to compare the particle sizes of nanotubes (surrounded with polymer) measured by DLS to those measured by AFM. They found that when PEO was used as the polymer, DLS and AFM measured similar lengths and diameters which were around 500nm and 5nm respectively. However when poly(amino benzene sulfonic acid) (PABS) was used as the polymer the length as obtained from DLS was almost double of that detected by AFM and the radius was about 4 times smaller. These differences were attributed to high concentrations of polymer present in the measured AFM samples, causing aggregation and the requirement of dry films which may have also promoted aggregation

during sample preparation process. These aggregations would subsequently lead to bundling of nanotubes.¹⁴³

2.6 Summary

To disperse carbon nanotubes is a lofty goal. Doing so will enable researchers and engineers to further tap into the multitude of properties that make carbon nanotubes an extremely attractive material. These include unprecedented mechanical strength, and outstanding electrical and thermal properties. Nanotube aggregation is a considerable problem due to the hydrophobic forces inherent in any graphitic structure. Surfactants and polymers, alone or in combination have been used to create nanotube dispersions using different mechanisms and structural features to achieve this goal. By understanding how these mechanisms work we can develop more effective methods for nanotube dispersion. To reiterate the motivation of this project – CTAB, a surfactant, and PVP, a polymer had previously been shown to form a stable dispersed solution of carbon nanotubes. Thus the project is to determine the mechanism of this system for the purposes of expanding the possibilities of CNTs for composite formation.

Chapter 3: Materials and Methods

3.1 Materials

The surfactant, cetyltrimethylammonium bromide (CTAB), sodium deoxycholate and polyvinylpyrrolidone (PVP) at molecular weights of 10 000 g/mol, 40 000 g/mol, 360 000 g/mol, and 1 300 000 g/mol were ordered from Sigma-Aldrich Chemicals. PVP at molecular weights 3 500 g/mol, and 8 000 g/mol were ordered from Acros Organics through Fisher Scientific. From this point onward, the different molecular weights of PVP will be denoted as PVP3.5, PVP8, PVP10, PVP40, PVP360, and PVP1300 where the digits correspond to the molecular weight in thousands. Single-walled carbon nanotubes (SWNT) at a purity of >90% (SKU#0101) and C70 fullerenes were ordered from CheapTubes Inc. These materials were used without further purification. GPC chromatography was used to confirm and evaluate the molecular weight distribution of the polymer.

3.2 Methods

3.2.1 Solution Preparation

CTAB at 0.1% wt/v and a specific molecular weight of PVP at concentrations of 0, 0.25, 0.75, 1.1, 4, 6, 9 %wt/v were dissolved together in pure water on a warm hot plate. From the resulting solution, 25mL was poured into a 40mL glass vial containing 5mg of either nanotubes or fullerenes to bring the carbonaceous compound to a concentration of 0.2 mg/mL. The solution was then mixed via sonication for 2 hours in an ice bath using a Fisher Scientific Model 500 Ultrasonic Dismembrator which had a step-horn and a half-inch nut attached. The horn frequency used was about 19.850 – 20.050 kHz. Other settings on the device include 180 W (i.e. 45% amplitude of a maximum of 400W) and a sonication interval of 0.3 seconds ON and 0.7 seconds OFF. The solution was then centrifuged at 50 000 RPM for 1 hour using a Thermo T-1270 Fixed Angle Titanium Rotor placed in a Sorvall WX series ultracentrifuge to separate dispersed and undispersed nanotubes. Lastly, the top half of the resulting supernatant was filtered through 2 pieces of Whatman Grade 1 Qualitative Filter Paper to remove any large undispersed solids.

3.2.2 Gel Permeation Chromatography (GPC)

To ensure the quality of the PVP from suppliers, samples were sent to PolyAnalytik in London, Ontario, Canada. Their procedure involved analyzed using 3 methacrylate-based gel columns PAA-206M, PAA-203, PAA-202 in a mobile phase of 0.1M NaNO₃ on a Viscotek Tetra Detector Array at a flow rate of 0.5mL/min and a temperature of 30 °C. The Tetra Detector Array included a Refractive Index detector (660nm LED), UV detector (variable wavelength, Deuterium lamp), Light Scattering detector (670nm laser, 7° and 90° degrees) and Viscometer detector (four-capillary bridge). The samples were dissolved in pure water and left on a rocker overnight shaking gently. The samples were filtered either through a 0.2µm (PVP samples) or a 0.45µm (nanotube) Nylon filter before injection with no resistance observed. The injection volume used was 100µL-150µL. For polymer samples, a combination of the Refractive Index and Light Scattering detector were used to determine the molecular mass while the Viscometer detector was used to determine the hydrodynamic radius. For samples containing SWNT, the a combination of the Refractive Index and UV detectors were used.

3.2.3 Spectroscopic Characterization

Absorbance spectra of the samples were obtained using a Shimadzu UV-3600 from wavelengths of 400nm to 1400nm with a slit width of 8.0 and a medium scan speed. The contents of the blanks of all nanotube dispersions were of the same material and concentrations of the samples themselves except without the nanotubes present in solution. The dispersion area was then analyzed using Origin 8.5s Peak Analyzer tool whereas the total area under the curve was analyzed with the Integration function available in the same program.

3.2.4 Atomic Force Microscopy

To obtain images of nanotube distributions for length and radius, 20 µL of sample was pipetted onto a cm² of silicon wafer and spread into a thin film using a disposable cell spreader. The wafer was then heated at approximately 185 °C for 4 hours followed by a wash with 1.5mL of pure water and dried again at the same temperature for 10 minutes. They were then brought to the atomic force microscope (AFM, Dimension 3100, Veeco Inc) for imaging. All images were captured under tapping mode with a silicon nitride cantilever from Nanoscience which has a nominal spring constant of 40 N/m and a tip radius of around 10 nm. Distributions from the images were then processed using the Gwyddion software.

3.2.5 Dynamic Light Scattering (DLS)

This technique was used to determine and verify the size distribution of the particles within the solutions. All samples were prepared at a polymer concentration of 1.1 %wt/v or less through simple mixing and diluting. This was done to avoid any significant viscosity changes which would effect results automatically calculated by the instrument software. The samples were then filtered using 2 pieces of Whatman Grade 1 Qualitative Filter Paper to remove large dust particles. Samples were then transferred into a cuvette and placed inside Brookhaven's ZetaPlus Zeta Potential Analyzer. Using the BIC Particle Sizing program (which runs Brookhaven's MAS OPTION software), 10 runs of each sample were analyzed at a temperature of 25 °C, angle of 90 °, and a wavelength of 659 nm. Note that the viscosity and refractive index were automatically set by choosing water as the solvent (viscosity of 0.89cP, refractive index of 1.330,). The run time of each experiment varied between samples and was set to the amount necessary to obtain a suitable exponential decay autocorrelation curve. The software then outputs the data in the standard "lognormal" format which essentially gives a distribution of the different sizes by solving the autocorrelation curve with the method of CUMULANTS. A deeper breakdown of the distribution can also be obtained with the Multi-modal Size Distribution (MSD) analysis tool which uses the non-negative least square (NNLS) algorithm to resolve multimodal particle distributions.

3.2.6 Surface Tension Characterization

Surface tension was characterized using a First Ten Angstroms 1000B Class contact angle and surface tension instrument. The corresponding software, FTA32, can be used to capture images and automatically uses the Young-Laplace equation relating interfacial tension to drop shape produced at the end of a needle. Before each sample was analyzed, 0.5mL of it was sacrificed for rinsing of the needle to minimize contamination. Afterwards, sufficient amounts of the sample was aspirated and the needle which had a blunt ended bevel was then loaded onto the machine apparatus. Important settings include setting the needle type and the interfacial density to that of the sample solvent and the environment around it. In this case, water and air, respectively. With each sample, several pictures were taken to avoid error that may occur from asymmetrical droplet formation which can cause minute errors in the determination of surface tension. After each sample, the needle was rinsed with pure water and compressed air was gently flowed through it to ensure no dilution when rinsing with the next sample. To obtain values such as the CMC, two lines were firstly drawn at regions of linearity: one with decreasing points of surface tension indicating the saturating droplet surface and the other

with points after the surface droplet had saturated with the surfactant. The intersection of these two lines was determined to be the CMC. The 95% confidence interval (CI) of the CMC values were calculated using a method described by Filliben *et al.* (1972).¹⁴⁴

3.2.7 pH Measurements

The pH of different samples were determined using a non-glass ISFET probe attached to a Hach H160 pH meter which was calibrated using buffers from BDH. The point of zero charge in particular was determined by initially preparing a series of 10mL solutions, each of which were adjusted to varying pHs between 1-10 by using either 0.1M sodium hydroxide or 0.1M hydrochloric acid. Then, about 1.5mg of the SWNT were placed into each solution and allowed to equilibrate. Each solutions final pH was then plotted with respect to its initial pH and the point of zero charge was then determined by finding where the trendline crosses the function $y = x$.

3.2.8 Viscosity Characterization

To obtain viscosity values, 1.5mL of the samples were placed onto the stage of an AR 1500EX rheometer. A 40mm 4° steel cone was lowered to a gap height of 162 μm and the sample was subjected to steady state flow tests with a shear rate ramp from 0.02864 s^{-1} to 2000 s^{-1} with a logarithmic step. The stage of the apparatus was also maintained at a temperature of 25 °C. As a control for studying the effects of viscosity on dispersion, several dispersion samples using glycerol were also prepared and characterized.

Chapter 4: Results

Nanotubes hold immense potential as a material that can lead to the development of new technology, however many of these potential products require nanotubes, which aggregate during synthesis, to be adequately dispersed and stabilized in solution otherwise their mechanical, electrical, and thermal properties remain locked in the bundle form. As previously discussed, one approach to stabilizing nanotubes in solution involves non-covalent modifications of the nanotube surface by mixing via ultrasonication in the presence of a stabilizing agent such as a polymer or surfactant. As the nanotubes are separating, these stabilizing agents would coat the surface of the nanotube making them less likely to bind with each other by providing an electrostatic or steric repulsing force to counteract the intrinsic van der Waals forces driving nanotube aggregation thereby lowering the surface energy of the nanotube as well. Although there has been a heavy amount of past research exploring the potential dispersing ability of different surfactant and polymers, using both in combination has been a fairly new approach. Davis *et al.* (2012) had previously used the surfactant, CTAB, and the polymer, PVP in the design of a chitosan-based composite, seeing a 20 times increase in the mechanical strength with the incorporation of nanotubes. To gain a better understanding of how these two types of molecules interact with each other and in the presence of nanotubes, a battery of techniques such as Vis-NIR absorption, atomic force microscopy (AFM), dynamic light scattering (DLS), surface tension, pH, and viscosity were used to assess the chemical and physical phenomena of the system. Here, the results of such experiments are presented, discussed and used to propose a model for the CTAB-PVP dispersion system.

4.1 Characterization of Nanotube Dispersions

4.1.1 Vis-NIR of Nanotube Suspensions

Vis-NIR spectroscopy was used to characterize nanotube dispersion. This technique was chosen to take advantage of the unique band structure of nanotubes. Nanotubes of different chirality require different levels of energy in order for electrons to be promoted from the conduction to the valence band. Assuming a suspension of nanotubes with a single chirality value, the theoretical spectra produced should show a single absorbance peak. In a sample with nanotubes of multiple chiralities, the peaks overlap and create a convoluted signal with multiple peaks. The resolution of the peaks nevertheless, is strongly dependent on how well dispersed the nanotubes are in solution. Nanotubes that are aggregated in bundles generally give poorly resolved spectra because of light scattering by

the nanotube bundles. Therefore, a well dispersed sample would be reflected by a spectra that gives sharp resolved peaks in the Vis-NIR region.

Prior research by Blanch *et al.* (2010), Haggemueller *et al.* (2008) and Tan *et al.* (2005) have used Vis-NIR absorbance spectroscopy to show that the surfactant cetyltrimonium bromide (CTAB) was moderately able to disperse nanotubes in aqueous solution.^{72,74,75} To validate our methodology, 5 mg of SWNT were placed in 25 mL of 0.1 %wt/v solution of CTAB, ultrasonicated to mix, and ultracentrifuged to remove impurities to ultimately achieve the dispersed sample. As a comparison, a suspension using an aqueous solution of 2 %wt/v sodium deoxycholate was also prepared the same way. Sodium deoxycholate was previously shown to be a much more effective dispersing agent compared to CTAB.⁷² Figure 4.1 provides the obtained spectral profile for the two samples.

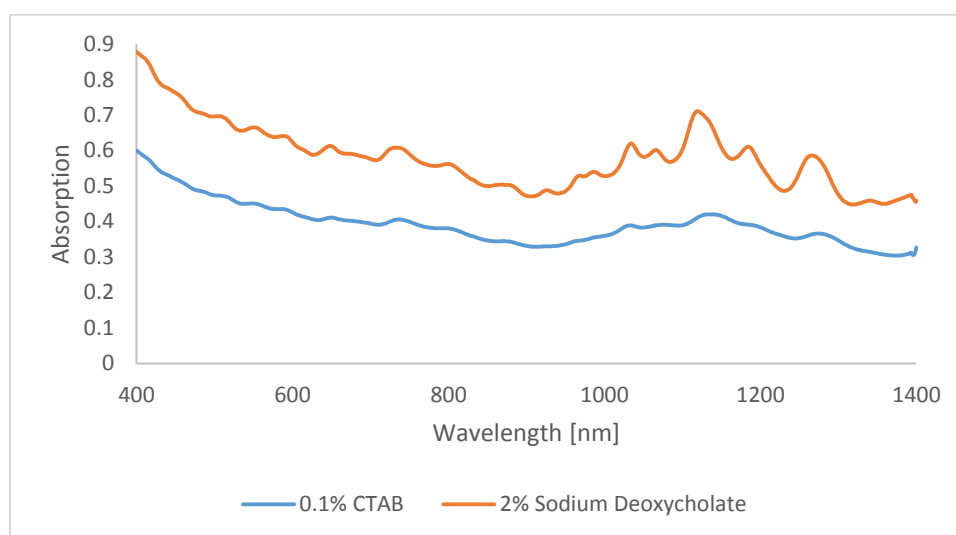


Figure 4.1: Absorption spectra of CTAB dispersed nanotubes

The presence of peaks in the spectra for CTAB as seen in Figure 4.1 is indicative of nanotubes being dispersed. In fact, the presence of multiple peaks indicates that there are multiple nanotube chiralities present within the solution. Many of these peaks could be convoluted though as stated previously, however using the theoretically predicted wavelengths required for electronic transitions by Bachilo *et al.* (2002) and Weisman *et al.* (2003) their identities can still be predicted. Among those most prominent are the [9,2], [8,7], and [7,5] species. Table 4.1 shows their measured wavelength against the values predicted in the aforementioned publications.

Species [m, n]	λ_{11} Measured	λ_{22} Measured	λ_{11} Predicted	λ_{22} Predicted
[9, 2]	1138	550	1138	551
[8, 7]	1275	735	1265	728
[7, 5]	1031	645	1024	645

Table 4.1: Nanotube species observable through peaks of CTAB-assisted dispersion of nanotubes. The measured and predicted van Hove wavelengths from research by Bachilo *et al.* (2002) and Weisman *et al.* (2003) are included.^{70,71}

To quantify the degree of nanotube dispersion using the optical absorption spectra, different methods have been proposed. Tan *et al.* (2005) obtained the resonance ratio by dividing the area of the absorbing peaks by the non-resonant background (Figure 2.6). Using this method, a total resonant area of approximately 26.8 was found for CTAB. This value corresponds to a resonance ratio of approximately 0.071 after dividing by the non-resonant background. Comparatively, this value is within range of values observed for different dispersants by Tan *et al.* (2005) however it is notably lower than their reported value of 0.119 for CTAB. The authors had also ran sodium cholate (SC) which differs from sodium deoxycholate by the absence of one hydroxyl group on the gonane template. Although not the same molecule, their dispersive ability should be similar given their similar structure. Then, for sodium cholate, they achieved a resonance ratio of 0.147 whereas we achieved a total resonant area of about 52.66 and a resonance ratio of about 0.094 for its derivative. Blanch *et al.* (2010) and Haggemueller *et al.* (2008) have both also confirmed similar results via Vis-NIR although neither used the resonance ratio. Blanch *et al.* (2010) relied solely on observing the sharpness of peaks however Haggemueller *et al.* (2008) determined the ratio of the nanotube absorbance to the background absorbance at the wavelength of 910 nm. For the obtained results, the wavelength of 1130 nm was used instead because there did not appear to be any nanotube chiralities present that could absorb at 910 nm given the obtained spectra. For sodium deoxycholate they obtained a value of 2.5 at a wavelength of 910 nm whereas a ratio of 1.73 for was achieved using 1130 nm for deoxycholate. CTAB gave a value of 1.32. Unfortunately, Haggemueller *et al.* (2008) did not test CTAB, but its value is most comparable to 1.50 which they obtained for imidazonium based cationic surfactants. While somewhat different, this comparison shows a trend in the dispersive ability of the tested surfactant molecules. Comparatively again, CTAB has dispersive abilities but is generally poor. The origins of the observed smaller values can be traced to purity of the initial nanotube sample (>90% in our case) as well as differences in synthesis method. Multiple sources such as Henrich *et al.* (2005) and Blanch *et al.* (2010) report clear differences in their nanotube dispersion spectra when nanotubes of different synthesis methods and catalysts were used.^{104,145}

We tested different molecular weights of polyvinylpyrrolidone (PVP) as well. To the best of our knowledge, there hasn't been a robust investigation on the effects of the molecular weights of a polymer on its nanotube dispersion ability. Prior research by Blanch *et al.* (2010) had shown that a 1 %wt/wt solution of PVP10 (where the 10 denotes the molecular weight in kg/mol) was relatively

poor at dispersing nanotubes compared to CTAB. To ensure this observation was not simply because the concentration was too low, an arbitrary concentration of 6 %wt/v for each molecular weight of PVP available was tested. The dispersions were then prepared in the same manner as described above in which 5 mg of SWNT were ultrasonicated in a 25mL aqueous solution of PVP at 6 %wt/v followed by ultracentrifugation. A collection of the resulting spectra is shown below in Figure 4.2.

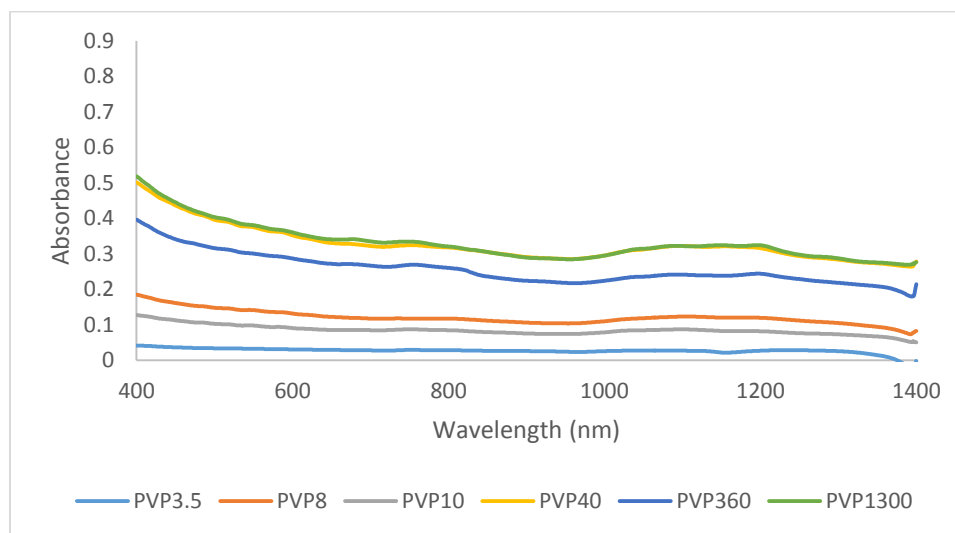


Figure 4.2: Absorption spectra of 6% PVP-dispersed nanotubes

In contrast to CTAB, the dispersion of nanotubes obtained using pure PVP was of poor quality. This is likely because PVP is a hydrophilic macromolecule and would not readily bind and stabilize hydrophobic SWNTs. There appears to be selected regions such as between 1000 nm - 1200nm where a slight increase in absorbance relative to the background could indicate nanotube dispersion though generally PVP appears ineffective overall. Manivannan *et al.* (2009) and Blanch *et al.* (2010) observed similar spectra and because of its poor quality, the authors did not quantitatively assess it. Haggemueller *et al.* (2008), however did test other hydrophilic polymers, namely carboxymethylcellulose and chitosan at two different molecular weights. Using the Haggemueller ratio method once again, the ratios of PVP are reported below:

Expected Polymer Molecular Weight (g/mol)	Peak Absorbance at 1130nm	Background Absorbance at 1130nm	Ratio
3500	N/A	N/A	N/A
8000	0.085	0.068	1.250
10 000	0.084	0.070	1.200
40 000	0.322	0.277	1.162
360 000	0.240	0.213	1.127
1 300 000	0.324	0.280	1.157

Table 4.2: Ratio of Absorbances for 6% PVP dispersion systems for 0.2 g/L SWNT calculated as described by Haggemueller *et al.* (2008)

Comparatively, Haggemueller *et al.* (2008) reported approximate values of 2.10, 2.05, 1.83, and 2.00 for carboxymethylcellulose at 90 000 g/mol, 250 000 g/mol, and chitosan at 20 000 g/mol and 200 000 g/mol, respectively. Overall, these values reveal that both polymers are better than PVP at dispersing nanotubes. This is likely due to their ionic character which aids in dispersion through electrostatic repulsion. In addition, there may be an influence from size. For example, with carboxymethylcellulose, the size of the polymer made no statistical difference in terms of effecting dispersion whereas for chitosan it did. These subtle differences are also noticeable within the collected results in Table 4.2 as it appears that smaller molecular weight polymers do lead to better dispersions. Overall though, it appears that PVP at every molecular weight is a poorer dispersing agent than CTAB.

For the next set of experiments it was decided that CTAB and PVP be mixed to observe the effects on dispersion. Recently, many research groups have looked into dispersion strategies using two different molecules especially for the purposes of nanotube chirality purification via ultracentrifugation.^{11,131} In 2011, Qiu *et al.* specifically used the CTAB-PVP system to purify iron nanoparticles via ultracentrifugation. Specifically, CTAB was used to coat the nanoparticles which were then passed through different viscosity layers generated by the presence of PVP at different concentrations. Authors found no significant changes in the nanoparticles after purification.¹³⁰ Recently Davis *et al.* (2012) also used both CTAB and PVP in conjunction to disperse nanotubes before incorporation into a chitosan matrix. The incorporation lead to substantial increases in mechanical strength of the SWNT-chitosan composite meaning SWNT were well dispersed. However within these tests, there again appeared to be no optimization for the molecular weight of PVP to use. Based on the observation presented in Table 4.2 above in which a lower molecular weight polymers can better disperse nanotubes and previous studies suggesting that for the case of nanomaterials dispersion the choice of molecular weight plays a critical role on the quality of the suspension obtained,¹⁴⁶ there is incentive to try and use different molecular weights of PVP to augment the dispersion of nanotubes even further. Thus, these samples were prepared as described above where 0.2 g/L of SWNT was ultrasonicated, however now the solution mixture contained both 0.1% wt/v CTAB and 6 %wt/v PVP at different molecular weights. It should be noted that upon performing these experiments, the non-resonant background did not appear stable as it shifted in terms of the overall absorption intensity. Despite this, the peaks which represent dispersion kept a more constant shape (Figure S 2, Appendix 1) therefore the use of the resonant area was selected beyond this point. Figure 4.3A shows the

obtained spectra of two molecular weights tested at 6 %wt/v, PVP10 and PVP40 where a distinct increase in peak resolution can be seen. Figure 4.3B compares and contrasts the quantified resonant area of all 3 of the previously described systems and contrast them with each other using the resonant area values obtained from the optical absorption spectra.

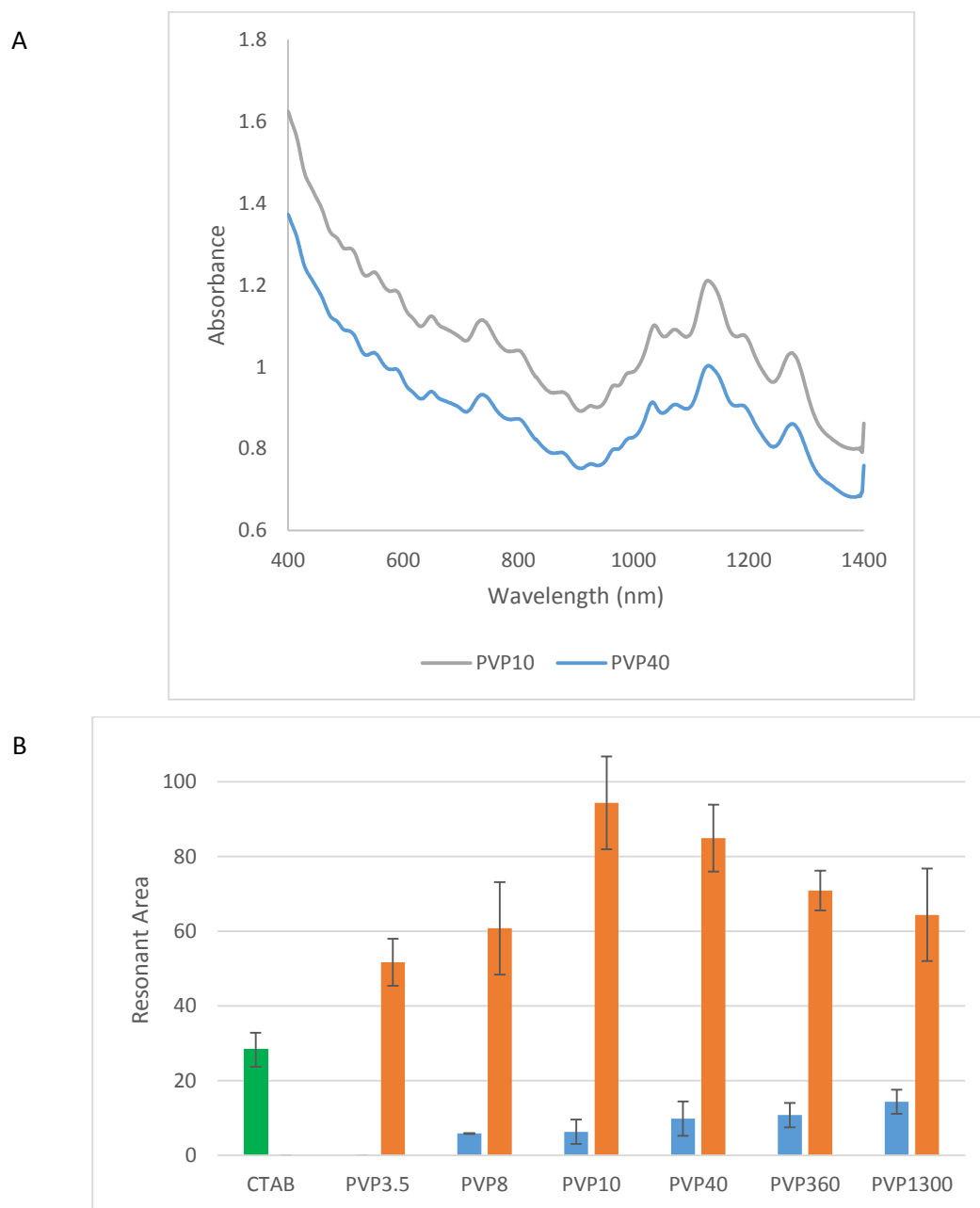


Figure 4.3: A) The obtained spectra of 0.1 %wt/v CTAB, 0.2 g/L SWNT, and 6 %wt/v PVP at different molecular weights. B) Resonant area comparison between 0.1 %wt/v CTAB (green), 6 %wt/v PVP (blue), and 0.1% CTAB with 6% PVP (orange) as obtained in (A) at dispersing 0.2 g/L SWNT.

In addition to the remarked observation that 0.1 %wt/v of CTAB is better at dispersing nanotubes than all samples containing pure PVP at 6 %wt/v, there are several observations worth noting on Figure 4.3. Firstly, in Figure 4.3A, it's observable that PVP10 appears to show the most prominent resonant

area. This is perhaps most observable in Figure 4.3B where quantifying the spectra reveals the dramatic increase in resonant area in all cases when both the surfactant and the polymer are present. For PVP10, there is almost a 3-fold increase compared to 0.1 %wt/v CTAB alone and almost a 9-fold increase compared to 6 %wt/v PVP10 alone. From this dramatic increase, the effect appears synergistic and not additive. Increasing or decreasing the molecular weight seemed to give poorer dispersions relative to PVP10 however the synergy remains present. To gain a better understanding on how the addition of polymer affects the resonant area, several different concentrations of PVP were tested. SWNT dispersions were thus prepared at the additional concentrations of 0.25 %wt/v, 0.75% wt/v, 1.1% wt/v, 4% wt/v, and 9% wt/v with each molecular weight. Figure 4.4 below shows the results.

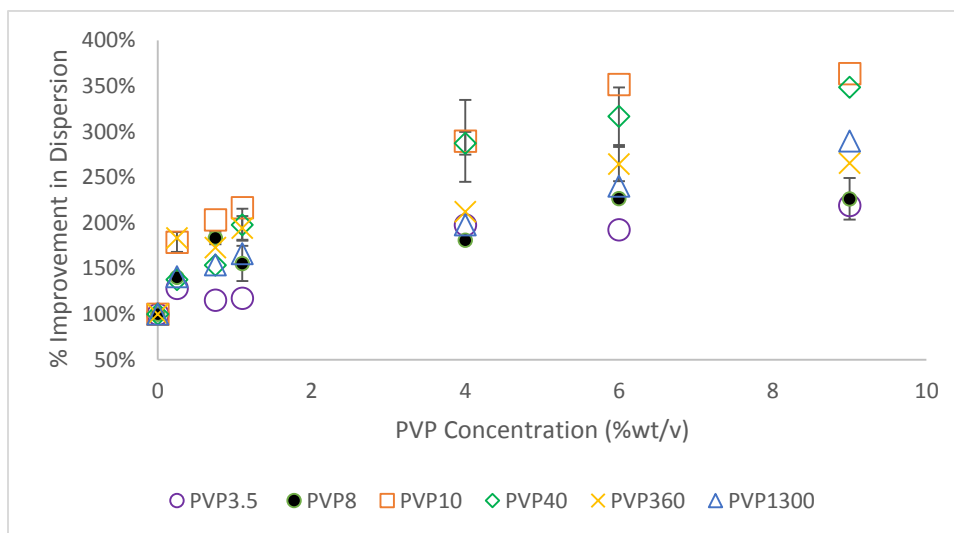


Figure 4.4: Resonant Area of PVP-CTAB-SWNT dispersions at a fixed CTAB concentration of 0.1 % wt/v and 0.2 g/L SWNT.

As indicated, the result shows an increase in dispersion with increasing polymer concentration for all molecular weights. It can also be observed that each trend appears to plateau at a concentration of 9% wt/v. Comparing each molecular weight of PVP used, PVP10 remains one of the better sizes to disperse nanotubes in terms of concentration. PVP40 was observed to have potential as well while other molecular weight polymers such as the smaller, PVP3.5 and PVP8, and the larger, PVP360 and PVP1300 show relatively poor nanotube dispersions.

The absorbance intensities of the Vis-NIR results can also be used to determine the final concentration of nanotubes in each dispersion tested. Beer-Lamberts Law which relates absorbance to the product of path length, concentration, and the extinction coefficient of the molecule is a common formula used to determine concentration from absorbance. Previously, for the purposes of gel permeation

chromatography (GPC), a separation and quantification technique, Bauer *et al.* (2008) determined the extinction coefficient for nanotubes to be 26 000 cm²/g at a wavelength of 690 nm by using samples of known nanotube concentration. Using this extinction coefficient, a path length of 1 cm, and the absorbance values at 690 nm for each spectra, the final concentrations of nanotubes in each sample were obtained and are shown below in Figure 4.5.

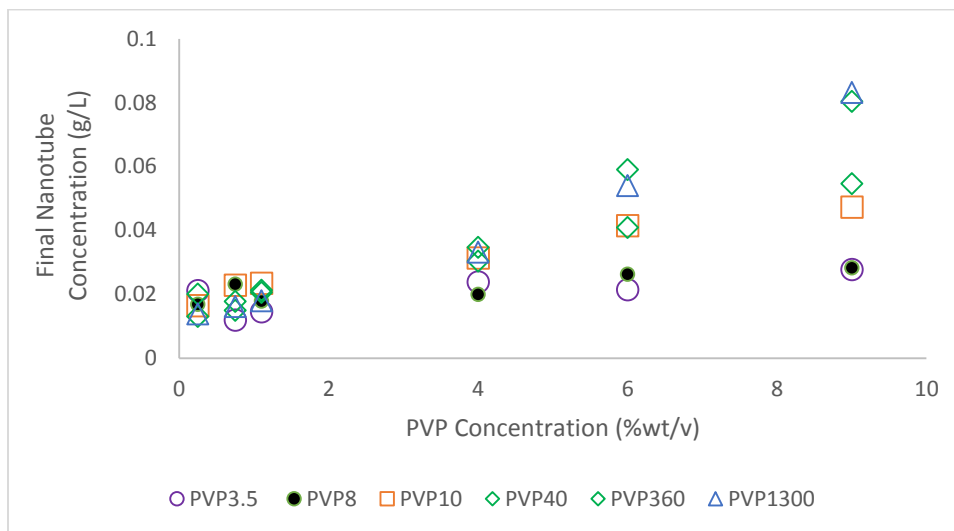


Figure 4.5: Final concentration of dispersed nanotube solution (g/L) with respect to the PVP concentration

From this, it appears that a higher molecular weight of the polymer leads to a higher overall retention of nanotubes (dispersed and aggregated) in the system. Indeed, with the smaller polymer, only 0.02 g/L or 10 % of SWNTs are retained whereas with larger polymers, 0.08 g/L or 40% of SWNTs are retained. This effect is likely related to the terminal velocity, the velocity at which a particle moves through a solution and is given as below when a solution is being centrifuged.

$$v_t = \frac{mr\omega^2}{6\pi\eta r_0} \quad (4.1)$$

where m is the mass of the particle, r is the distance of a particle to the axis of rotation, ω^2 is the angular velocity, η is the viscosity of the medium, and r_0 is the radius of the particle. Increases in viscosity with the addition of polymer is a well-known phenomenon and has been shown to change in our working concentration range (Figure S 5, Appendix 1) as well. Thus, a higher viscosity would lead to a lower terminal velocity meaning that at a set centrifugation speed and time, particles would take longer to sediment. This result was reaffirmed by using C70 fullerenes, another carbonaceous nanoparticle much smaller than SWNT at: 0.2 g of fullerenes/L dispersed with 0.1 %wt/v CTAB and 6% wt/v PVP. Results (Figure S 3, Appendix 1) indicate that a higher molecular weight of PVP led to higher concentration of fullerenes in suspension after centrifugation as indicated by differences in

absorption intensity. It is worth noting that Qi *et al.* (2007) were able to retain a maximum of 0.075 g/L SWNT from an initial concentration of 0.1 g/L which translates into a 75% retention however, their procedure did not involve centrifugation. Additionally, their zeta potential results indicated that at least 75% of their retained nanotubes were saturated with surfactant when a CTAB concentration of 1 mM was used.¹⁴⁷ Given the lower concentration of nanotubes retained in our case and the amount of CTAB used (0.1 %wt/v is approximately 3 mM), it is very likely that all the nanotubes in our samples are saturated with surfactant as well.

4.1.2 Atomic Force Microscopy

Many researchers have previously reported that nanotubes can be fragmented during ultrasonication resulting in nanotubes with smaller lengths.^{74,79} To assess whether this was a phenomenon occurring within our system, AFM was used to acquire the length and diameter distributions of nanotubes in our dispersed samples. Unlike traditional forms of microscopy which visualize a sample based on how it interacts with particles from a particular source (light, electrons, etc), AFM uses a cantilever probe with a fine tip to scan the surface of prepared samples. In this case, the sample for AFM was prepared by aliquoting a solution containing 0.1 %wt/v CTAB and 0.2 g/L SWNT onto a polished silicon wafer. The wafer which serves as a smooth non-interfering surface for analysis was then dried at 180 °C and washed profusely with pure water to remove surfactant molecules. It was then dried again and analyzed immediately on the AFM. This sample was chosen in particular instead of samples containing polymers to avoid misinterpretation of polymers for nanotubes and vice versa. Figure 4.6 shows a sample image that was acquired.

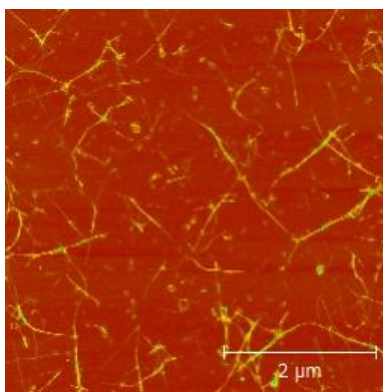


Figure 4.6: Sample AFM image of CTAB-suspended SWNT dried over a silicon wafer

From the image, there does appear to be nanotube strands of varying degrees of diameter and length. Using several images, the diameter and length of the observable strands were subsequently measured using the computer program, Gwyddion and presented below in Figure 4.7 in the form of histograms.

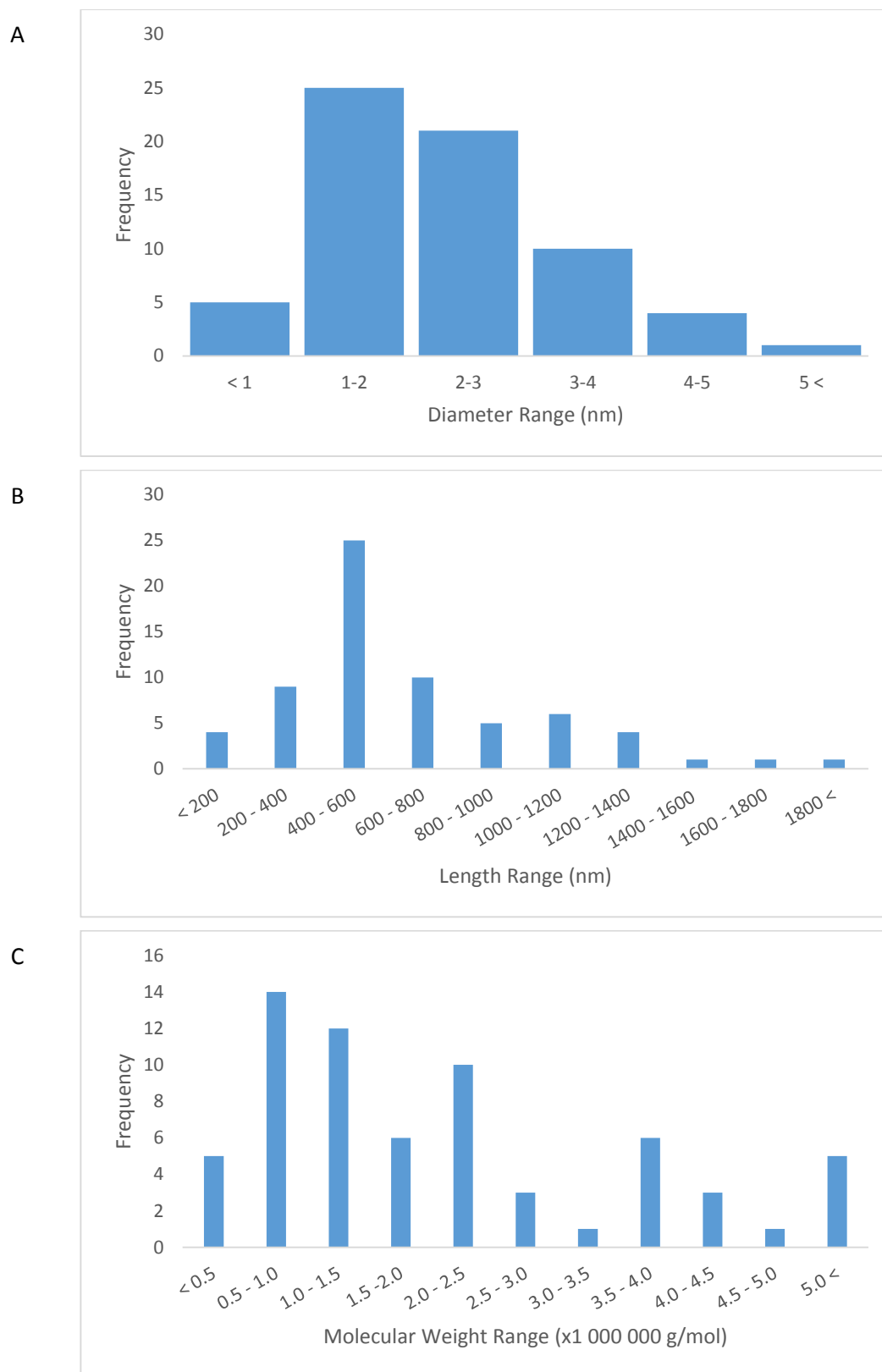


Figure 4.7: Distributions of A) diameter B) length and C) Molecular Weight as gathered from AFM images.

These distributions show that most prevalent nanotube characteristics include a diameter of about 1 nm - 2 nm and a length of about 400 nm - 600 nm. Using these dimensions, a molecular weight distribution of about 500 000 – 1 000 000 g/mol was also calculated stoichiometrically by using a density of 1.33 g/cm³, as specified by Hadjiev *et al* (2001)¹⁴⁸, and assuming the nanotube as a rigid cylinder. The acquired outer diameter and length were in range of those reported in previous research in which sonication was part of the dispersion methodology (Table 4.3).^{101,121,149,150}

Sonication Type	Power (W)	Power/Area (W/inch ²)	Time (h)	Length (nm)	Diameter (nm)	Reference
<i>1" Tip</i>	<i>180</i>	<i>229.30</i>	<i>2</i>	<i>400-600</i>	<i>1-2</i>	<i>Own results</i>
0.125" Tip	3	244.59	1.5	100-200	1-2	Zheng <i>et al.</i> (2003) ¹²¹
0.125" Tip	6	489.17	1	141-393	1-5	Islam <i>et al.</i> (2003) ¹⁴⁹
0.157" Tip	13	671.51	1	200-500	N/A	Su <i>et al.</i> (2007) ¹⁵¹
0.0785" Tip	N/A	N/A	0.0167	100-400	N/A	Yehia <i>et al.</i> (2007) ¹⁵²
Tip (Size N/A)	40	N/A	0.0333	500	N/A	Elgrabli <i>et al.</i> (2007) ¹⁵³
Tip (Size N/A)	N/A	N/A	0.0167	2000	2.5-3	Hecht <i>et al.</i> (2006) ¹⁵⁴
Tip (Size N/A)	N/A	N/A	15	500-1000	2-3	Paredes <i>et al.</i> (2004) ¹⁵⁵
Tip (Size N/A)	N/A	40	N/A	400-700	1.3	Islam <i>et al.</i> (2003) ¹⁴⁹
Bath	12	N/A	1	230-802	1-2	

Table 4.3: Reported lengths and radii from various research groups after sonication. The italicized results are the results obtained in our experiments

As seen, given the conditions used it's reasonable that the nanotubes are being fragmented especially considering that they are sold at a length of 5 – 30 μm . It's noticeable as well that there doesn't seem to be much correlation between the power applied, time, nor the resulting length as it seems the mere application of ultrasonication is enough to fragment nanotubes into various sizes. This is especially true given that bath sonication can fragment nanotubes as well. Curiously, Islam *et al.* (2003) observed bath sonication give a wider distribution of lengths but a fairly narrow diameter distribution while tip sonication gave a wide distribution of diameters but a narrow distribution of length. Although a reason was not stated, this is likely due to how the ultrasonics are applied to the sample.

The discrepancy seen in the different reported ranges of nanotubes could be a result of aggregation during sample preparation. Because of the drying and washing steps, there's a large chance that fragments could clump together thus leading to overestimation of sizes in the produced images.¹⁴³ Nevertheless, it was also observed that the molecular weight of nanotubes obtained using GPC, 646 103 g/mol, (Table S 2, Appendix 1) falls within the expected range calculated using AFM data thereby reconfirming the results.

The fact that nanotubes become fragmented during ultrasonication has several implications. Most likely, it affects sample preparation in terms of ultracentrifugation. Seen in equation (4.1), smaller nanotubes equates to a lower mass in determining the terminal velocity for separation during ultracentrifugation, therefore fragmented nanotubes would remain in solution more readily than their uncut forms leading to an overall increase in retention. Also, having a reduced length may also help in dispersion as the shorter the nanotube, the less flexibility it has to coil with either itself or adjacent nanotubes for the formation of aggregates. This is especially true considering the persistent length of a nanotube is typically on the order of several microns, 32 – 174 μm as reported by Duggal *et al.* (2006).¹⁵⁶ Given that the persistent length is a measurement of stiffness and the obtained lengths are almost a hundred times smaller, this means that the nanotubes in solution would be extremely rigid.

4.1.3 Dynamic Light Scattering (DLS)

As a means of validating the size characterization by AFM and to observe any potential changes to surfactant or polymer morphology in aqueous solution, the different chemical components of a dispersed system were analyzed using DLS. DLS as its name implies is a light scattering-based technique which uses fluctuations in the light scattered by particles over time and under the effects of Brownian motion to determine suspended particle size distributions. Brownian motion is the movement of particles from random collisions imparted by surrounding molecules. Scattering intensity and time are related through an autocorrelation function which can subsequently be solved by using different mathematical transformations. Two that are readily available are the CUMULANT and non-negative least squares (NNLS) method. The CUMULANT algorithm estimates the autocorrelation curve by expanding it as a sum of exponentials as defined previously in equation (2.21) whereas the NNLS uses the least-square fitting with the constraint that the weighting factor, C_p , in

equation (2.21) is positive. The method of CUMULANTS typically projects size distributions as a quadratic curve due to a lack of information beyond the third expansion term.

Having validated the molecular weight of the different PVP using GPC as mentioned above, the distributions between these two techniques were compared. Aqueous PVP samples of different molecular weights were ran at a concentration of 1.1 %wt/v because it was determined previously through trial and error that the polymers were sufficiently concentrated to generate a satisfactory autocorrelation curve. Table 4.4 below summarizes the results for a lognormal analysis which uses the CUMULANT method.

Expected Polymer Molecular Weight (g/mol)	Obtained Molecular Weight (g/mol)	Hydrodynamic Radius (nm) (lognormal)
3500	4870 ± 325	1.8 ± 0.1
8000	10 900 ± 835	2.5 ± 0.1
10 000	53 567 ± 10 086	3.3 ± 0.5
40 000	256 333 ± 14 978	6.6 ± 0.4
360 000	1 173 333 ± 104 083	12.6 ± 0.9
1 300 000	1 360 000 ± 113 137	13.5 ± 0.9

Table 4.4: Summary table of DLS results for the analysis of the different molecular weights of PVP

The outputted hydrodynamic radius and molecular weights obtained from the lognormal distributions of DLS follow an increasing trend. However they appear larger compared to the listed supplier values and are certainly larger than values obtained from GPC as reported in Table S 1, Appendix 1. At this point it is necessary to comment on the similarity between PVP360 and PVP1300 in both DLS and GPC. This observation was unexpected but also helps to explain the similarity in trends observed in previous dispersion experiments. Differences in the readings between DLS and GPC could arise due to a difference in technique as DLS relates scattering intensity to time and calculates molecular weight based on the diffusion coefficient whereas the data collected via GPC involved the combination of a low-angle laser static light scattering detector and refractive index detector. The former is a technique based around solving the Zimm equation (4.2) by bringing the particle scattering function, $P(\theta)$, to unity and reducing the equation to its linear form equation (4.3):

$$\frac{Kc}{R(\theta)} = \frac{1}{M_w P(\theta)} + 2A_2c + \dots \quad (4.2)$$

$$\frac{Kc}{R(\theta)} = \frac{1}{M_w} + 2A_2c \quad (4.3)$$

Additional terms are c , for concentration, $R(\theta)$ for the Rayleigh ratio, and A_2 for the second virial coefficient. It can therefore be seen that the theory is vastly different. The later involves building a refractive index profile based on solutions containing a known polymer of known concentration and molecular weight. The signal from the sample is then compared to the profile of the standard solutions. Therefore, having two detectors would lead to greater accuracy and is likely the source of discrepancy.

Having assessed the techniques precision, the next set of data presented will deal with the use of the NNLS algorithm in conjunction with the CTAB-PVP-SWNT system as it allows for greater insight into the dispersivity of the system. The results will be interpreted after all the data is presented to provide a more inclusive explanation.

Figure 4.8 below shows the distribution of aqueous 1.1 %wt/v PVP10 and serves as an example as to what was seen using NNLS for other polymer solutions as well. As can be seen, two separate distributions are presented indicating the presence of two differently sized forms of the polymer. It is important to note that this observation was seen with 0.1 %wt/v CTAB as well. Table 4.5 reports the sizes in which the smaller and larger forms are centered.

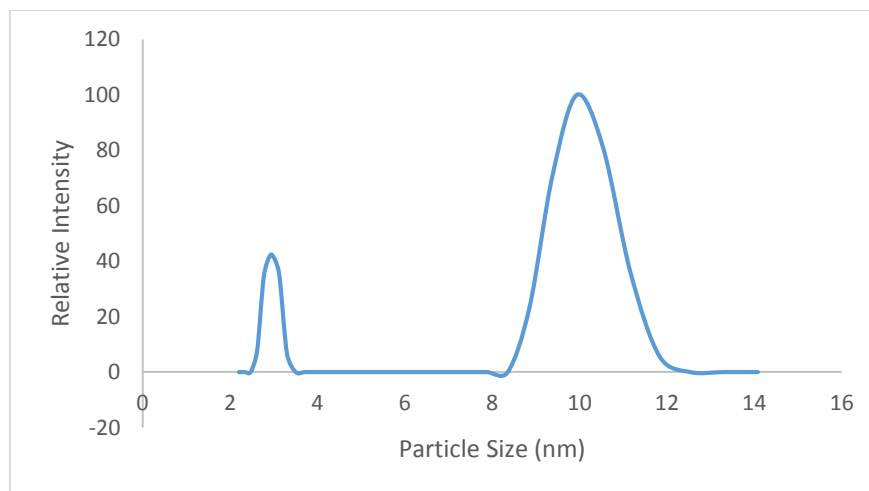


Figure 4.8: Example of bimodal distribution seen in the MSD analysis of PVP at different molecular weights. This particular example was obtained for 1.1% PVP10

Expected Polymer Molecular Weight (g/mol)	Radius of PVP Smaller Form using NNLS (nm)	Radius of PVP Larger Form using NNLS (nm)
3500	1.6 ± 0.9	7.4 ± 5.1
8000	1.1 ± 0.5	5.5 ± 1.4
10 000	0.9 ± 1.0	4.1 ± 1.6
40 000	3.7 ± 0.6	13.4 ± 3.5

360 000	7.5 ± 0.5	27.2 ± 5.1
1 300 000	7.1 ± 1.0	29.5 ± 9.2

Table 4.5: Values of the small and large forms of PVP under the MSD analysis option.

CTAB alone at a concentration of 0.1 %wt/v was also ran (Figure 4.9). In addition to obtaining an overall hydrodynamic radius of 106.4 nm from the lognormal analysis, it can be seen that the distribution derived from NNLS is quite complex as there appears to be three different domain sizes with two of the three being convoluted and centered around diameters of 136.6 nm and 417.7 nm. The third and also smallest distribution appears around 2.4 nm and are likely to be micelles. The identity of the other two species will be discussed below. The first peak sitting at a diameter of approximately 2.4 nm is likely that of micelles which can be predicted to be approximately 1.67 nm – 4.36 nm by taking the end-to-end distance of two CTAB molecules using a bond length of 0.120 nm - 0.157 nm and a bond angle of 109.5°. Additionally it is also in the vicinity of the hydrodynamic radius of 2.92 nm reported by Movchan *et al.* (2012).¹⁵⁷ However, the other distributions centered at larger sizes are more difficult to interpret. Initially, it was thought that these species may be worm-like micelles making them anisotropic in solution thereby giving radial and translational readings based on its orientation to light. However a careful inspection of the phase diagram of CTAB (Figure 2.7) indicates that worm-like micelles should not form at the conditions used in our experiments. Lee *et al.* (2005) have also observed these multiple size distributions for CTAB and proposed that they represent chemical byproducts formed from radical-containing surfactant molecules generated during sonication. This seems unlikely as we have analyzed CTAB without sonication and have observed distributions about the same size. However, we have experimentally observed that crystals can form in CTAB solutions over time at room temperature. Indeed, Ray *et al.* (2005) and Movchan *et al.* (2012) have reported self-aggregation of alkyltrimethylammonium bromide surfactants of various sizes. According to the phase diagram (Figure 2.7), at working conditions, CTAB is very close to the crystalline phase such that aggregates are a possibility. Based on this observations we attribute the distributions peaks observed above 100nm to surfactant aggregates.

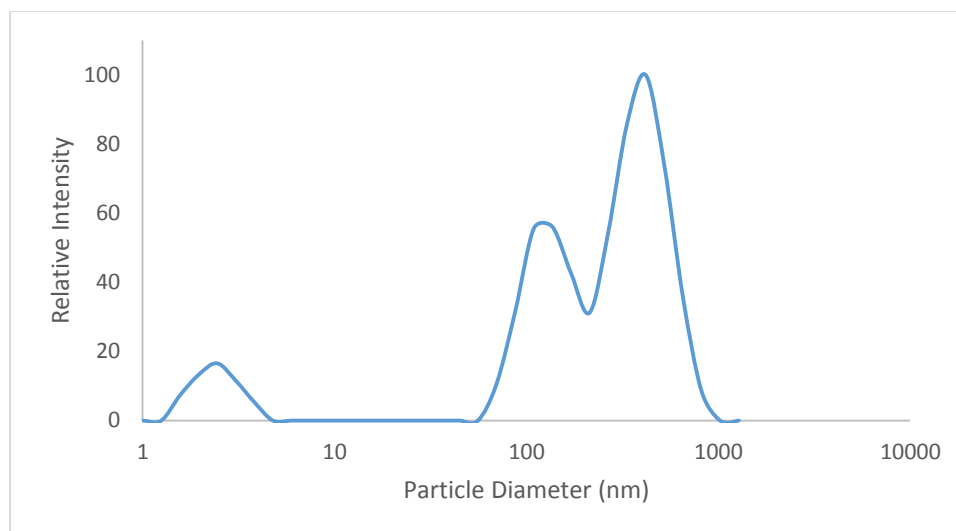
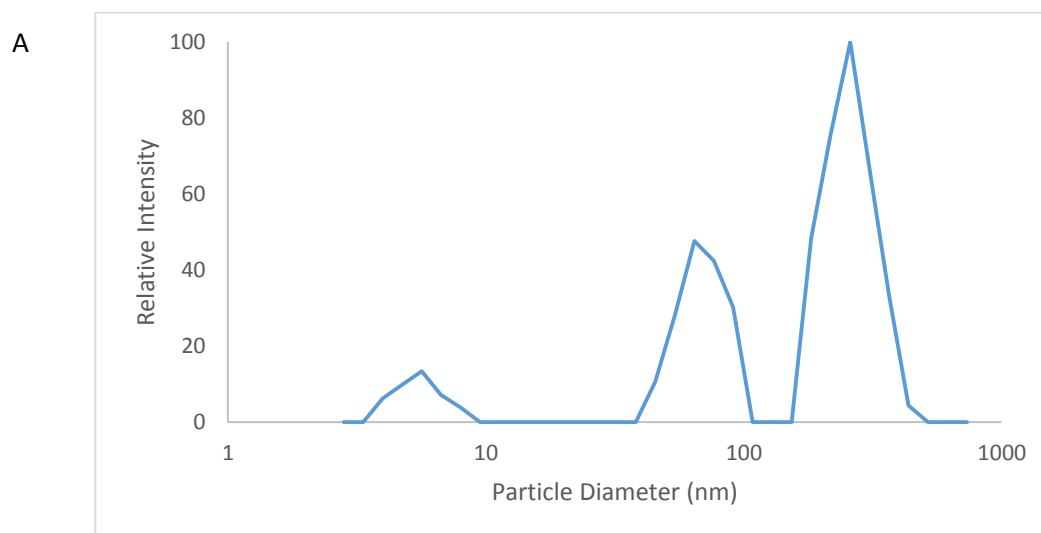


Figure 4.9: Particle size distribution of 0.1% CTAB in solution

Having observed the distributions of both aqueous PVP and aqueous CTAB, dispersed nanotube solutions were also analyzed using DLS. In choosing which molecular weight of PVP to use to prepare dispersed samples, it was decided that PVP40-SWNT, PVP360-SWNT, and PVP1300-SWNT would provide the most reliable data due to the limits of resolution. For PVP-SWNT, 0.25 %wt/v of the polymer and 0.2 g/L of SWNT were used as it was noticed that higher concentrations of PVP would interfere with SWNTs readings. As mentioned above, PVP360-SWNT and PVP1300 are very similar in size and so should provide similar results. The resulting particle size distributions are given below in Figure 4.10.



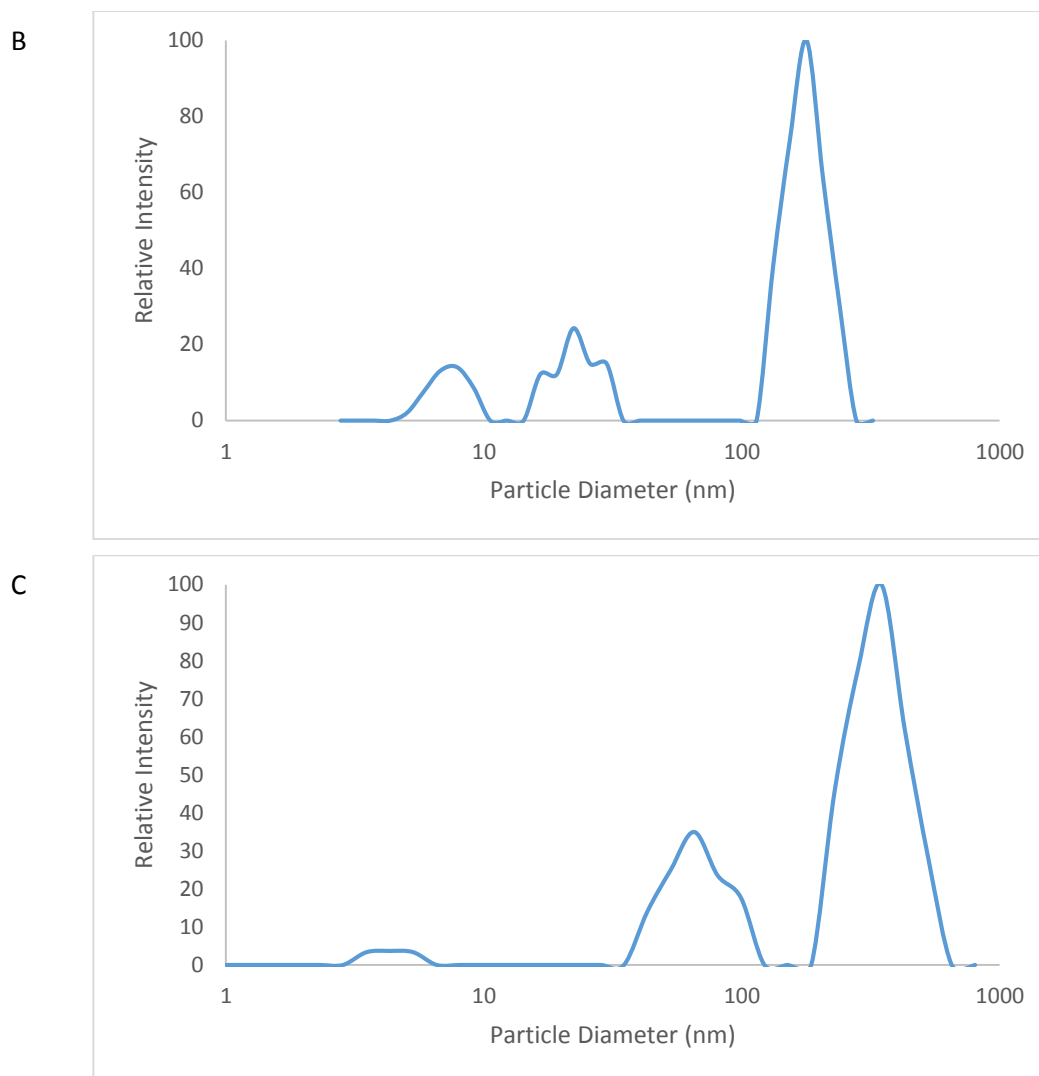


Figure 4.10: DLS of SWNT suspended with 0.25% A) PVP40, B) PVP360, and PVP1300

In both cases, the distribution is trimodal. In the figure the diameter distributions seem to be centered around: 5.6 nm, 64.3 nm, and 258.5 nm for the PVP40-SWNT system; 7.9 nm, 22.3 nm, and 178.0 nm for the PVP360-SWNT system; and 4.3 nm, 65.4 nm, and 348.0 nm for the PVP1300 system. Because nanotubes are rod-like in nature, they are anisotropic in the way they scatter light as mentioned previously.¹⁴¹ Because of this, two of the three distributions can be associated with the diameter and length of the nanotubes. Given the AFM data above, it is very likely then that the distributions of smallest and largest size represent the diameter and length of a nanotube (centered around 1-2 nm and 400 – 600nm respectively as obtained by AFM). In each case though, there also exist a third distribution in between. In the case of PVP360-SWNT, this size is centered around 22.28 nm whereas for PVP40 and PVP1300 it is centered around 65 nm. It was expected that PVP360-SWNT and PVP1300-SWNT would give very similar results given previously mentioned GPC results but the size of

the middle distribution between the two are not the same. In the case of PVP360, this size is approximately that of the larger species detected in aqueous PVP360 without nanotubes. These bimodal distributions seen in aqueous solutions of PVP will now be discussed.

The double distribution profile observed in aqueous PVP was also observed by Xu *et al.* (1991) in which they encountered a similar problem studying PS-PEO block polymers using DLS as a main technique of investigation. They noted hypotheses from previous authors such as incomplete dissolution of the polymer; solvent-driven aggregation between smaller species; and thermodynamically-driven aggregation where the smaller species cluster due to favorability of a crystalline-like phase. The authors postulated that these aggregates may appear as a large entity with a nucleus, an onion-like particle, or several small particles aggregated together. Although in their report the authors could not decisively conclude what the larger species was, later reports by various authors do seem to indicate that they are indeed smaller polymers clustered together.^{158,159} Indeed, considering the possibility of aggregation, the size we obtained of the larger species (as reported in Table 4.5) always seems bigger than the smaller particles by a ratio of 4:1 approximately. We could postulate then that every agglomerate of PVP consists of approximately 4 polymeric chains. The particle of size 22.3 nm for PVP360 could just be one of these agglomerates. However, this conclusion doesn't seem to fit with the middle peak observed for PVP40 and PVP1300. Given the literature, there are two other plausible explanations: 1) PVP aggregate with carbonaceous compounds to produce larger clusters or 2) PVP chains are swelling. With regards to the first hypothesis, since PVP is hydrophilic and nanotubes are hydrophobic this hypothesis seem unlikely at first, however it is important to recall research by Dror *et al.* (2005) and Cotiuga *et al.* (2006) in which they observed hydrophilic polymers such as a styrene and maleate copolymer (PSSty), a polystyrene-polyethylene oxide copolymer, and gum arabic aggregated together with amorphous carbon using cryo-TEM.^{123,124} The sizes of these aggregates did vary but many of the images show particles do fall within the size domains we observed for the middle peak. In addition, when CTAB-SWNT was ran at the working concentration of 0.1% wt/v it was found to give detection patterns similar to those obtained on PVP samples with nanotubes. Three peaks were also observed with the center peak around 71 nm in size. Due to the absence of PVP but the presence of nanotubes, this suggests that the middle peak has carbonaceous origins. With the second hypothesis, Tuteja *et al.* (2008) observed that with the incorporation of polystyrene nanoparticles into a solution of polystyrene chains, the radius of gyration of the chains increased by 10%-20% due to swelling. This only happened when the radius of gyration of the polymer was larger than the nanoparticle radius.¹⁶⁰ It's possible that a similar phenomenon is occurring in our system however with only a maximum of 20% seen in the increase of the polymer, hypothesis 1 seems more likely.

Given that PVP360 and PVP1300 are very similar in terms of molecular weight, the reason why the middle peak appears in different positions could also be influenced by the resolution of DLS. Typically a minimum of 2:1 difference in particle size is necessary for two particles to be resolved confidently. For instance, if a particle is 100 nm, only a particle at a size of 200nm or greater in solution will show up as separate entities. However, this difference could expand depending on the distribution of sizes in solution.^{161,162} The middle species differ from another by a ratio of only 3:1 approximately and considering the potential distribution of sizes available in an aqueous polymer solution, it's possible that the peak appears in different positions due to resolution. It's important to note that this does not mean that the two peaks are the same type of particle appearing at a different size but rather simply pointing out that both polymer aggregates and amorphous carbon can exist in solution but the apparatus could be having trouble differentiating the two as DLS is again a method based on changes in scattering intensity.

4.2 Surface Tension

Due to the potentially complex and sensitive behavior of CTAB in aggregating and crystallizing, its behavior in the presence of PVP was tested. Analyzing the surface tension is one possible method to do this as the air-liquid boundary of a surfactant solution is directly related to surfactant concentration and behavior. Specifically, because surfactant molecules are amphipathic, they would only want to present its hydrophilic region to polar solvents like water while the non-polar region would project away from the solution and into the air. This behavior would cause the surface tension to drop due to interference of normal water molecule interactions. At the surface saturation point, surfactant molecules at the air-liquid boundary would then form micelles, spherical structures in which the non-polar region of surfactants are located in the core of the structure – protected from the aqueous environment. Figure 4.11 illustrates an experiment carried to obtain this critical micelle concentration (CMC) of CTAB.

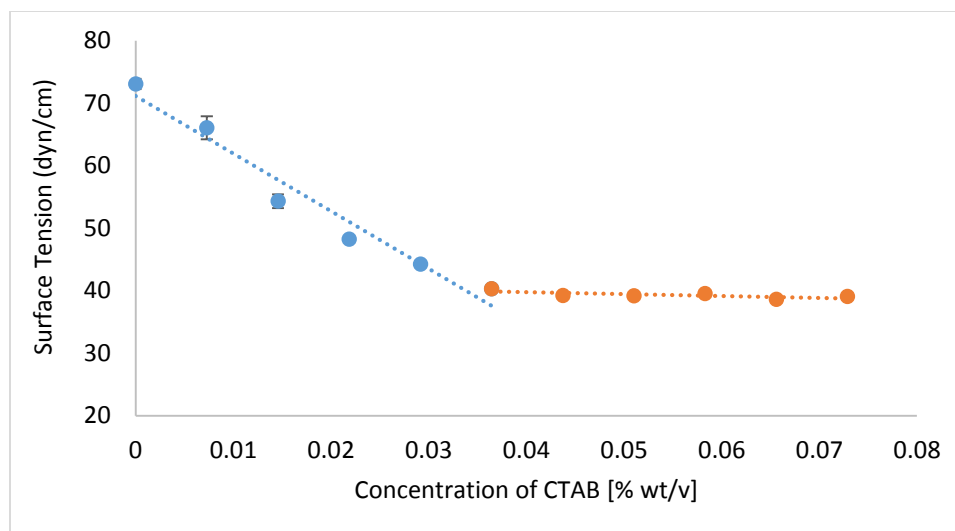


Figure 4.11: Surface tension behavior of CTAB

Given that the surface tension decreases from 72 dyn/cm (surface tension of water) to a stagnant value of 38 dyn/cm, the CMC which occurs at the breaking point is approximately 0.0338 %wt/v or 0.93 mM. This is within the generally reported range of 0.9-1.0 mM determined by a variety of techniques including calorimetry, surface tension, conductivity, viscometry, and fluorimetry.¹⁶³⁻¹⁶⁵ Additionally, using an abscissa confidence interval method described by Filliben *et al.* (1972) the CMC has a determined 95% CI range of about 0.058 mM. This value indicates that the true CMC value is within the 0.93 ± 0.029 mM range with a 95% confidence level. Similarly, PVP was also tested however being a hydrophilic polymer, there was minimal change compared to the value of water (Figure S 4, Appendix 1). Also tested were samples at working conditions of 0.1% wt/v CTAB and the concentration range previously stated for PVP: 0.25 %wt/v, 0.75 %wt/v, 1.1% wt/v, 4 %wt/v, 6% wt/v, 9% wt/v. When the two were combined (for each molecular weight), the surface tension value was consistently about 38 dyn/cm meaning that the surface of samples were still saturated with CTAB. Lastly, the CMC was also tested in response to PVP at different molecular weights. It was found that within the confidence interval, there weren't any significant changes with the addition of the polymer as shown in Table 4.6.

M_w of Polymer (g/mol)	Concentration [%wt/v]	CMC [mM]	95% CI Range [mM]
3500	0.25	1.055	0.0642
	1.10	1.137	0.0448
	4.00	1.111	0.0746
10 000	0.25	1.013	0.0721

	1.10	0.965	0.0696
	4.00	0.883	0.2258
40 000	0.25	1.022	0.2054
	1.10	1.044	0.0690
	4.00	1.040	0.0833
360 000	0.25	1.068	0.0668
	1.10	0.940	0.0669
	4.00	0.920	0.1482

Table 4.6: Estimated CMC values of CTAB with different molecular weights of PVP at different concentrations with the 95% interval that the true CMC value lies between.

Overall, the CMC of CTAB acquired is consistent with previous reports. With the addition of PVP, Table 4.6 also shows that there are no significant changes in the CMC of CTAB no matter the molecular weight or concentration. This can be surprising especially given as PVP has been shown to interact with alkali metals and cationic nanoparticles.^{166,167} Nonetheless, this coincides well with reports such as those by Feng *et al.* (2003), Bury *et al.* (1997), Wang *et al.* (1998), and Wan-Badhi *et al.* (1993) all of whom have observed through various techniques such as calorimetry, H-NMR, and electrochemical kinetics that CTAB and PVP don't directly interact with one another.^{115,116,168,169} However, a recent report by Ali *et al.* (2009) reported that the CMC of CTAB can increase quite sensitively to the addition of PVP. In fact, they reported that the CMC of CTAB changed from the range of 0.9mM – 1.0 mM to 2.64mM with 0.02 %wt/v PVP40 and 3.87mM with 0.15 %wt/v PVP40.¹⁷⁰ We tested these concentrations as well (data not shown) using surface tension however, no changes in CMC were observed. The origin of these inconsistencies may be due to a difference in technique. Conductivity works on the premise of detecting how well an electric current can pass through a solution. At CMC, the conductivity shifts due to the formation of micelles. Although PVP is largely considered a neutral molecule with minimal conductivity readings¹⁷¹ (compared to those observed by Ali *et al.* (2009)) it has been reported to contain cationic groups¹⁶⁹ which may play a role in changing conductivity. Indeed, Yang *et al.* (2012) observed that treatment of PVP-MWNT in an acidic solution of aqueous PVP at a pH of 3.0 lead to the development of a positive charge on PVP.¹⁷² In addition, PVP is known to have possible resonance structures through the shift in electron density from the nitrogen to the oxygen as seen below in Figure 4.12.^{173,174}

Briefly, the pH is a measure of the concentration of protons in solutions and is one of the fundamental measurements of acidity and basicity in solutions. As mentioned previously, the pH of the system should be considered as there may be changes influenced by the bromide counter-ion of CTAB. At the working concentration of 0.1 %wt/v, CTAB was determined to have a pH of 4.81 ± 0.11 . At the arbitrary polymer concentration of 6 %wt/v as previously used to disperse nanotubes, solutions possessed a pH less than 4 for all molecular weights of the polymer (Figure 4.13).

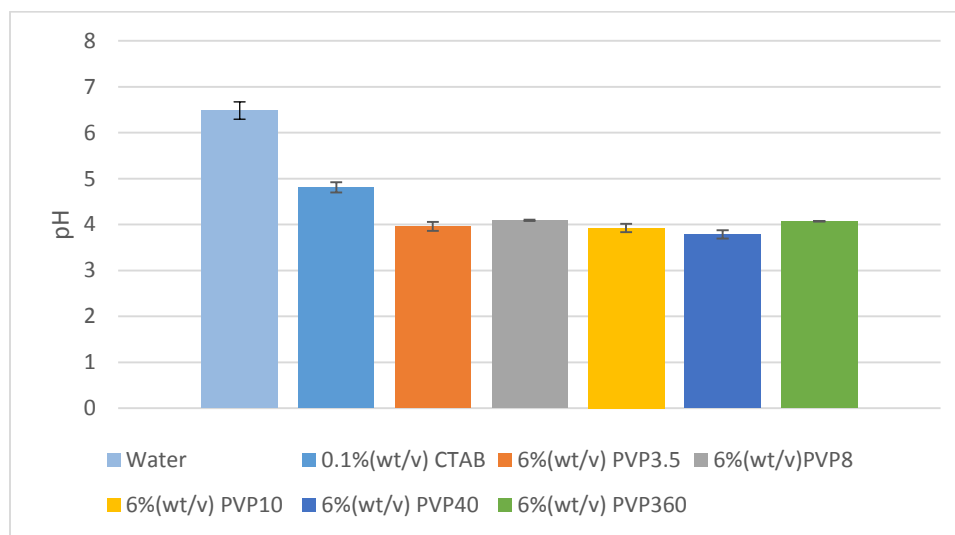
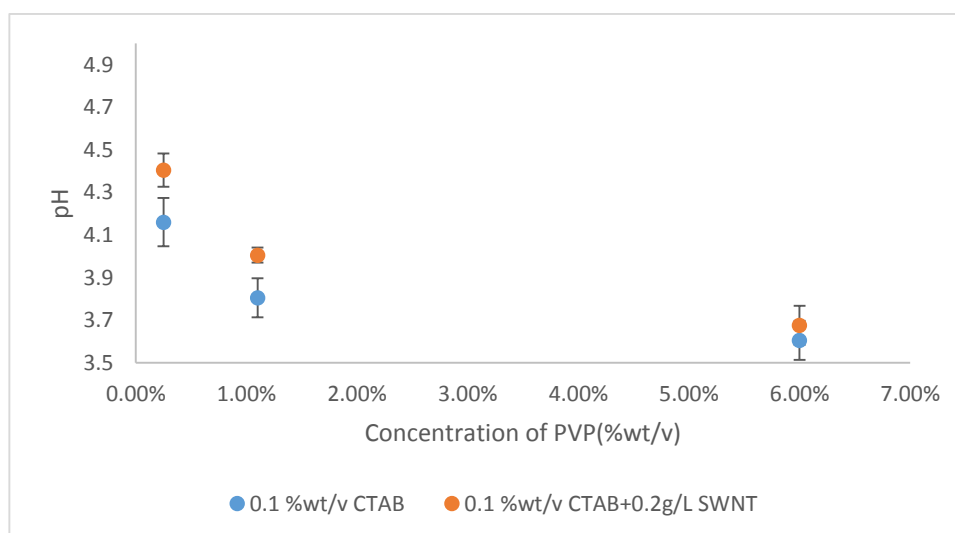


Figure 4.13: The pH value of standard control solutions such as 0.1% CTAB and 6% of the different molecular weights of the polymer.

In mixtures containing both PVP at concentrations of either 0.25 %wt/v, 1.1% wt/v or 6% wt/v and 0.1% wt/v CTAB, the pH appeared to decrease with increasing concentrations of PVP for all molecular weights (Figure 4.14).

A



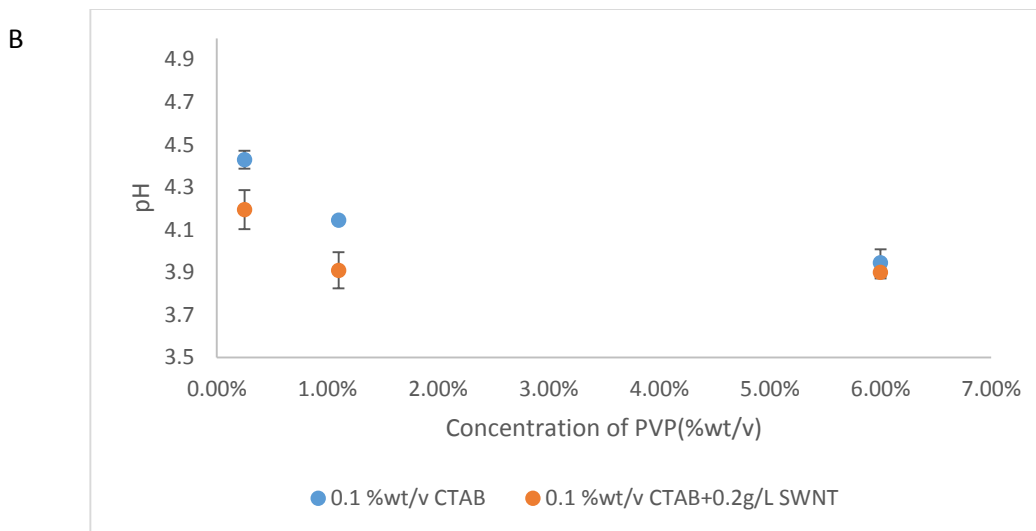


Figure 4.14: pH reading of A) PVP40 and B) PVP360 at different concentrations. The blue represents of samples with 0.1 %wt/v CTAB whereas the orange represents samples with both 0.1 %wt/v CTAB and 0.2g/L SWNT.

This suggest that changes in pH seem largely driven by PVP. Compared to CTAB, the mechanism behind PVP driven pH appears rather complex. Nikiforova *et al.* (2012) sought to describe the acid-base properties of PVP by presenting the tautomeric structures seen in Figure 4.15 below.

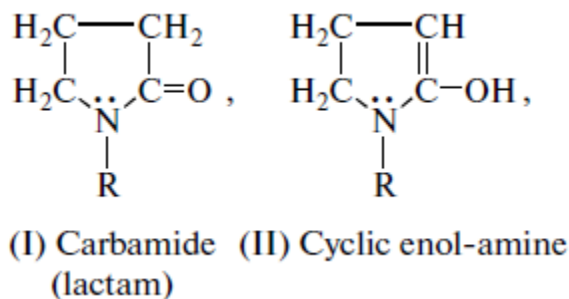


Figure 4.15: Possible Tautomerism of PVP as shown in Nikiforova et al. (2012).¹⁷⁹

Theoretical comparisons of the energies (difference of 133.62 kJ/mol) and dipole moments of these tautomers show that the normal carbamide form (I) is should be more stable. However, the authors noted the rather mobile hydrogen atom at the alpha position of the carbonyl group (I) and the hydroxyl group of (II). With regards to structure (II), it is expected that a very high pH would be necessary to extract the hydroxyl proton however a range of 4.2-6.8 had been previously reported as one in which the existence of structure (II) is a possibility and one that would subsequently drive a solution towards lower pH.¹⁷⁹ The authors also remark on the ability of each pyrrolidone monomer in the polymer to be able to retain a water molecule even in the driest of states. This monohydration effect can lead to other significant phenomena including the breaking of the lactam ring at the bond

between the carbonyl carbon and the nitrogen as well as delocalization of positive and/or negative charge depending on the solvent conditions.¹⁷⁹

With the incorporation of nanotubes, there were minor changes in pH as can be seen in Figure 4.14 above. With low molecular weight polymers (PVP40 and below), the pH at the tested concentrations seemed to increase whereas with higher molecular polymers such as PVP360 the pH seemed to decrease with the presence of nanotubes. This result suggest that with low molecular weight polymers and nanotubes, the amount of detectable protons in solution is lowered once nanotubes were incorporated and vice versa with PVP360. To better understand the surface charge state of a nanotube at different pH values, the point of zero charge of the nanotubes was determined. This was done by measuring the initial and final pH of multiple aqueous solutions with an adjusted pH range of 2-10 after the addition of nanotubes.

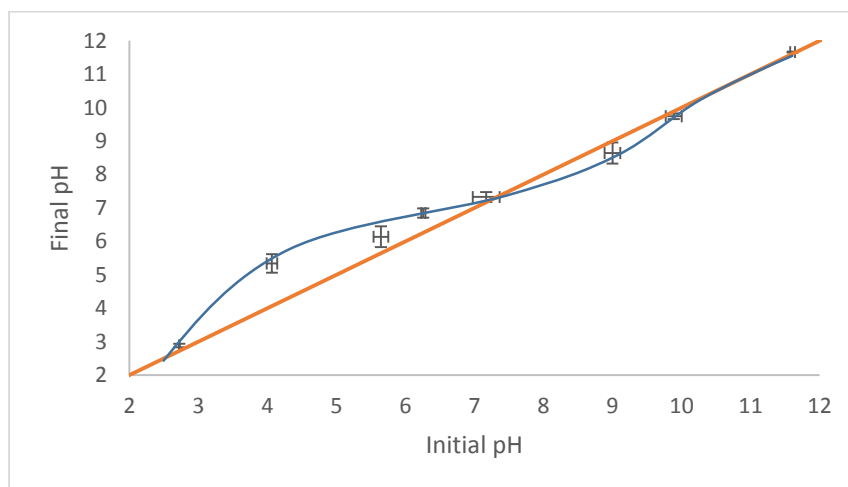


Figure 4.16: A) Demonstrates the determination of the point of zero charge while B) gives the pH value of standard control solutions such as 0.1% CTAB and 6% of the different molecular weights of the polymer.

Figure 4.16 above reveals that the initial and final pH are equal at a value of 7.5, meaning that at this point, there is a charge of 0 on the surface of the nanotube. This value was relatively close to nanotubes that were purified using NaOH treatment by Matarredona *et al.* (2003).⁵⁸ Thus, given previous pH measurements, this implies that the nanotube surface is likely positively charged. The increase in pH when using molecular weights below 40 000 g/mol might be influencing hydrogen adsorption onto the surface of nanotubes – the basis for nanotube application in hydrogen storage.^{180,181} This would mean less hydrogen in solution and an increase in pH as the nanotubes are essentially buffering the system. However, this hypothesis doesn't hold true when using high molecular weight polymers such as PVP360 as the pH is decreasing instead of increasing. This suggest then that nanotubes are encouraging more protons to be in solution. This observation may be because

protons can no longer be adsorbed onto the surface of the nanotube or there is a change in the behavior of CTA^+ or Br^- in solution however given the observations in section 4.2 there's no reason to suggest that either has changed in the presence of nanotubes making the former hypothesis more reasonable. It's interesting to note as well that high levels of dispersion occur in acidic conditions – the link being increases in PVP concentration. Therefore, given the ability of nanotubes to adsorb protons, there would be an increased positive surface charge on the nanotube which may help dispersion through electrostatic repulsion. However, it's important to consider that the change in pH is most significant at lower PVP concentrations but in these regions, dispersion is barely increased whereas at high PVP concentrations, the change in pH is low but the dispersion is significantly augmented. If electrostatic repulsion was the main driving factor, then the change in pH should be more correlated with changes in dispersion therefore electrostatic repulsion if present should not be the only force driving dispersion.

4.4 Viscosity

Our results indicate that nanotube dispersion generally increases with PVP concentration. However, because of the molecular weight of each polymer, the resulting viscosity in each solution increases at a different rate (Figure S 5, Appendix 1). Therefore, it became necessary to determine whether or not viscosity played a role in the dispersion of nanotubes. To meet this objective the dynamic viscosity of the PVP-CTAB system was acquired at PVP concentrations previously specified with each molecular weight using a rheometer with the cone and plate geometry. Glycerol-CTAB suspensions of nanotubes were also prepared to act as a positive control. Figure 4.17 presents these results.

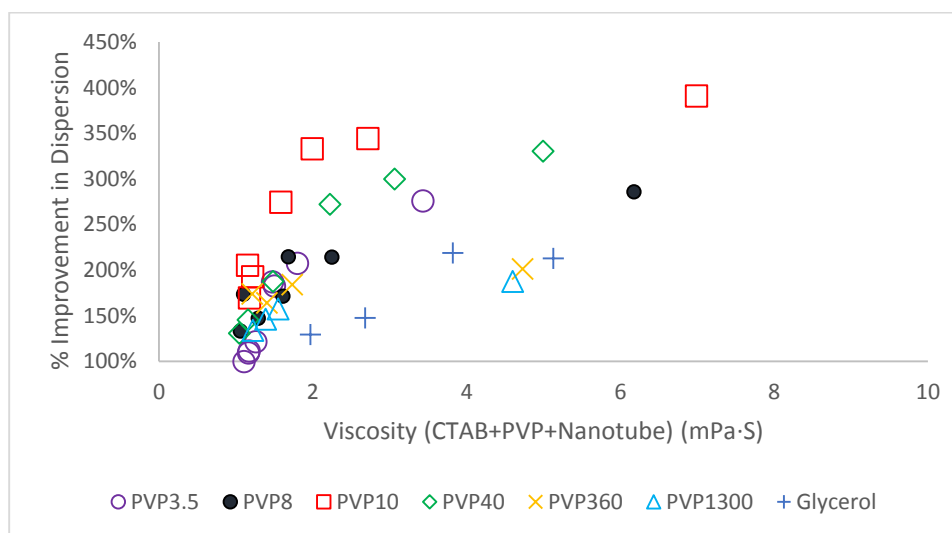


Figure 4.17: Relationship between viscosity and the total area of dispersion acquired from UV data

Interestingly, from the figure above, it is seen that viscosity does indeed play a role in dispersing nanotubes as generally dispersion increases with viscosity. The results obtained using glycerol particularly illustrate this effect. However, the molecular weight of the polymer seems to play a bigger role than that of viscosity in nanotube dispersion as PVP10 remains the most potent dispersing agent while PVP3.5, PVP8, and PVP40 all cluster about the same region slightly below that of PVP10 while PVP360 and PVP1300 are even poorer. In addition, another interesting observation is the presence of two regions where the dispersion is being improved at different rates. The change in regions appears to happen at approximately 2 – 3 mPa·S. Using equation (2.10)^{111,113} and the hydrodynamic radii determined from GPC in Table S 1, Appendix, the overlap concentrations (c^*) of PVP and its corresponding viscosity values can be determined (Table 4.7). The overlap concentration is the concentration at which polymers are abundant enough in solution such that polymer chains begin crossing with each other. The determined overlap concentrations are consistent with values seen in the literature^{182–184} and are also reasonable in terms of it being high with low molecular weights of PVP and vice versa as there would need to be more a smaller polymer in order for overlap to occur. With regards to the overlap viscosity It can be seen that the 2 – 3 mPa·S viscosity range is where PVP molecules begin to overlap. Therefore, dispersion augmentation with PVP seems to be most significant before the overlap concentration and after the polymer overlaps, the improvement is only slight. These methods will be further discussed in section 4.5, nevertheless, based on this observation, it seems PVP is likely augmenting dispersion through a physical mechanism.

Expected Polymer Molecular Weight (g/mol)	Overlap Concentration (%wt/v)	Overlap Viscosity (mPa·S)
PVP3.5	14.53	2.50
PVP8	13.28	3.01
PVP10	9.28	2.44
PVP40	3.91	2.12
PVP360	0.61	2.06
PVP1300	0.68	2.35

Table 4.7: Overlap Concentration and the corresponding overlap viscosity of PVP as estimated using GPC and equation (2.10)^{111,113}.

Another observation with regards to viscosity stems from its decrease in the system with higher molecular weight polymers such as PVP360 when nanotubes are included as shown in Figure 4.18C and compared to Figure 4.18A and Figure 4.18B below in which PVP3.5 and PVP10 were used.

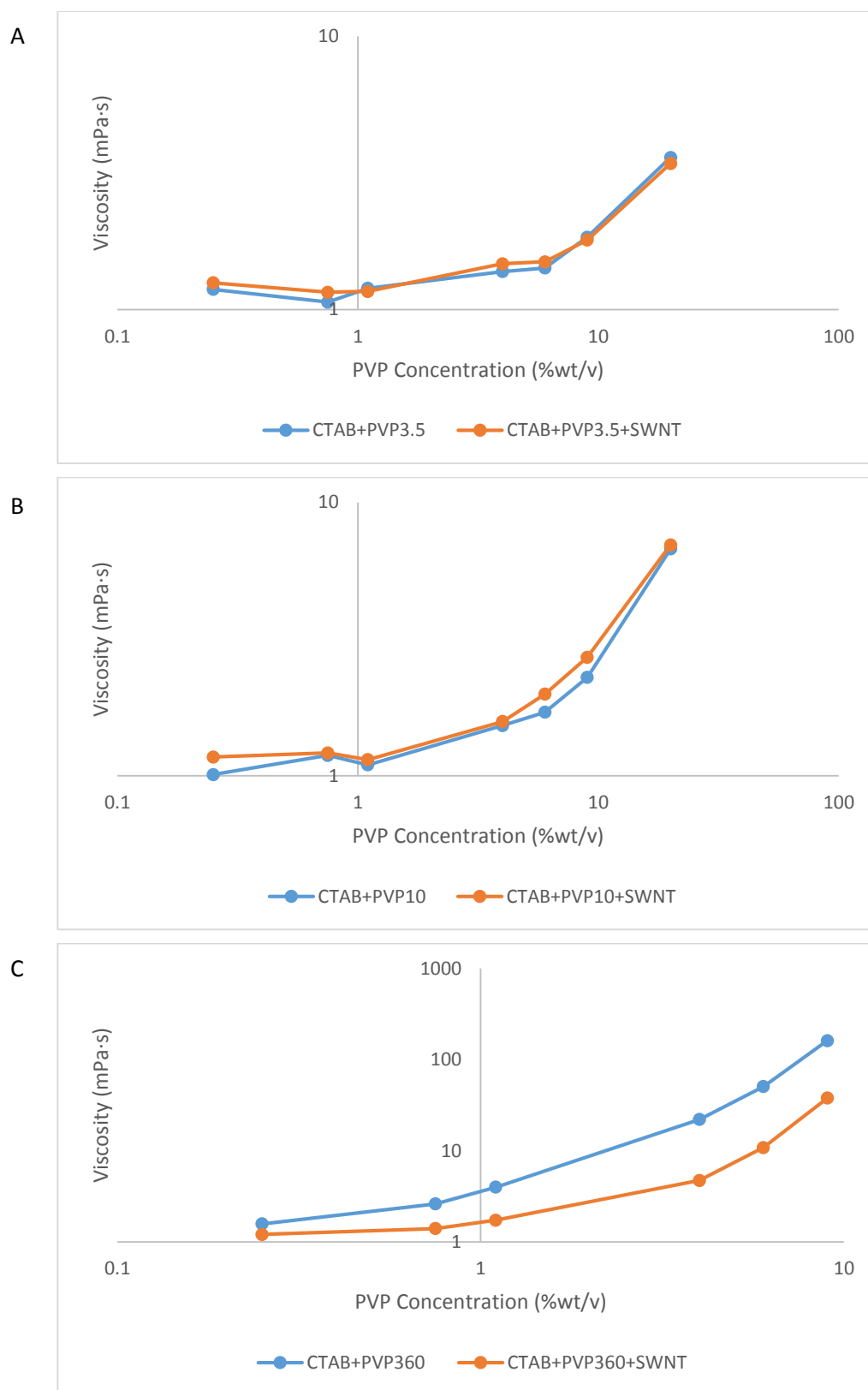


Figure 4.18: Dynamic viscosity of CTAB+PVP system with and without SWNT at a PVP molecular weight of A) 3500 g/mol B) 10 000 g/mol C) 360 000 g/mol.

Indeed, there was an observed maximum of 77% decrease using 9 %wt/v aqueous PVP360. This is interesting since Einstein once predicted that the inclusion of spherical particles in a fluid should increase viscosity as described by the formula:

$$\eta = \eta_0(1 + 2.5\phi) \quad (4.4)$$

where η is the final viscosity, η_0 is the viscosity of the fluid without the particles, and ϕ is the volume fraction of the particles.¹⁸⁵ With the inclusion of nanotubes which have a large aspect ratio, the viscosity should then increase. Clearly, this does not seem to be the case. Several research groups have reported similar observations. For example, Mackay *et al.* (2003) incorporated modified polystyrene nanoparticles into linear polystyrene melts. They found that with the introduction of about 50 %wt/v of nanoparticles, the viscosity decreased fourfold. They proposed that an increase in free volume of 10% was the cause of the decrease where free volume is the amount of free space available for a polymer to adopt different conformations and to move around in solution. The data presented here could also be used to theoretically calculate the excluded volume. Given a single nanotube, the free volume generated can be given by:

$$v_f = \pi dL\Delta \quad (4.5)^{186}$$

where d is the diameter of the nanotube, L is the length of the nanotube, and Δ is the thickness of the excluded volume shell, respectively. The overall size of the excluded volume shell can be calculated separately using the following formula:

$$v_{ex} = \frac{32}{3}\pi r^3 + 8\pi Lr^2 + 4L^2r\langle\sin(\gamma)\rangle \quad (4.6)^{187}$$

where in addition to the above terms, r is the radius of the nanotube and $\langle\sin(\gamma)\rangle$ is a term that takes into consideration the orientation of nanotubes with respect to one another in solution. It is given by the formula:

$$\sin(\gamma) = \sqrt{1 - [\sin\theta_I\sin\theta_J \cos(\phi_I - \phi_J) + \cos\theta_I\cos\theta_J]^2} \quad (4.7)^{187}$$

where I and J denote two different nanotube species in 3D space with angle θ along the X-Y plane and ϕ along the Z-XY plane. To do these calculations, we can use the most predominant nanotube sizes acquired from the AFM seen in Figure 4.7. In particular the length of 500 nm and diameter of 2.5nm were used. With regards to the contact angle (γ) between the nanotubes, Néda *et al.* (1999) found that $\sin(\gamma)$ had an average value of approximately $\frac{\pi}{4}$ or 0.785 in a solution of isotropic cylinders.¹⁸⁸ From this value, the excluded volume is approximately $1.00 \times 10^6 \text{ nm}^3$. This gives a Δ value of about

25.28 nm. Based on this, the free volume of a single nanotube is approximately $9.92 \times 10^4 \text{ nm}^3$. Taking the extreme case of 9% PVP360, the concentration of nanotubes retained is roughly 0.08 g/L which equates to approximately 6.42×10^{16} individual nanotubes. Using a molecular weight of 750 000 g/mol and assuming a volume of 1 L, the total free volume is approximately 6.37×10^{-3} L. Compared to the original assumed volume of 1 L, this value is very small and therefore the concept of free volume at the extremely low working concentration of nanotubes (0.2 g/L) should not play a significant role in our system.

There are other theories as well such as those by Jain *et al.* (2008) whom have suggested that decreases in viscosity are linked to adsorption between the polymer and the particle.¹⁸⁹ It is very unlikely this is occurring given the hydrophobic nature of nanotubes and the hydrophilicity of PVP. Even if CTAB were adsorbed onto the nanotube surface, CTAB-PVP interactions are not known to occur as stated above. A publication by Roberts *et al.* (2001) also noted decreases in viscosity when small silica particles (0.35 nm) were blended with polydimethylsiloxane however when larger particles (2.2 nm), were included the viscosity increased.¹⁹⁰ Given the size of nanotubes, this seems counter to our observations. Xie *et al.* (2004) had used CaCO_3 particles during their composite formation and explained decreases in viscosity by suggesting that under stress, their rotating spherical particles created zones of increased shear. These shearing zones then allowed polymers to align more readily which decreased viscosity. This can only be true with spherical particles however and nanotubes being rod-like would not create these zones as readily.¹⁹¹ Perhaps the most significant theory though comes from Tuteja *et al.* (2005) in which their results show that viscosity decreases only arise if the polymer is entangled. Otherwise, the viscosity would increase. The mechanism they claim is one in which the added particles has a “constraint release” effect in which the particle interferes with the entanglement of polymers chains.¹⁹² Additionally, combined with the well-known observation that macromolecules can align to the direction of shear¹⁹³, nanotubes could be increasing the responsiveness of polymers to shearing forces thereby facilitating alignment. This seems to be the most reasonable as given the size of PVP360, it would be heavily entangled at 9% wt/v. A review of Table 4.7 shows that it occurs at 0.61 %wt/v, much more prominently than other molecular weights. Also, given smaller molecular weight polymers, chains would not be as intertwined thus the “constraint release” effect would be more negligible in those cases. This effect is also supported by electrophoretic mobility in that, based on the observation of Figure S 6, Appendix 1, it seems that there is an overall increase in the mobility of CTAB when nanotubes were added to a solution of a heavily entangled PVP360 chains but not when nanotubes were added to a solution containing looser PVP10 chains.

It's worth noting as well that there are also reports where this phenomenon does not seem to appear despite similar test conditions. For instance, Camponeschi *et al.* (2006) used carboxymethylcellulose with a molecular weight of 350 000 g/mol at a concentration of 1% wt/v and found that the viscosity was no different with the addition of nanotubes despite the polymer being entangled at that concentration according to overlap concentrations determined by Troszynska *et al.* (2008).^{194,195}

4.5 Discussion

The results presented above detailed the rationale and design of experiments as well as the data acquired. SWNTs were dispersed in systems containing CTAB, PVP, or both and analyzed using Vis-NIR spectroscopy. With regards to PVP, multiple molecular weights were tested to determine whether there was an optimum. Subsequent tests were then used to characterize the system and elucidate a potential mechanism for the improved dispersion.

Initial sample preparation using only 0.1 %wt/v CTAB to disperse nanotubes resulted in a stable suspension in which nanotubes were appreciably dispersed. Although not as effective as 2 %wt/v sodium deoxycholate, the use of CTAB as the dispersing agent yielded observable nanotube chiralities in solution (from Vis-NIR absorbance). Suspensions prepared using PVP alone were, in contrast, a lot poorer in separating different nanotube chiralities as Vis-NIR could not resolve any corresponding peaks. Surprisingly then, the addition of PVP to a system already containing CTAB resulted in an unexpected synergism in the augmentation of SWNT dispersions. This phenomenon was most prominent with PVP10 with respect to the concentration and viscosity of the polymer as larger and smaller molecular weights of PVP were less effective at dispersing nanotubes.

Probing the system using AFM and DLS to observe any changes in dimensionality of the system components showed that the nanotube had been fragmented likely due to ultrasonication as previously reported. In addition DLS revealed that the PVP appeared unaffected by the presence of CTAB as sizes remained relatively constant throughout all experiments. Checking for changes in the behavior of CTAB in the presence of PVP using surface tension also revealed no significant changes with regards to the formation of micelles or the behavior of CTAB in general. PVP on its own was also explored using tensiometry and was found to play little role in affecting surface tension. It appears then that there are no direct changes in the behavior of PVP or CTAB when one is added to the other. However, there may be some indirect effects between CTAB and PVP. As indicated in Figure 4.15, PVP does have several resonance forms, of which the nitrogen can have a positive dipole moment and the carbonyl oxygen can have a negative dipole moment. This may lead to slight interactions with the

bromide ion on the nitrogen or the cationic head of CTAB on the oxygen, both of which could then indirectly influence the formation of micelles. However, in addition to the studies listed above in which a multitude of techniques were used to show no PVP and CTAB interaction,^{115,116,168,169} Hamada *et al.* (1976) noted that alkylammonium surfactants were poorly influenced by PVP when bromide was the counter-ion therefore any potential interactions would definitely be rare given what has been seen. There was a report though by Shirahama *et al.* (1994) which stated cationic surfactants could interact with PVP but only at pH values above 11.3¹⁹⁶ however in our solutions when CTAB and PVP were together, the conditions were definitely acidic. Therefore, again, it appears that CTAB and PVP don't interact.

There were detectable changes in pH however and this appeared to be largely PVP driven since the pH decreased beyond that of CTAB alone with increasing PVP concentrations irrespective of the molecular weight. This latter fact indicates that this effect is likely related to the individual pyrrolidone monomers and their ability to donate the alpha hydrogen in the pyrrolidone ring. When nanotubes were added to the solution, there was a slight recovery of the pH which can be explained by hydrogen adsorption onto the surface of nanotubes. This result is supported by the point of zero charge which is a value of 7.5 indicating that hydrogen would adsorb onto the surface of nanotubes in acidic solutions. Thus, the surface of nanotubes are most certainly positively charged not just from expected CTAB adsorption but also protons as well. Jiang *et al.* (2003) noticed the same effect on the basic end of the pH scale when they used SDS as their dispersing surfactant and noticed that at high pH values, the surface of nanotubes became more negatively charged due to hydroxyl ion adsorption.⁹⁷ Such a phenomenon may aid in the electrostatic repulsion that keeps nanotubes separated, however this was deemed unlikely as the magnitude of the changes in pH did not correspond to the magnitude of changes in dispersion.

Expectedly there will be interactions between CTAB and the nanotube but with regards to PVP interactions with the nanotube, Granite *et al.* (2012) showed that any interactions would be very weak. In 1996, Smith *et al.* showed that if PVP was forming strong adsorbing interactions, it would lead to decreased recovery of the polymer in GPC.¹⁸⁷ Table S 2, Appendix 1, shows that there was a recovered concentration of 0.80 %wt/v at a retention volume of 23.8mL. This detected concentration is very close to the starting concentration aimed to be 0.75 %wt/v, therefore the fact that there was full recovery corresponds with conclusions by Granite *et al.* (2012) regarding PVP weak interactions. According to viscosity though, the PVP despite not interacting, can still augment dispersion at an appreciable rate especially for PVP10 until which they overlap. Then, the increase is less pronounced.

With regards to overlap, the incorporation of nanotubes into heavily entangled polymers such as PVP360 resulted in a decrease of the viscosity when compared to solutions without the polymer. This result was attributed by Tuteja *et al.* (2005) to have arisen from particles being able to disrupt the magnitude of polymer entanglement which would help polymers align better to shearing forces.

Therefore, it seems CTAB is the molecule that adsorbs to the surface of nanotubes, fully saturating it given prior literature reports,¹⁴⁷ and enabling dispersion then PVP augments this effect mainly through a physical mechanism, possibly by taking up space in solution and sterically buffering nanotubes in solution as shown in Figure 4.19. A similar model in which coiled polymers are present with nanotubes was proposed by Grunlan *et al.* (2006) in which they used just poly(acrylic acid) as the dispersing agent.¹⁹⁷

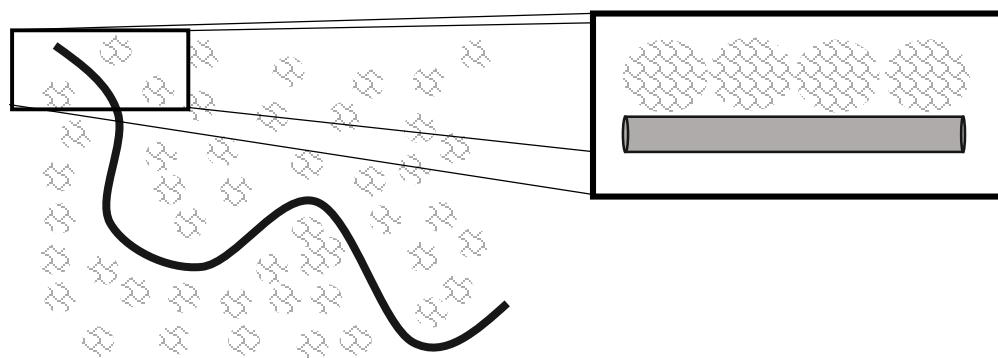


Figure 4.19: Hypothesized interaction of polymer with nanotube. The nanotube is illustrated here as the black-gray cylinder with an outer covering of surfactant (red glow). The spheres on top represent the PVP polymers.

Preliminary calculations were done to assess whether the polymer content was high enough to provide such an effect. This was done by comparing the total available surface area of nanotubes in solution and the area of a polymer projected onto the nanotubes surface assuming dimensions remain constant throughout the solution. It's important to note as well that the concentration of nanotube is different for each sample therefore the total amount of available surface area is also different as well. Thus, the total nanotube surface areas for each CTAB-PVP system was calculated using concentration values from Beer-Lambert calculations presented in section 4.1.1 and the dimensions assessed from AFM (i.e. a length of 500 nm, a radius of 0.75 nm and a molecular weight of 750 000 g/mol). The numerical values are presented in Table S 3, Appendix 1. To calculate the projected area of the polymer, the projection was considered circular so that the hydrodynamic radius obtained via GPC could be used. The results of these calculations are presented in Table S 4, Appendix 1. By taking the ratio between the total projectable area and the total available nanotube area, it can be seen that

the polymer can provide an excess amount of contact between it and the nanotube surface (Table 4.8) meaning that the surface of nanotube is fully covered and in contact with PVP.

Concentration [% wt/v]	PVP3.5	PVP8	PVP10	PVP40	PVP360	PVP1300
0.25	2779	2201	1595	1122	218	371
0.75	14773	4795	3451	2933	739	958
1.1	17733	9114	4930	3029	935	1261
4	39459	29788	13444	6761	2301	2493
6	65635	33904	15223	8590	1779	2295
9	76151	47295	20044	9648	1961	2236

Table 4.8: Ratio of total surface area projectable by the polymer to total surface area available of nanotubes

In addition, plotting the dispersion with respect to the total area provided by the polymer yields the following trend:

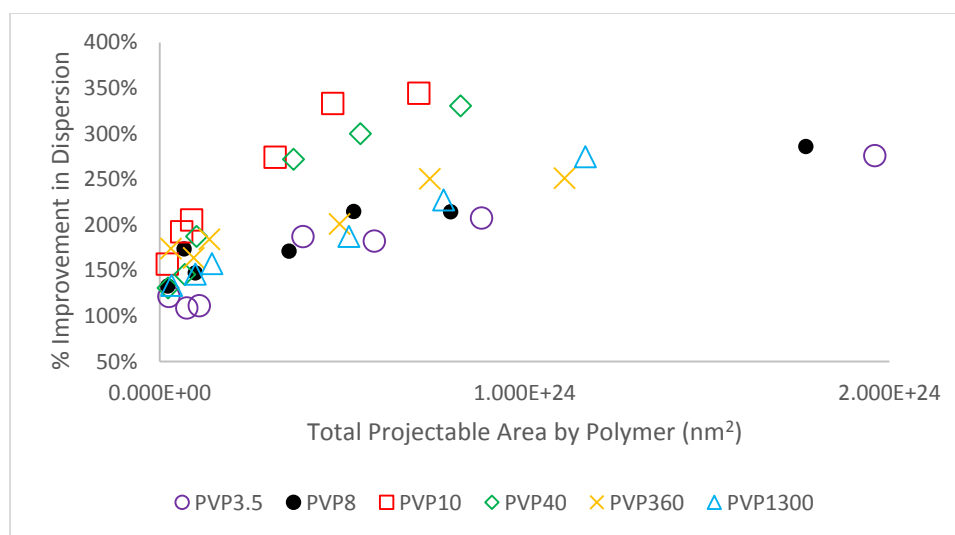


Figure 4.20: Percent increase in dispersion over the total projectable area by PVP

Comparing Figure 4.20 to Figure 4.4, the plots appear similar in that PVP10 again is the most effective molecular weight to use while other weights are worst for dispersion. This confirms that the observed improvement on nanotube dispersion is the result of the physical presence of the polymer and the likelihood that it is buffering the system.

To understand this physical effect more, a comparison was done with results by Smith *et al.* (1996). In their study, the stabilizing ability of PVP on polystyrene nanoparticles was investigated using the molecular weights: 10 000 g/mol, 40 000 g/mol, 360 000 g/mol, and 2 500 000 g/mol. They noted that dispersions were only stable with molecular weights 40 000 g/mol or greater and above a polymer concentration sufficient to give full surface coverage. Full coverage was stated to be important due to steric repulsions between the adsorbed polymer layers. Their potential energy curve (reproduced

below in Figure 4.21) shows a large vertical rise at particle separations corresponding to twice the adsorbed layer thickness. For the effective molecular weights, a shallow secondary minimum was also deemed important as they noted that the secondary minimum for PVP10 was sufficiently deep such that flocculation could occur.¹⁹⁸

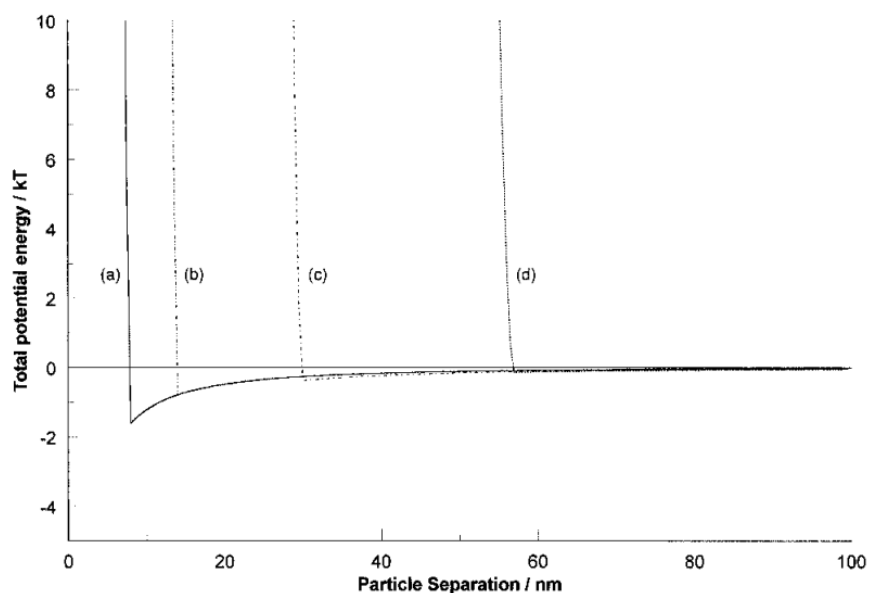


Figure 4.21: Potential energy of polystyrene nanoparticles stabilized with different molecular weights of PVP. A) PVP10, B) PVP40, C) PVP360, and D) PVP2500 as produced by Smith et al. (1996).¹⁹⁸

This result is useful not only because it shows the existence of a potential cutoff for which PVP can augment dispersion but a potential mechanism for it. This mechanism is centered around a link between the thickness of the adsorbed layer of polymer and the interparticle separation distance it can provide. This observation was also observed by Nativ-Roth *et al.* (2007) noting a minimum of 20 monomeric units of PEO in order for nanotubes to be sterically driven apart to a stable separation distance of 2.5 nm in their experiments. This distance (2.5 nm) is the minimum required in order for there to be no intertube attraction as indicated by Figure 2.4. Given the hydrodynamic diameters of PVP as presented in Table S 1, Appendix 1, it is worth pointing out that PVP10 has a determined hydrodynamic radius of 2.432 nm which is very close to the minimum separation distance of 2.5 nm required. It is postulated that this may be an important factor governing the system as PVP3.5 and PVP8, which have smaller hydrodynamic radii are less effective. It appears then that there needs to be a particle with a hydrodynamic radius approximately the same size as the minimum intertube distance in order for nanotubes to be effectively spaced out. On inspection though, it may be noticed that PVP10 would provide a total separation distance of approximately 5 nm between each nanotube

assuming rigidity. This is twice as large as the minimum intertube distance required however the key should still lie in the hydrodynamic radius. Although rarely touched upon it was observed previously by Bandyopadhyaya *et al.* (2002) in which the polymer gum arabic (GA) was found to generate repulsive forces only at a distance twice its radius of gyration (1.54 times the hydrodynamic radius for random coil polymer¹⁹⁹) therefore the 5 nm would be the minimum separation distance required in order for the polymer generate an effect. The origins of this repulsive effect was attributed to a net gain in translational entropy as ropes of 100 tubes separated could lead to a 2 fold increase in translational entropy (i.e. the disorder of the system associated with movement of the particle).²⁰⁰ Interestingly, a supporting piece of information for this may lie in the determination of nanotube concentration after sample preparation. A close inspection of Figure 4.5 shows that there is a large difference between the retention ability of PVP8 and PVP10 despite the fact that the two are only on average 2000 g/mol apart from one another. This observation seems to indicate that PVP3.5 and PVP8 can't support nanotubes in solution and that nanotubes are easily passing through the polymers during centrifugation. Although this model may serve to explain why PVP3.5 and PVP8 are ineffective, it doesn't explain why PVP360 and PVP1300 are also ineffective thus it could be that these two are worse for a different reason.

To answer this question, we sought to delve deeper into the contact mechanics between the polymer and nanotube, specifically the contact area, as given by the Hertzian model. This approach contrast the model considered previously in that the Hertzian model is specifically used to look at contact mechanics whereas previously, only a projection was considered. Perhaps, the most common derivation of Hertzian contact area (A) comes in the form of a sphere indenting an elastic surface and is given by the formula:

$$A = \pi a^2 = \pi \left[\frac{3LR}{4E} \right]^{\frac{2}{3}} \quad (4.8)$$

where a is the contact radius, and L is the force of the load, R is the radius of the indenter, and E is the combined Young's modulus of the two materials in contact respectively as given below:

$$E = \left[\frac{1 - \nu_1^2}{E_1} + \frac{1 - \nu_2^2}{E_2} \right]^{-1} \quad (4.9)$$

where ν is Poisson's ratio. Unfortunately, many of these terms are unknown however in 2007, Geike *et al.* proposed that the 3D Hertzian model can be approximated 1D by considering a circle penetrating an elastic surface given by the formula below:

$$A = a^2\pi = Rd\pi \quad (4.10)^{201,202}$$

where d is the depth of penetration. This model was therefore used to get a deeper understanding of our system due to its clear simplicity. Given that CTAB and PVP don't significantly interact, the depth of penetration should be negligible and constantly small across all molecular weights used. Therefore, for ease, the depth of indentation was arbitrarily picked as 0.1 nm across all calculations whereas the hydrodynamic radius is used as the radius of the indenter. It's noticed then that the contact area is proportional to the hydrodynamic radius. Interestingly, by converting all PVP concentrations to the amount of "contact area" (i.e multiplying mols of the polymer by the hydrodynamic radius) then plotting with the percent increase in dispersion gives the resulting plot is given below in

Figure 4.22.

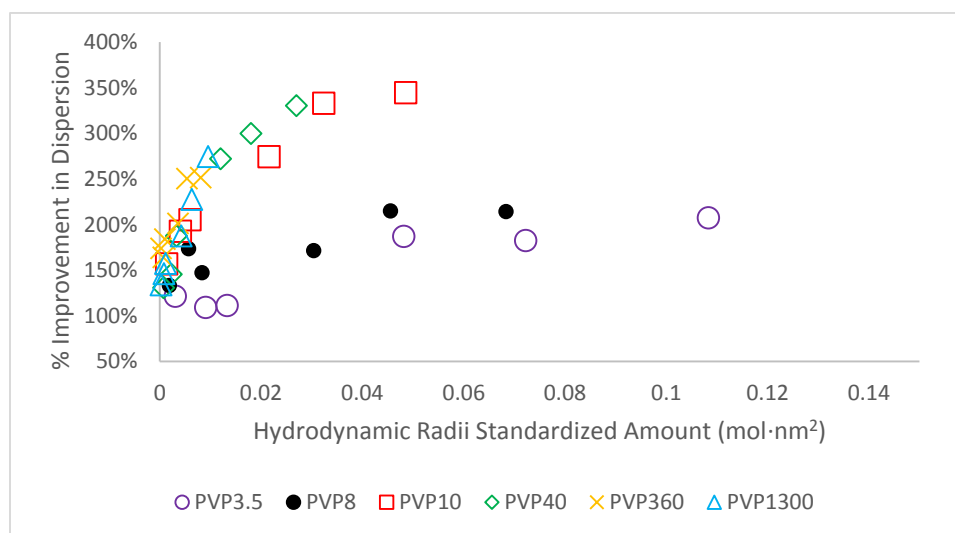


Figure 4.22: Percent increase in dispersion versus the total possible contact area by PVP

Interestingly, unlike the previous plots such as Figure 4.4 and Figure 4.20, the trend of PVP360 and PVP1300 shift and match that of PVP10 and PVP40. This result appears to cement the fact that the quality of dispersion by different molecular weights of PVP is linked to the polymers hydrodynamic radius. PVP3.5 and PVP8 remain as poor dispersing agents presumably because of its small size but PVP360 and PVP1300 disperse nanotubes based on the same mechanism as PVP10 and PVP40. The reason why PVP360 and PVP1300 could be worse than PVP10 and PVP40 as shown in Figure 4.4 and Figure 4.20 is because given any specific concentration, the number of larger polymers in solution will

always be a lot lower than the smaller polymer given stoichiometry. This means that even though concentrations may be equal between different molecular weight, the number of molecules in solution are different. Thus, when everything is standardized based off of contact area, the dispersion profiles of PVP (>10 000 g/mol) match up as shown above. In addition, PVP360 and PVP1300, being bigger polymers, have very low overlap concentrations (0.61 %wt/v) as described in section 4.4 meaning that these PVPs can overlap significantly at low concentrations where surface coverage is far less than optimal. Given the overall results and the subsequent rationale, it appears then that the data agrees well with the proposed mechanism in Figure 4.19.

4.6 Summary

Presented here were the results of several experiments to determine how a surfactant-polymer system, namely the CTAB-PVP system worked to disperse nanotubes. It was seen using Vis-NIR that CTAB had reasonable dispersion ability but PVP was relatively poorer. Together though, the dispersion increased significantly with PVP10 being able to augment dispersion by almost 3 times compared to CTAB alone and 9 times compared to PVP alone. Checking the state of nanotubes using AFM revealed that the nanotubes were being fragmented as a result of sonication. This was confirmed using DLS and references to the literature. In addition, DLS showed that PVP was not changing at the working concentrations of CTAB, as the shape stayed relatively the same size. The effects of PVP on CTAB were also investigated using surface tension and although there was a small amount of controversy in the literature, it appears that PVP has no effect on CTAB as well. PVP does seem to increase the acidity of the solution overall however in the presence of nanotubes, this effect is buffered as hydrogen can adsorb onto the surface of nanotubes given a point of zero charge of 7.5. Interestingly, this only occurs when using molecular weight polymers of 40 000 g/mol or less. The presence of nanotubes in a solution of 0.1 %wt/v CTAB and PVP360 at all concentrations resulted in an increase in pH compared to controls. The origins of this is still unknown however. In solutions of PVP360, it was also observed that the presence of nanotubes lead to a decrease in viscosity. This is likely because nanotubes blocked the larger PVP from becoming too entangled and served to ease shear alignment as well. Overall, given the deficiency of chemical evidence, it is likely that both CTAB and PVP behaved independently of one another. This implies that the long hydrophobic alkyl chain, CTAB is likely the one binding to the nanotube surface while PVP is likely stabilizing the dispersion through steric repulsion. Although, the exact mechanism isn't fully characterized, the origins likely lie with relation to the hydrodynamic radius of the polymer and its ability to separate nanotubes at a distance high enough that nanotubes do not self-aggregate. In this regard, further tests towards validating the

entropic origins are recommended however overall we find that the data gathered and presented here seem to support the model displayed in Figure 4.19 in which PVP is essentially buffering a CTAB-assisted dispersion of nanotubes.

Chapter 5: Conclusion

A carbon nanotube is a recently discovered carbonaceous material expected to be able to elevate modern technology to the next frontier as it has extraordinary electrical, mechanical, and thermal properties. However, nanotubes are strongly driven to aggregate due to their hydrophobic nature thereby their overall applicability is still limited. In its aggregated state, nanotubes are not as electrically or thermally conductive and cannot provide mechanical support due to low percolation. To remedy this, there are two chemical approaches to modifying nanotubes to make them more homogeneously dispersed in solution: covalent and non-covalent modifications. Covalent modifications involve attaching different functional groups to the surface of nanotubes however, these processes typically involve harsh treatments with acids as the initial step which can lead to destruction of the nanotube's structure and therefore properties. Non-covalent modifications involve using amphiphatic molecules such as surfactants or different polymers to coat the nanotube so it becomes stabilized to the environment around it. This strategy preserves much of the nanotubes intrinsic properties therefore it is a much more appealing strategy. To this end, many different types of surfactants (cationic, anionic, non-ionic, and zwitterionic) and polymers have been investigated for their dispersal ability however, only recently have researchers begun to combine these two types of molecules together in dispersing nanotubes.

This thesis presented work describing the investigation of a surfactant and polymer based system for the homogeneous dispersion of carbon nanotubes in solution through non-covalent modifications. The approach involved the characterization of a system containing both the hydrophilic polymer, polyvinylpyrrolidone (PVP) at different molecular weight, and the cationic surfactant, cetyltrimonium bromide (CTAB). The chosen molecular weights were: 3 500 g/mol (PVP3.5) , 8 000 g/mol (PVP8), 10 000 g/mol (PVP10), 40 000 g/mol (PVP40), 360 000 g/mol (PVP360), and 1 300 000 g/mol (PVP1300). Solutions with a volume of 25 mL were prepared using ultrasonication to mix CTAB, SWNT, and/or PVP to concentrations of 0.1 %wt/v, 0.2 g/L, and one of 0.25 %wt/v, 0.75 %wt/v, 1.1 %wt/v, 4 %wt/v, 6 %wt/v, or 9%wt/v respectively. From there, samples were ultracentrifuged to remove unsuspected aggregates. These samples were then systematically analyzed using a battery of techniques including Vis-NIR, atomic force microscopy (AFM), dynamic light scattering (DLS), surface tension, pH, and viscosity. From these results, there were several observations worth noting such as:

- Synergy in the CTAB-PVP system at dispersing nanotubes as compared to both CTAB alone and PVP alone. The most synergistic molecular weight was PVP10.

- More nanotubes were retained with the use of higher molecular weights of PVP.
- SWNT were fragmented as a result of ultrasonication.
- PVP appears to aggregate in solution in the presence and absence of nanotubes.
- No changes in the behavior of CTAB or PVP in the presence of one another.
- CTAB and PVP drives the formation of an acidic solution with PVP being more of a significant contributor.
- The point of zero charge of nanotubes is at a pH of approximately 7.5.
- Dramatic increase in dispersion before PVP overlap concentration and then subtle increases afterwards
- Decrease in viscosity when nanotubes are incorporated into a solution containing CTAB and PVP360 or PVP1300.

After compiling these observations and comparing to those of literature the following conclusions were drawn:

1. The fragmentation of nanotubes likely contributed to its retention in solution during the ultracentrifugation step due to a decrease in the terminal velocity.
2. Because there were no changes in the behavior of CTAB nor PVP, the two act as they normally would individually in the presence of nanotubes thus it is CTAB that adsorbs to the surface of nanotubes through hydrophobic interactions while PVP remains as a separate entity in solution.
3. Working in acidic conditions, hydronium ions are likely adsorbing onto the surface of nanotubes in addition to CTAB.
4. Nanotubes are decreasing the viscosity of large polymers by reducing the extent of intermolecular entanglement between different chains thereby allowing polymers to align more readily to shearing forces.

With regards to the second point above, because PVP and CTAB acted without the influence of the other in the presence of nanotubes, PVP is augmenting nanotube dispersion through a physical mechanism. It was stated previously that dispersions were most amplified when PVP10 was used as the molecular weight of choice. After reviewing prior research by Smith *et al.* (1996), PVP10 was noticed to possess a hydrodynamic radius very close to that of the minimum separation distance required in order for nanotubes to not be attracted to one another. Bandyopadhyaya *et al.* (2002) also noted that steric repulsion only occurs at a distance twice that of the radius of gyration for

polymers therefore PVP10 possesses the exact size requirements to drive nanotubes through steric repulsion.²⁰⁰ This served to explain why PVP3.5 and PVP8 were ineffective at dispersing nanotubes as they both possessed smaller hydrodynamic radii however this reason doesn't explain why PVP360 and PVP1300 were poor as well. From there, an approximation analysis of the contact area between a single polymer and the nanotube was done and revealed that PVP360 and PVP1300 in fact behaved under the same mechanism as PVP10. More specifically, when the amount of each molecular weight of PVP was multiplied by the hydrodynamic radius of either PVP10, PVP40, PVP360 or PVP1300, their respective dispersion trends overlapped. The fact that PVP360 and PVP1300 are poorer on the basis of concentration was attributed to the fact that at any given concentration, there would be more chains of the smaller polymer in solution (given the differences in mass) therefore there was a greater total amount of potential contact when using smaller polymers such as PVP10 or PVP40. In addition, PVP360 and PVP1300 are much larger, therefore they would overlap with each other more readily at low concentrations.

Overall, PVP appears to be augmenting a normal CTAB-PVP dispersion system by physically buffering its presence. This result brings great potential for the use of carbon nanotubes in a variety of applications as aqueous processing is one of the most preliminary steps in customizing products for its desired use. PVP is a cheap and readily available polymer and has been shown to possess no interactive ability with alkylammonium surfactants such as CTAB. Nevertheless, it's important to investigate and further diversify the potential of this system to develop a more well-rounded understanding. This thesis will conclude by presenting potential follow-up experiments to build on what was learned here.

5.1 Future Directions

In response to the above, the following experiments are recommended below:

- Based on the results of the pH, it would be insightful to further investigate the exact nature of hydrogen adsorption onto the nanotube surface in the presence of a cationic surfactant such as CTAB. In relation, Grunlan *et al.* (2006) noted that increases in pH led to poly(acrylic acid) being better able to interact with nanotubes. Thus, a dispersion study carried at different pH values is suggested.
- Reports by Granite *et al.* (2012) and by Dror *et al.* (2005) have reported on the likely conformation of polymer molecules in solution in the presence of nanotubes however none of these were in the presence of a surfactant. Despite DLS results showing no significant

changes in size, it may still be advantageous to perform small angle neutron scattering to reaffirm these results.

- PVP is one of many hydrophilic polymers. The effects of other hydrophilic polymers such as polyethylene oxide and polyvinyl alcohol. The use of polypyrrole or polypyridine may also be insightful due to similarities in structure.
- It was suggested that the counter-ion of CTAB, bromide, may be playing an important role in the behavior of the system. The effects of other alkylammoniumhalide surfactant variants possessing different counter-ions and a different chain length can be tested as well.

References

1. Khare, R. & Bose, S. Carbon Nanotube Based Composites- A Review. *J. Miner. Mater. Charact. Eng.* **04**, 31 (2005).
2. Spitalsky, Z., Tasis, D., Papagelis, K. & Galiotis, C. Carbon nanotube–polymer composites: Chemistry, processing, mechanical and electrical properties. *Prog. Polym. Sci.* **35**, 357–401 (2010).
3. Bandaru, P. R. Electrical Properties and Applications of Carbon Nanotube Structures. *J. Nanosci. Nanotechnol.* **7**, 1239–1267 (2007).
4. Yao, Z., Kane, C. L. & Dekker, C. High-Field Electrical Transport in Single-Wall Carbon Nanotubes. *Phys. Rev. Lett.* **84**, 2941–2944 (2000).
5. Ajayan, P. M. & Tour, J. M. Materials Science: Nanotube composites. *Nature* **447**, 1066–1068 (2007).
6. Zhang, X. *et al.* Optically- and Thermally-Responsive Programmable Materials Based on Carbon Nanotube-Hydrogel Polymer Composites. *Nano Lett.* **11**, 3239–3244 (2011).
7. Dai, G.-P., Liu, C., Liu, M., Wang, M.-Z. & Cheng, H.-M. Electrochemical Hydrogen Storage Behavior of Ropes of Aligned Single-Walled Carbon Nanotubes. *Nano Lett.* **2**, 503–506 (2002).
8. Liu, C. *et al.* Hydrogen Storage in Single-Walled Carbon Nanotubes at Room Temperature. *Science* **286**, 1127–1129 (1999).
9. Herrera, J. E., Isimjan, T. T., Abdullahi, I., Ray, A. & Rohani, S. A novel nanoengineered VO_x catalyst supported on highly ordered TiO₂ nanotube arrays for partial oxidation reactions. *Appl. Catal. Gen.* **417–418**, 13–18 (2012).
10. Strano, M. S. *et al.* The Role of Surfactant Adsorption during Ultrasonication in the Dispersion of Single-Walled Carbon Nanotubes. *J. Nanosci. Nanotechnol.* **3**, 81–86 (2003).
11. Ghosh, S., Bachilo, S. M. & Weisman, R. B. Advanced sorting of single-walled carbon nanotubes by nonlinear density-gradient ultracentrifugation. *Nat. Nanotechnol.* **5**, 443–450 (2010).
12. Tsuchiya, K. *et al.* High Purity and Yield Separation of Semiconducting Single-Walled Carbon Nanotubes Dispersed in Aqueous Solutions with Density Gradient Ultracentrifugation Using Mixed Dispersants of Polysaccharides and Surfactants. *Jpn. J. Appl. Phys.* **52**, 035102 (2013).
13. Ning, J., Zhang, J., Pan, Y. & Guo, J. Surfactants assisted processing of carbon nanotube-reinforced SiO₂ matrix composites. *Ceram. Int.* **30**, 63–67 (2004).
14. Davis, T. J., Zhang, J. & Herrera, J. E. Surfactant Assisted Incorporation of Single-Walled Carbon Nanotubes into a Chitosan-Polyvinylpyrrolidone Polymer. *J. Nanoeng. Nanomanufacturing* **1**, 320–324 (2011).
15. Maity, A., Sinha Ray, S. & Hato, M. J. The bulk polymerisation of N-vinylcarbazole in the presence of both multi- and single-walled carbon nanotubes: A comparative study. *Polymer* **49**, 2857–2865 (2008).
16. Iijima, S. Helical microtubules of graphitic carbon. *Nature* **354**, 56–58 (1991).

17. Ajayan, P. M., Stephan, O., Colliex, C. & Trauth, D. Aligned Carbon Nanotube Arrays Formed by Cutting a Polymer Resin-Nanotube Composite. *Science* **265**, 1212–1214 (1994).
18. Kroto, H. W., Heath, J. R., O'Brien, S. C., Curl, R. F. & Smalley, R. E. C60: Buckminsterfullerene. *Nature* **318**, 162–163 (1985).
19. Thostenson, E. T., Ren, Z. & Chou, T.-W. Advances in the science and technology of carbon nanotubes and their composites: A review. *Compos. Sci. Technol.* **61**, 1899–1912 (2001).
20. Dresselhaus, M. S., Dresselhaus, G. & Saito, R. Physics of carbon nanotubes. *Carbon* **33**, 883–891 (1995).
21. Baughman, R. H. Carbon Nanotubes--the Route Toward Applications. *Science* **297**, 787–792 (2002).
22. Garg, A. & Sinnott, S. B. Effect of chemical functionalization on the mechanical properties of carbon nanotubes. *Chem. Phys. Lett.* **295**, 273–278 (1998).
23. Mintmire, J. W., Dunlap, B. I. & White, C. T. Are fullerene tubules metallic? *Phys. Rev. Lett.* **68**, 631–634 (1992).
24. Hong, S. & Myung, S. Nanotube Electronics: A flexible approach to mobility. *Nat. Nanotechnol.* **2**, 207–208 (2007).
25. Kim, H. M. *et al.* Charge transport properties of composites of multiwalled carbon nanotube with metal catalyst and polymer: application to electromagnetic interference shielding. *Curr. Appl. Phys.* **4**, 577–580 (2004).
26. Pötschke, P., Bhattacharyya, A. R. & Janke, A. Carbon nanotube-filled polycarbonate composites produced by melt mixing and their use in blends with polyethylene. *Carbon* **42**, 965–969 (2004).
27. Bauhofer, W. & Kovacs, J. Z. A review and analysis of electrical percolation in carbon nanotube polymer composites. *Compos. Sci. Technol.* **69**, 1486–1498 (2009).
28. Shulaker, M. M. *et al.* Carbon nanotube computer. *Nature* **501**, 526–530 (2013).
29. Reich, S., Thomsen, C. & Ordejón, P. Electronic band structure of isolated and bundled carbon nanotubes. *Phys. Rev. B* **65**, 155411 (2002).
30. Anantram, M. P. Physics of carbon nanotube electronic devices. *Rep. Prog. Phys.* **69**, 507–561 (2006).
31. Dergan, A. Electronic and transport properties of carbon nanotubes. *Univ. Ljubl.* 2–6 (2010).
32. Saito, R., Fujita, M., Dresselhaus, G. & Dresselhaus, M. S. Electronic structure of chiral graphene tubules. *Appl. Phys. Lett.* **60**, 2204–2206 (1992).
33. Cabria, I., Mintmire, J. W. & White, C. T. Metallic and semiconducting narrow carbon nanotubes. *Phys. Rev. B* **67**, 121406 (2003).
34. Weisman, R. B. & Subramoney, S. Carbon nanotubes. *INTERFACE-PENNINGTON-* **15**, 42 (2006).
35. Futaba, D. N. *et al.* Shape-engineerable and highly densely packed single-walled carbon nanotubes and their application as super-capacitor electrodes. *Nat. Mater.* **5**, 987–994 (2006).

36. Schaefer, D. W. *et al.* Structure and dispersion of carbon nanotubes. *J. Appl. Crystallogr.* **36**, 553–557 (2003).
37. Treacy, M. M. J., Ebbesen, T. W. & Gibson, J. M. Exceptionally high Young's modulus observed for individual carbon nanotubes. *Nature* **381**, 678–680 (1996).
38. Wong, E. W., Sheehan, P. E. & Lieber, C. M. Nanobeam Mechanics: Elasticity, Strength, and Toughness of Nanorods and Nanotubes. *Science* **277**, 1971–1975 (1997).
39. Krishnan, A., Dujardin, E., Ebbesen, T. W., Yianilos, P. N. & Treacy, M. M. J. Young's modulus of single-walled nanotubes. *Phys. Rev. B* **58**, 14013–14019 (1998).
40. Li, F., Cheng, H. M., Bai, S., Su, G. & Dresselhaus, M. S. Tensile strength of single-walled carbon nanotubes directly measured from their macroscopic ropes. *Appl. Phys. Lett.* **77**, 3161–3163 (2000).
41. Yu, M.-F. *et al.* Strength and Breaking Mechanism of Multiwalled Carbon Nanotubes Under Tensile Load. *Science* **287**, 637–640 (2000).
42. Yu, M.-F., Files, B. S., Arepalli, S. & Ruoff, R. S. Tensile Loading of Ropes of Single Wall Carbon Nanotubes and their Mechanical Properties. *Phys. Rev. Lett.* **84**, 5552–5555 (2000).
43. Modulus of Elasticity - Young Modulus for some common Materials. at http://www.engineeringtoolbox.com/young-modulus-d_417.html
44. Popov, M., Kyotani, M., Nemanich, R. J. & Koga, Y. Superhard phase composed of single-wall carbon nanotubes. *Phys. Rev. B* **65**, 033408 (2002).
45. Di, J. *et al.* Ultrastrong, Foldable, and Highly Conductive Carbon Nanotube Film. *ACS Nano* **6**, 5457–5464 (2012).
46. Wang, X. Ultrastrong, Stiff and Multifunctional Carbon Nanotube Composites. **1**, 19–25 (2013).
47. Sobolkina, A. *et al.* Dispersion of carbon nanotubes and its influence on the mechanical properties of the cement matrix. *Cem. Concr. Compos.* **34**, 1104–1113 (2012).
48. Huang, Y. *et al.* Poly(vinyl pyrrolidone) wrapped multi-walled carbon nanotube/poly(vinyl alcohol) composite hydrogels. *Compos. Part Appl. Sci. Manuf.* **42**, 1398–1405 (2011).
49. Coleman, J. N., Khan, U., Blau, W. J. & Gun'ko, Y. K. Small but strong: A review of the mechanical properties of carbon nanotube–polymer composites. *Carbon* **44**, 1624–1652 (2006).
50. Kim, P., Shi, L., Majumdar, A. & McEuen, P. L. Thermal transport measurements of individual multiwalled nanotubes. *Phys. Rev. Lett.* **87**, (2001).
51. Pop, E., Mann, D., Wang, Q., Goodson, K. & Dai, H. Thermal Conductance of an Individual Single-Wall Carbon Nanotube above Room Temperature. *ArXivcond-Mat0512624* (2005). at <http://arxiv.org/abs/cond-mat/0512624>
52. Anthony, T. R. *et al.* Thermal diffusivity of isotopically enriched ¹²C diamond. *Phys. Rev. B* **42**, 1104–1111 (1990).
53. Thermal Conductivity In Advanced Chips | Solid State Technology. at <http://electroiq.com/blog/2005/07/thermal-conductivity-in-advanced-chips/>

54. Young, H. D. in *Univ. Phys.*
55. Berber, S., Kwon, Y.-K. & Tománek, D. Unusually High Thermal Conductivity of Carbon Nanotubes. *Phys. Rev. Lett.* **84**, 4613–4616 (2000).
56. Gojny, F. H. *et al.* Evaluation and identification of electrical and thermal conduction mechanisms in carbon nanotube/epoxy composites. *Polymer* **47**, 2036–2045 (2006).
57. Han, Z. & Fina, A. Thermal conductivity of carbon nanotubes and their polymer nanocomposites: A review. *Prog. Polym. Sci.* **36**, 914–944 (2011).
58. Matarredona, O. *et al.* Dispersion of Single-Walled Carbon Nanotubes in Aqueous Solutions of the Anionic Surfactant NaDDBS. *J. Phys. Chem. B* **107**, 13357–13367 (2003).
59. Kyrilyuk, A. V. & van der Schoot, P. Continuum percolation of carbon nanotubes in polymeric and colloidal media. *Proc. Natl. Acad. Sci.* **105**, 8221–8226 (2008).
60. Girifalco, L. A., Hodak, M. & Lee, R. S. Carbon nanotubes, buckyballs, ropes, and a universal graphitic potential. *Phys. Rev. B* **62**, 13104 (2000).
61. Nativ-Roth, E. *et al.* Physical Adsorption of Block Copolymers to SWNT and MWNT: A Nonwrapping Mechanism. *Macromolecules* **40**, 3676–3685 (2007).
62. Sahoo, N. G., Rana, S., Cho, J. W., Li, L. & Chan, S. H. Polymer nanocomposites based on functionalized carbon nanotubes. *Prog. Polym. Sci.* **35**, 837–867 (2010).
63. Szleifer, I. Polymers and carbon nanotubes—dimensionality, interactions and nanotechnology. *Polymer* **46**, 7803–7818 (2005).
64. Angelikopoulos, P. & Bock, H. The science of dispersing carbon nanotubes with surfactants. *Phys. Chem. Chem. Phys.* **14**, 9546–9557 (2012).
65. Kim, K. K. *et al.* Design of Dispersants for the Dispersion of Carbon Nanotubes in an Organic Solvent. *Adv. Funct. Mater.* **17**, 1775–1783 (2007).
66. Bahr, J. L., Mickelson, E. T., Bronikowski, M. J., Smalley, R. E. & Tour, J. M. Dissolution of small diameter single-wall carbon nanotubes in organic solvents? *Chem. Commun.* 193–194 (2001). doi:10.1039/b008042j
67. Ausman, K. D., Piner, R., Lourie, O., Ruoff, R. S. & Korobov, M. Organic Solvent Dispersions of Single-Walled Carbon Nanotubes: Toward Solutions of Pristine Nanotubes. *J. Phys. Chem. B* **104**, 8911–8915 (2000).
68. Rouse, J. H. Polymer-Assisted Dispersion of Single-Walled Carbon Nanotubes in Alcohols and Applicability toward Carbon Nanotube/Sol–Gel Composite Formation. *Langmuir* **21**, 1055–1061 (2005).
69. Kataura, H. *et al.* Optical properties of single-wall carbon nanotubes. *Synth. Met.* **103**, 2555–2558 (1999).
70. Bachilo, S. M. *et al.* Structure-Assigned Optical Spectra of Single-Walled Carbon Nanotubes. *Science* **298**, 2361–2366 (2002).

71. Weisman, R. B. & Bachilo, S. M. Dependence of Optical Transition Energies on Structure for Single-Walled Carbon Nanotubes in Aqueous Suspension: An Empirical Kataura Plot. *Nano Lett.* **3**, 1235–1238 (2003).
72. Tan, Y. & Resasco, D. E. Dispersion of Single-Walled Carbon Nanotubes of Narrow Diameter Distribution. *J. Phys. Chem. B* **109**, 14454–14460 (2005).
73. Attal, S., Thiruvengadathan, R. & Regev, O. Determination of the Concentration of Single-Walled Carbon Nanotubes in Aqueous Dispersions Using UV–Visible Absorption Spectroscopy. *Anal. Chem.* **78**, 8098–8104 (2006).
74. Blanch, A. J., Lenehan, C. E. & Quinton, J. S. Parametric analysis of sonication and centrifugation variables for dispersion of single walled carbon nanotubes in aqueous solutions of sodium dodecylbenzene sulfonate. *Carbon* **49**, 5213–5228 (2011).
75. Haggemueller, R. *et al.* Comparison of the Quality of Aqueous Dispersions of Single Wall Carbon Nanotubes Using Surfactants and Biomolecules. *Langmuir* **24**, 5070–5078 (2008).
76. Wenseleers, W. *et al.* Efficient Isolation and Solubilization of Pristine Single-Walled Nanotubes in Bile Salt Micelles. *Adv. Funct. Mater.* **14**, 1105–1112 (2004).
77. Fantini, C. *et al.* Investigation of the light emission efficiency of single-wall carbon nanotubes wrapped with different surfactants. *Chem. Phys. Lett.* **473**, 96–101 (2009).
78. Xie, X.-L., Mai, Y.-W. & Zhou, X.-P. Dispersion and alignment of carbon nanotubes in polymer matrix: A review. *Mater. Sci. Eng. R Rep.* **49**, 89–112 (2005).
79. Hilding, J., Grulke, E. A., George Zhang, Z. & Lockwood, F. Dispersion of Carbon Nanotubes in Liquids. *J. Dispers. Sci. Technol.* **24**, 1–41 (2003).
80. Qian, D., Dickey, E. C., Andrews, R. & Rantell, T. Load transfer and deformation mechanisms in carbon nanotube-polystyrene composites. *Appl. Phys. Lett.* **76**, 2868–2870 (2000).
81. Badaire, S., Poulin, P., Maugey, M. & Zakri, C. In Situ Measurements of Nanotube Dimensions in Suspensions by Depolarized Dynamic Light Scattering. *Langmuir* **20**, 10367–10370 (2004).
82. Sandler, J. *et al.* Development of a dispersion process for carbon nanotubes in an epoxy matrix and the resulting electrical properties. *Polymer* **40**, 5967–5971 (1999).
83. Huang, Y. Y. & Terentjev, E. M. Dispersion of Carbon Nanotubes: Mixing, Sonication, Stabilization, and Composite Properties. *Polymers* **4**, 275–295 (2012).
84. Kharisov, B. I., Kharissova, O. V., Leija Gutierrez, H. & Ortiz Méndez, U. Recent Advances on the Soluble Carbon Nanotubes. *Ind. Eng. Chem. Res.* **48**, 572–590 (2009).
85. Vaisman, L., Wagner, H. D. & Marom, G. The role of surfactants in dispersion of carbon nanotubes. *Adv. Colloid Interface Sci.* **128-130**, 37–46 (2006).
86. Zhao, W., Song, C. & Pehrsson, P. E. Water-soluble and optically pH-sensitive single-walled carbon nanotubes from surface modification. *J. Am. Chem. Soc.* **124**, 12418–12419 (2002).

87. Alvaro, M. *et al.* Synthesis, Photochemistry, and Electrochemistry of Single-Wall Carbon Nanotubes with Pendent Pyridyl Groups and of Their Metal Complexes with Zinc Porphyrin. Comparison with Pyridyl-Bearing Fullerenes. *J. Am. Chem. Soc.* **128**, 6626–6635 (2006).
88. Bahr, J. L. & Tour, J. M. Covalent chemistry of single-wall carbon nanotubes. *J. Mater. Chem.* **12**, 1952–1958 (2002).
89. Zhou, W. *et al.* Structural characterization and diameter-dependent oxidative stability of single wall carbon nanotubes synthesized by the catalytic decomposition of CO. *Chem. Phys. Lett.* **350**, 6–14 (2001).
90. Rinzler, A. g. *et al.* Large-scale purification of single-wall carbon nanotubes: process, product, and characterization. *Appl. Phys. Mater. Sci. Process.* **67**, 29 (1998).
91. Du, J.-H. The present status and key problems of carbon nanotube based polymer composites. *EXPRESS Polym. Lett.* **1**, 253–273 (2007).
92. Brinker, C. J., Lu, Y., Sellinger, A. & Fan, H. Evaporation-induced self-assembly: nanostructures made easy. *Adv. Mater.* **11**, 579–585 (1999).
93. Feitosa, E. *et al.* Structural organization of cetyltrimethylammonium sulfate in aqueous solution: The effect of Na₂SO₄. *J. Colloid Interface Sci.* **299**, 883–889 (2006).
94. Joshi, J. V., Aswal, V. K., Bahadur, P. & Goyal, P. S. Role of counterion of the surfactant molecule on the micellar structure in aqueous solution. *Curr. Sci.-BANGALORE-* **83**, 47–49 (2002).
95. Aswal, V. K. Role of different counterions and size of micelle in concentration dependence micellar structure of ionic surfactants. *Chem. Phys. Lett.* **368**, 59–65
96. Yurekli, K., Mitchell, C. A. & Krishnamoorti, R. Small-Angle Neutron Scattering from Surfactant-Assisted Aqueous Dispersions of Carbon Nanotubes. *J. Am. Chem. Soc.* **126**, 9902–9903 (2004).
97. Jiang, L., Gao, L. & Sun, J. Production of aqueous colloidal dispersions of carbon nanotubes. *J. Colloid Interface Sci.* **260**, 89–94 (2003).
98. Zhang, Y., Yuan, S., Zhou, W., Xu, J. & Li, Y. Spectroscopic evidence and molecular simulation investigation of the pi-pi interaction between pyrene molecules and carbon nanotubes. *J. Nanosci. Nanotechnol.* **7**, 2366–2375 (2007).
99. Lu, Q. *et al.* RNA Polymer Translocation with Single-Walled Carbon Nanotubes. *Nano Lett.* **4**, 2473–2477 (2004).
100. Moore, V. C. *et al.* Individually Suspended Single-Walled Carbon Nanotubes in Various Surfactants. *Nano Lett.* **3**, 1379–1382 (2003).
101. O’Connell, M. J. *et al.* Band Gap Fluorescence from Individual Single-Walled Carbon Nanotubes. *Science* **297**, 593–596 (2002).
102. Xin, X., Xu, G. & Li, H. in *Phys. Chem. Prop. Carbon Nanotub.* (ed. Suzuki, S.) (InTech, 2013). at <<http://www.intechopen.com/books/physical-and-chemical-properties-of-carbon-nanotubes/dispersion-and-property-manipulation-of-carbon-nanotubes-by-self-assemblies-of-amphiphilic-molecules>>

103. Thomassin, J.-M., Huynen, I., Jerome, R. & Detrembleur, C. Functionalized polypropylenes as efficient dispersing agents for carbon nanotubes in a polypropylene matrix; application to electromagnetic interference (EMI) absorber materials. *Polymer* **51**, 115–121 (2010).
104. Blanch, A. J., Lenehan, C. E. & Quinton, J. S. Optimizing Surfactant Concentrations for Dispersion of Single-Walled Carbon Nanotubes in Aqueous Solution. *J. Phys. Chem. B* **114**, 9805–9811 (2010).
105. Ishibashi, A. & Nakashima, N. Individual Dissolution of Single-Walled Carbon Nanotubes in Aqueous Solutions of Steroid or Sugar Compounds and Their Raman and Near-IR Spectral Properties. *Chem. – Eur. J.* **12**, 7595–7602 (2006).
106. Lin, S. & Blankschtein, D. Role of the Bile Salt Surfactant Sodium Cholate in Enhancing the Aqueous Dispersion Stability of Single-Walled Carbon Nanotubes: A Molecular Dynamics Simulation Study. *J. Phys. Chem. B* **114**, 15616–15625 (2010).
107. Shigeta, M., Komatsu, M. & Nakashima, N. Individual solubilization of single-walled carbon nanotubes using totally aromatic polyimide. *Chem. Phys. Lett.* **418**, 115–118 (2006).
108. Teraoka, I. *Polymer Solutions: An Introduction to Physical Properties*. (John Wiley & Sons, 2002).
109. Mutch, K. J., Duijneveldt, J. S. van & Eastoe, J. Colloid–polymer mixtures in the protein limit. *Soft Matter* **3**, 155–167 (2007).
110. Ying, Q. & Chu, B. Overlap concentration of macromolecules in solution. *Macromolecules* **20**, 362–366 (1987).
111. Clasen, C. *et al.* How dilute are dilute solutions in extensional flows? *J. Rheol.* **50**, 849 (2006).
112. Daoud, M. *et al.* Solutions of Flexible Polymers. Neutron Experiments and Interpretation. *Macromolecules* **8**, 804–818 (1975).
113. Graessley, W. W. Polymer chain dimensions and the dependence of viscoelastic properties on concentration, molecular weight and solvent power. *Polymer* **21**, 258–262 (1980).
114. O’Connell, M. J. *et al.* Reversible water-solubilization of single-walled carbon nanotubes by polymer wrapping. *Chem. Phys. Lett.* **342**, 265–271 (2001).
115. Bury, R., Desmazières, B. & Treiner, C. Interactions between poly(vinylpyrrolidone) and ionic surfactants at various solid/water interfaces: a calorimetric investigation. *Colloids Surf. Physicochem. Eng. Asp.* **127**, 113–124 (1997).
116. Wang, G. & Olofsson, G. Titration Calorimetric Study of the Interaction between Ionic Surfactants and Uncharged Polymers in Aqueous Solution. *J. Phys. Chem. B* **102**, 9276–9283 (1998).
117. Pei, X., Hu, L., Liu, W. & Hao, J. Synthesis of water-soluble carbon nanotubes via surface initiated redox polymerization and their tribological properties as water-based lubricant additive. *Eur. Polym. J.* **44**, 2458–2464 (2008).
118. Cheng, F. Soluble, Discrete Supramolecular Complexes of Single-Walled Carbon Nanotubes with Fluorene-Based Conjugated Polymers. *Macromolecules* **41**, 2304–2308
119. Yang, L. *et al.* In situ synthesis of amylose/single-walled carbon nanotubes supramolecular assembly. *Carbohydr. Res.* **343**, 2463–2467 (2008).

120. Chou, S. G. *et al.* Phonon-Assisted Excitonic Recombination Channels Observed in DNA-Wrapped Carbon Nanotubes Using Photoluminescence Spectroscopy. *Phys. Rev. Lett.* **94**, 127402 (2005).
121. Zheng, M. *et al.* DNA-assisted dispersion and separation of carbon nanotubes. *Nat. Mater.* **2**, 338–342 (2003).
122. Pedersen, J. S. Form factors of block copolymer micelles with spherical, ellipsoidal and cylindrical cores. *J. Appl. Crystallogr.* **33**, 637–640 (2000).
123. Dror, Y., Pyckhout-Hintzen, W. & Cohen, Y. Conformation of Polymers Dispersing Single-Walled Carbon Nanotubes in Water: A Small-Angle Neutron Scattering Study. *Macromolecules* **38**, 7828–7836 (2005).
124. Cotiuga, I. *et al.* Block-Copolymer-Assisted Solubilization of Carbon Nanotubes and Exfoliation Monitoring Through Viscosity. *Macromol. Rapid Commun.* **27**, 1073–1078 (2006).
125. Manivannan, S. *et al.* Dispersion of single-walled carbon nanotubes in aqueous and organic solvents through a polymer wrapping functionalization. *J. Mater. Sci. Mater. Electron.* **20**, 223–229 (2009).
126. Gong, X., Liu, J., Baskaran, S., Voise, R. D. & Young, J. S. Surfactant-Assisted Processing of Carbon Nanotube/Polymer Composites. *Chem. Mater.* **12**, 1049–1052 (2000).
127. Fukushima, T. *et al.* Molecular Ordering of Organic Molten Salts Triggered by Single-Walled Carbon Nanotubes. *Science* **300**, 2072–2074 (2003).
128. Bellayer, S. *et al.* Preparation of Homogeneously Dispersed Multiwalled Carbon Nanotube/Polystyrene Nanocomposites via Melt Extrusion Using Trialkyl Imidazolium Compatibilizer. *Adv. Funct. Mater.* **15**, 910–916 (2005).
129. Ma, P.-C., Siddiqui, N. A., Marom, G. & Kim, J.-K. Dispersion and functionalization of carbon nanotubes for polymer-based nanocomposites: A review. *Compos. Part Appl. Sci. Manuf.* **41**, 1345–1367 (2010).
130. Qiu, P. & Mao, C. Viscosity Gradient as a Novel Mechanism for the Centrifugation-Based Separation of Nanoparticles. *Adv. Mater.* **23**, 4880–4885 (2011).
131. Hároz, E. H. *et al.* Enrichment of Armchair Carbon Nanotubes *via* Density Gradient Ultracentrifugation: Raman Spectroscopy Evidence. *ACS Nano* **4**, 1955–1962 (2010).
132. Tucker, W. B. Surface Tension by Pendant Drops. (1938). at <<https://dspace.mit.edu/bitstream/handle/1721.1/44474/35158026.pdf?sequence=1>>
133. Woodward, R. P. Surface Tension Measurements Using the Drop Shape Method. at <<http://www.firsttenangstroms.com/pdfdocs/STPaper.pdf>>
134. Dinh, S. M. & Armstrong, R. C. A Rheological Equation of State for Semiconcentrated Fiber Suspensions. *J. Rheol. 1978-Present* **28**, 207–227 (1984).
135. Ahmad, B., Ahmad, N., Saeed, A. & Nazar, U.-I. Rheology of Poly(Vinyl Pyrrolidone) in Aqueous and Organic Media. *Jour. Chem. Soc. Pak* **17**, 7–10 (1991).
136. Grady, B. P. The Use of Solution Viscosity to Characterize Single-Walled Carbon Nanotube Dispersions. *Macromol. Chem. Phys.* **207**, 2167–2169 (2006).

137. Fan, Z. Rheology of multiwall carbon nanotube suspensions. **51**, 585–604 (2007).
138. Cowie, J. M. G. *Polymers: Chemistry and Physics of Modern Materials, 2nd Edition*. (CRC Press, 1991).
139. Manual, I. BI-FOQELS. at <<http://www.ceic.unsw.edu.au/centers/Partcat/facilities/FOQELS.pdf>>
140. Chowdhury, D. F. & Cui, Z. F. Carbon nanotube length reduction techniques, and characterisation of oxidation state using quasi-elastic light scattering. *Carbon* **49**, 862–868 (2011).
141. Finsy, R. Particle sizing by quasi-elastic light scattering. *Adv. Colloid Interface Sci.* **52**, 79–143 (1994).
142. Maeda, T. & Fujime, S. Spectrum of light quasielastically scattered from solutions of very long rods at dilute and semidilute regimes. *Macromolecules* **17**, 1157–1167 (1984).
143. Shetty, A. M., Wilkins, G. M. H., Nanda, J. & Solomon, M. J. Multiangle Depolarized Dynamic Light Scattering of Short Functionalized Single-Walled Carbon Nanotubes. *J. Phys. Chem. C* **113**, 7129–7133 (2009).
144. Filliben, J. J. & McKinney, J. E. *Confidence limits for the abscissa of intersection of two linear regressions*. (National Bureau of Standards, 1972). at <<http://archive.org/details/jresv76Bn3-4p179>>
145. Hennrich, F. *et al.* Raman Spectroscopy of Individual Single-Walled Carbon Nanotubes from Various Sources. *J. Phys. Chem. B* **109**, 10567–10573 (2005).
146. Brenntag Specialties. PVP (Polyvinylpyrrolidone). at <http://www.brenntag specialties.com/en/downloads/Products/Multi_Market_Principals/Ashland/VP_-_PVP_VA/PVP_Brochure.pdf>
147. Qi, X., Wang, P., Ji, L., Tan, X. & Ouyang, L. 分散剂 CTAB 对碳纳米管悬浮液分散性能的影响. *J. Inorg. Mater.* **22**, 1122–1126 (2007).
148. Hadjiev, V. G., Iliiev, M. N., Arepalli, S., Nikolaev, P. & Files, B. S. Raman scattering test of single-wall carbon nanotube composites. *Appl. Phys. Lett.* **78**, 3193–3195 (2001).
149. Islam, M. F., Rojas, E., Bergey, D. M., Johnson, A. T. & Yodh, A. G. High Weight Fraction Surfactant Solubilization of Single-Wall Carbon Nanotubes in Water. *Nano Lett.* **3**, 269–273 (2003).
150. Heller, D. A. *et al.* Concomitant Length and Diameter Separation of Single-Walled Carbon Nanotubes. *J. Am. Chem. Soc.* **126**, 14567–14573 (2004).
151. Su, Z., Mui, K., Daub, E., Leung, T. & Honek, J. Single-Walled Carbon Nanotube Binding Peptides: Probing Tryptophan's Importance by Unnatural Amino Acid Substitution. *J. Phys. Chem. B* **111**, 14411–14417 (2007).
152. Yehia, H. N. *et al.* Single-walled carbon nanotube interactions with HeLa cells. *J. Nanobiotechnology* **5**, 8 (2007).
153. Elgrabli, D. Effect of BSA on carbon nanotube dispersion for in vivo and in vitro studies. *Nanotoxicology* **1**, 266–278 (2007).
154. Hecht, D., Hu, L. & Gruner, G. Conductivity scaling with bundle length and diameter in single walled carbon nanotube networks. *Appl. Phys. Lett.* **89**, 133112–133112–3 (2006).

155. Paredes, J. I. & Burghard, M. Dispersions of Individual Single-Walled Carbon Nanotubes of High Length. *Langmuir* **20**, 5149–5152 (2004).
156. Duggal, R. & Pasquali, M. Dynamics of Individual Single-Walled Carbon Nanotubes in Water by Real-Time Visualization. *Phys. Rev. Lett.* **96**, (2006).
157. Movchan, T. G., Soboleva, I. V., Plotnikova, E. V., Shchekin, A. K. & Rusanov, A. I. Dynamic light scattering study of cetyltrimethylammonium bromide aqueous solutions. *Colloid J.* **74**, 239–247 (2012).
158. Webber, S. E. Polymer Micelles: An Example of Self-Assembling Polymers. *J. Phys. Chem. B* **102**, 2618–2626 (1998).
159. Halperin, A., Tirrell, M. & Lodge, T. P. in *Macromol. Synth. Order Adv. Prop.* 31–71 (Springer Berlin Heidelberg, 1992). at <<http://link.springer.com/chapter/10.1007/BFb0051635>>
160. Tuteja, A., Duxbury, P. M. & Mackay, M. E. Polymer Chain Swelling Induced by Dispersed Nanoparticles. *Phys. Rev. Lett.* **100**, 077801 (2008).
161. Tscharnuter, W. Photon correlation spectroscopy in particle sizing. *Encycl. Anal. Chem.* (2000). at <<http://onlinelibrary.wiley.com/doi/10.1002/9780470027318.a1512/full>>
162. Bryant, G. & Thomas, J. C. Improved Particle Size Distribution Measurements Using Multiangle Dynamic Light Scattering. *Langmuir* **11**, 2480–2485 (1995).
163. Bielska, M. Micellar enhanced ultrafiltration of nitrobenzene and 4-nitrophenol. *J. Membr. Sci.* **243**, 273–281
164. Gravsholt, S. Viscoelasticity in highly dilute aqueous solutions of pure cationic detergents. *J. Colloid Interface Sci.* **57**, 575–577
165. Ray, G. B., Chakraborty, I., Ghosh, S., Moulik, S. P. & Palepu, R. Self-Aggregation of Alkyltrimethylammonium Bromides (C10-, C12-, C14-, and C16TAB) and Their Binary Mixtures in Aqueous Medium: A Critical and Comprehensive Assessment of Interfacial Behavior and Bulk Properties with Reference to Two Types of Micelle Formation. *Langmuir* **21**, 10958–10967 (2005).
166. Khan, M. S., Gul, K. & Rehman, N. U. INTERACTION OF POLYVINYLPIRROLIDONE WITH METAL CHLORIDE AQUEOUS SOLUTIONS INTERACTION OF POLYVINYLPIRROLIDONE WITH METAL CHLORIDE AQUEOUS SOLUTIONS. *高分子科学* **22**, 581–584 (2004).
167. McFarlane, N. L., Wagner, N. J., Kaler, E. W. & Lynch, M. L. Calorimetric Study of the Adsorption of Poly(ethylene oxide) and Poly(vinyl pyrrolidone) onto Cationic Nanoparticles. *Langmuir* **26**, 6262–6267 (2010).
168. Feng, Y. *et al.* Interaction of poly(vinylpyrrolidone) with cationic and nonionic surfactants in aqueous solution studied by ¹H NMR. *Colloid Polym. Sci.* **281**, 902–906 (2003).
169. Wan-Badhi, W. A., Wan-Yunus, W. M. Z., Bloor, D. M., Hall, D. G. & Wyn-Jones, E. Equilibrium and kinetic studies associated with the interaction between sodium dodecyl sulfate and polyvinylpyrrolidone in aqueous solution. *J. Chem. Soc. Faraday Trans.* **89**, 2737–2742 (1993).

170. Ali, M. S., Suhail, M., Ghosh, G., Kamil, M. & Kabir ud, D. Interactions between cationic gemini/conventional surfactants with polyvinylpyrrolidone: Specific conductivity and dynamic light scattering studies. *Colloids Surf. Physicochem. Eng. Asp.* **350**, 51–56 (2009).
171. Rawat, A., Mahavar, H. K., Tanwar, A. & Singh, P. J. Study of electrical properties of polyvinylpyrrolidone/polyacrylamide blend thin films. *Bull. Mater. Sci.* **37**, 273–279 (2014).
172. Yang, Y. J., Li, W. & Zhang, H. Electrodeposition of Polyvinylpyrrolidone-Grafted Multi-Walled Carbon Nanotubes from Dimethylformamide. *Fuller. Nanotub. Carbon Nanostructures* **20**, 743–749 (2012).
173. Mishra, A., Ram, S. & Ghosh, G. Dynamic Light Scattering and Optical Absorption in Biological Nanofluids of Gold Nanoparticles in Poly(vinyl pyrrolidone) Molecules. *J. Phys. Chem. C* **113**, 6976–6982 (2009).
174. Karbowski, M., Cichos, J. & Buczek, K. Interaction of Lanthanide β -Diketonate Complexes with Polyvinylpyrrolidone: Proton-Controlled Switching of Tb³⁺ Luminescence. *J. Phys. Chem. B* **118**, 226–239 (2014).
175. Mishra, A. & Ram, S. Selective Light Emission in Nonbonding Electron Transitions in Poly(vinyl pyrrolidone) Molecules on Spin-Coating in Thin Layers. *J. Phys. Chem. A* **113**, 14067–14073 (2009).
176. Rubingh, D. *Cationic Surfactants: Physical Chemistry*. (CRC Press, 1990).
177. Fried, J. R. *Polymer Science and Technology*. (Prentice Hall Professional Technical Reference, 2003).
178. Sa, V. & Kornev, K. G. Analysis of Stability of Nanotube Dispersions Using Surface Tension Isotherms. *Langmuir* **27**, 13451–13460 (2011).
179. Nikiforova, T. E., Kozlov, V. A. & Islyaikin, M. K. Acid-base interactions and complex formation while recovering copper(II) ions from aqueous solutions using cellulose adsorbent in the presence of polyvinylpyrrolidone. *Russ. J. Phys. Chem. A* **86**, 1836–1846 (2012).
180. Callejas, M. A. Enhanced hydrogen adsorption on single-wall carbon nanotubes by sample reduction. *Mater. Sci. Eng. B* **108**, 120–123
181. Chen, P., Wu, X., Lin, J. & Tan, K. L. High H₂ Uptake by Alkali-Doped Carbon Nanotubes Under Ambient Pressure and Moderate Temperatures. *Science* **285**, 91–93 (1999).
182. Norwood, D. P., Minatti, E. & Reed, W. F. Surfactant/Polymer Assemblies. 1. Surfactant Binding Properties. *Macromolecules* **31**, 2957–2965 (1998).
183. Desbrieres, J., Borsali, R., Rinaudo, M. & Milas, M. χ .F Interaction parameter and the single-chain diffusion coefficients of dextran/poly(vinylpyrrolidone)/water: dynamic light scattering experiments. *Macromolecules* **26**, 2592–2596 (1993).
184. Kim, Y. & Kim, H. Effect of extensional properties of polymer solutions on the droplet formation via ultrasonic atomization. *Polym. Eng. Sci.* **51**, 2446–2452 (2011).
185. Einstein, A. *Ann Phys.* **19**, 1911 (1906).
186. Ge, R. Rheology of Solutions of Polyisophrene and Polyisoprene-Carbon Nanotube Composites. *Univ. West. Ont. - Electron. Thesis Diss. Repos.* (2013). at <<http://ir.lib.uwo.ca/etd/1812>>

187. Pham, G. T. *Characterization and Modeling of Piezo-resistive Properties of Carbon Nanotube-based Conductive Polymer Composites*. (ProQuest, 2008).
188. Néda, Z., Florian, R. & Brechet, Y. Reconsideration of continuum percolation of isotropically oriented sticks in three dimensions. *Phys. Rev. E* **59**, 3717–3719 (1999).
189. Jain, S., Goossens, J. G. P., Peters, G. W. M., Duin, M. van & Lemstra, P. J. Strong decrease in viscosity of nanoparticle-filled polymer melts through selective adsorption. *Soft Matter* **4**, 1848–1854 (2008).
190. Roberts, C., Cosgrove, T., Schmidt, R. G. & Gordon, G. V. Diffusion of Poly(dimethylsiloxane) Mixtures with Silicate Nanoparticles. *Macromolecules* **34**, 538–543 (2001).
191. Xie, X.-L. Rheological and mechanical properties of PVC/CaCO₃ nanocomposites prepared by in situ polymerization. *Polymer* **45**, 6665–6673
192. Tuteja, A., Mackay, M. E., Hawker, C. J. & Van Horn, B. Effect of Ideal, Organic Nanoparticles on the Flow Properties of Linear Polymers: Non-Einstein-like Behavior. *Macromolecules* **38**, 8000–8011 (2005).
193. Papthanasious, T. D. & Guell, D. C. *Flow-Induced Alignment in Composite Materials*. (Elsevier, 1997).
194. Camponeschi, E. *et al.* Uniform Directional Alignment of Single-Walled Carbon Nanotubes in Viscous Polymer Flow. *Langmuir* **22**, 1858–1862 (2006).
195. Troszyn'ska, A., Narolewska, O., Wolejszo, A. & Ostaszyk, A. Effect of carboxymethyl cellulose (CMC) on perception of astringency of phenolic compounds. *Pol. J. Food Nutr. Sci.* **58**, 241–245 (2008).
196. Shirahama, K., Mukae, K. & Iseki, H. A cationic surfactant is bound to poly(vinylpyrrolidone) in high pH media. *Colloid Polym. Sci.* **272**, 493–496 (1994).
197. Grunlan, J. C., Liu, L. & Kim, Y. S. Tunable Single-Walled Carbon Nanotube Microstructure in the Liquid and Solid States Using Poly(acrylic acid). *Nano Lett.* **6**, 911–915 (2006).
198. Smith, J. N., Meadows, J. & Williams, P. A. Adsorption of Polyvinylpyrrolidone onto Polystyrene Latices and the Effect on Colloid Stability. *Langmuir* **12**, 3773–3778 (1996).
199. Weiner, B. B. What is Particle Size? (2010). at http://www.brookhaveninstruments.com/pdf/What_is_Particle_Size.pdf
200. Bandyopadhyaya, R., Nativ-Roth, E., Regev, O. & Yerushalmi-Rozen, R. Stabilization of Individual Carbon Nanotubes in Aqueous Solutions. *Nano Lett.* **2**, 25–28 (2002).
201. Popov, V. L. *Contact Mechanics and Friction: Physical Principles and Applications*. (Springer Science & Business Media, 2010).
202. Geike, T. & Popov, V. L. Mapping of three-dimensional contact problems into one dimension. *Phys. Rev. E* **76**, 036710 (2007).

Appendix 1

GPC

To check the quality of the polymers received from suppliers. Table S 1 below shows the assessment of the different molecular weights ordered from Sigma-Aldrich and Acros Organics:

Sample	Peak Ret. Vol. (mL)	Mn (g/mol)	Mw (g/mol)	Mz (g/mol)	Mp (g/mol)	Mw/Mn	IV (dL/g)	R _H (nm)
3500	22.414	1551	3527	6296	4328	2.279	0.053	1.352
8000	21.723	3568	8009	14 720	7381	2.247	0.068	1.937
10 000	23.694	4359	14 171	37 087	11 340	3.252	0.083	2.432
40 000	22.373	21 516	53 200	131 185	36 236	2.474	0.197	5.078
360 000	19.731	279 736	803 087	2 128 000	448 660	2.872	1.262	22.891
1 300 000	19.862	240 318	605 688	1 395 000	385 208	2.524	1.126	20.383

Table S 1: Summary table of GPC results for the analysis of the different molecular weights of PVP

The distribution of all the polymers is in general agreement with the expected molecular weights provided by the manufacturer, with the exception of PVP1300. It should be noted that PVP3.5 and PVP8 have elution times out of trend from other samples likely because they were ran after the apparatus had undergone maintenance. CTAB alone was also ran before the maintenance occurred and was found to elute at a volume of 29.6 mL. A dispersed nanotube sample in 0.75% PVP10, 0.1% CTAB, and 0.2 g/L SWNT was also injected for separation and characterization via GPC. The outputted data is given in Figure S 1 and Table S 2.

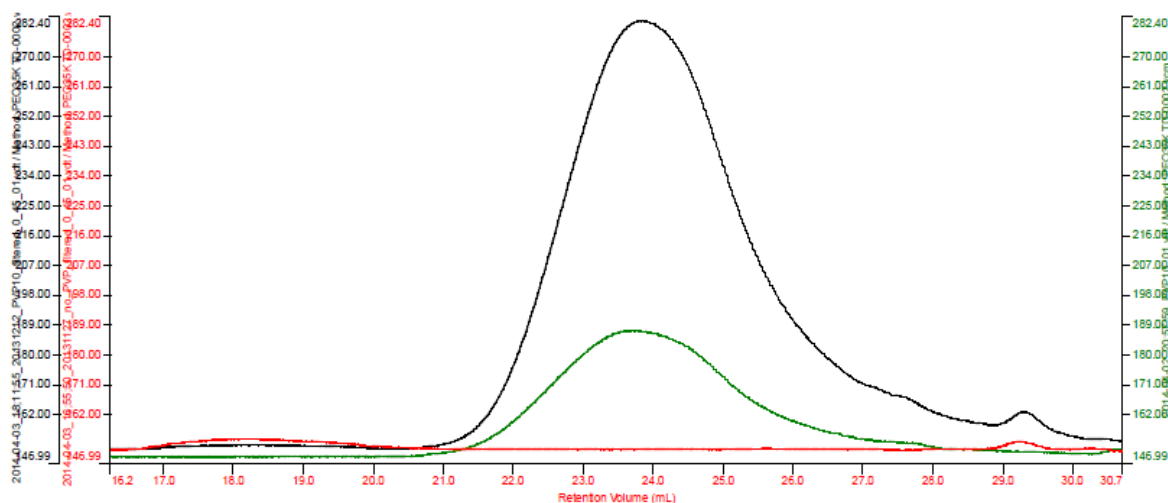


Figure S 1: Obtained chromatogram of 0.75 %wt/v PVP10, 0.1 %wt/v CTAB, and 0.2 g/L SWNT from GPC purification.

Sample	Peak Ret. Vol. (mL)	Mn (g/mol)	Mw (g/mol)	Mz (g/mol)	Mp (g/mol)	Mw/Mn	IV (dL/g)	Concentration (mg/mL)
Peak 1	18.153	358 736	646 103	1 020 000	520 901	1.801	15.526	0.027
Peak 2	23.837	6 056	12 696	28 583	10 301	2.093	0.0761	7.959

Table S 2: Summary table of GPC results for the resolution of SWNT in a dispersed solution of 0.75% PVP10, 0.1% CTAB, and 0.2 g/L SWNT.

Three distributions were detected after the run was complete. Peak 1 appeared at a retention volume of 18.153, Peak 2 appeared at a retention volume of 23.837, while Peak 3 was seen at a retention of approximately 29.4 mL (data not provided by PolyAnalytik). Given the retention times of Peak 2 and Peak 3, these species likely correspond to PVP10 and CTAB. Thus, it is very likely then that Peak 1 represents purified nanotubes. Notable is that there was a detected amount of 0.027 mg/mL whereas the initial concentration was targeted to be 0.2 g/L therefore there is a 10% retention after ultracentrifugation.

Vis-NIR Spectra

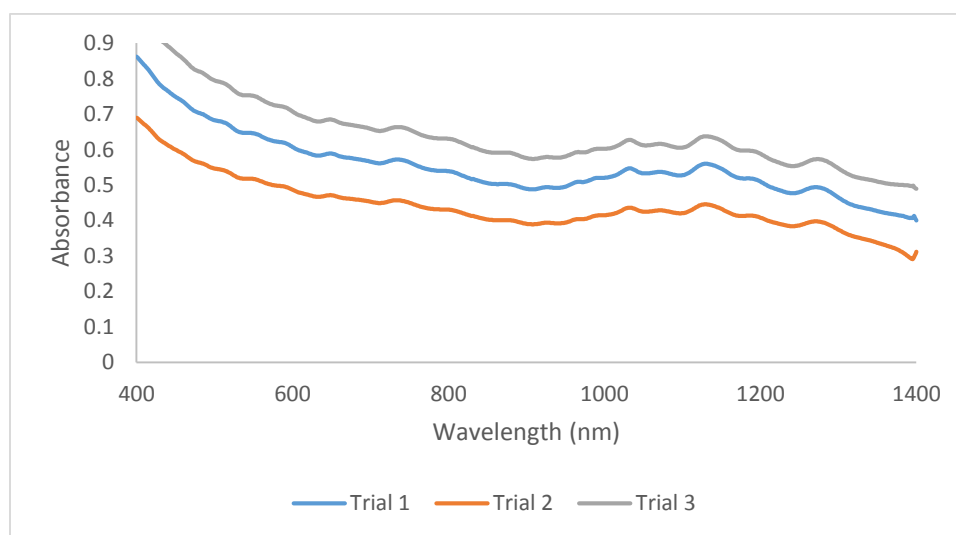


Figure S 2: Three separate trials of dispersions prepared with 0.1 %wt/v CTAB, 6 %wt/v PVP40, and 0.2 g/L SWNT. Shown are triplicates of 0.1 %wt/v CTAB, 6% wt/v PVP40, and 0.2 g/L SWNT each of which were prepared separately. As seen, there is variation in the overall intensity of each spectra, which contributes to the magnitude of the non-resonant background however the shape of the resonant peaks stay fairly similar.

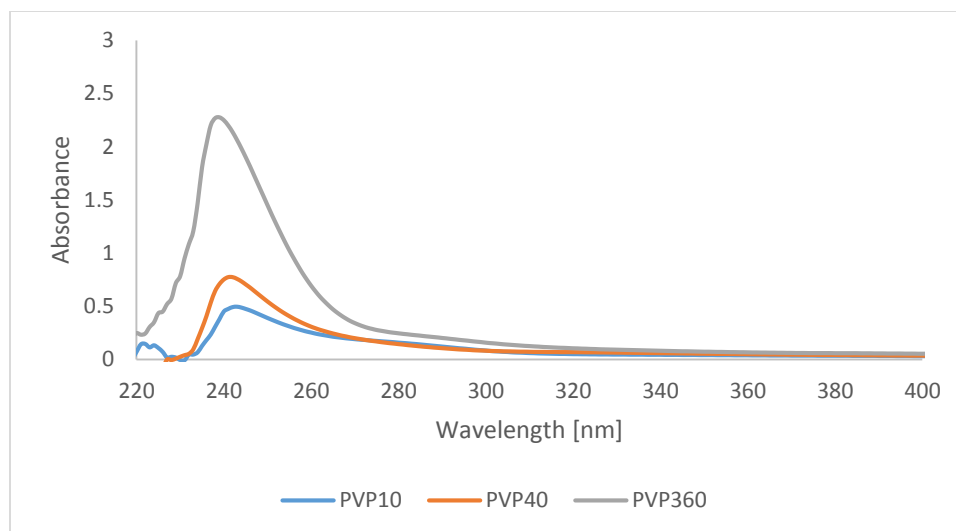


Figure S 3: Absorbance spectra of C70 fullerenes dispersed with 0.1% CTAB and 6% PVP of different molecular weights.

The above shows the absorbance spectra of C70 fullerene suspensions prepared with either 6% wt/v PVP10, 6 %wt/v PVP40, or 6 %wt/v PVP360. As can be seen, the absorption intensity is significantly higher in the solution prepared with 6 %wt/v PVP360. This is an indication that there are more fullerenes suspended when using PVP360.

Surface Tension

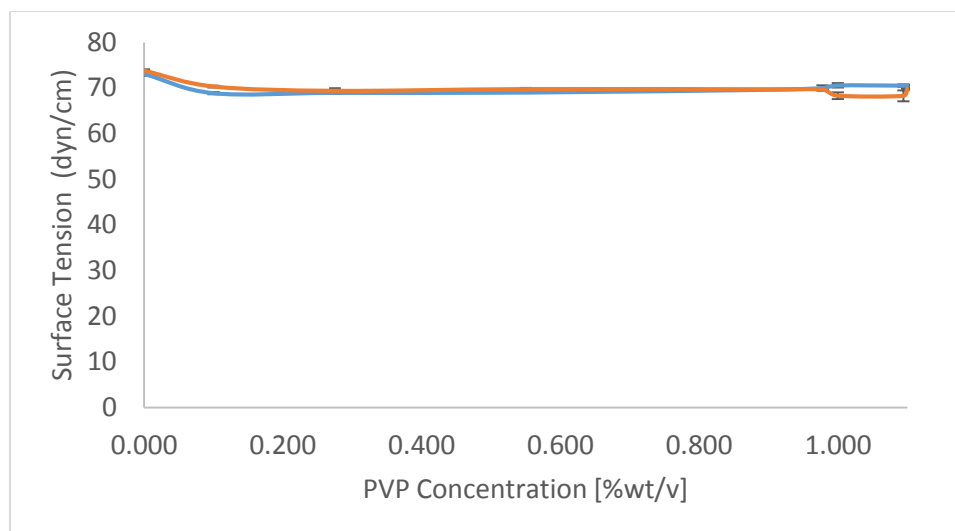


Figure S 4: Surface tension behavior of PVP40 and PVP360

Figure S 4 reveals the surface tension behavior of PVP as demonstrated by PVP40 and PVP360. As indicated, PVP does affect the surface tension of water slightly however the deviation is from the normal surface tension of water (72 dyn/cm) is very minute.

Viscosity

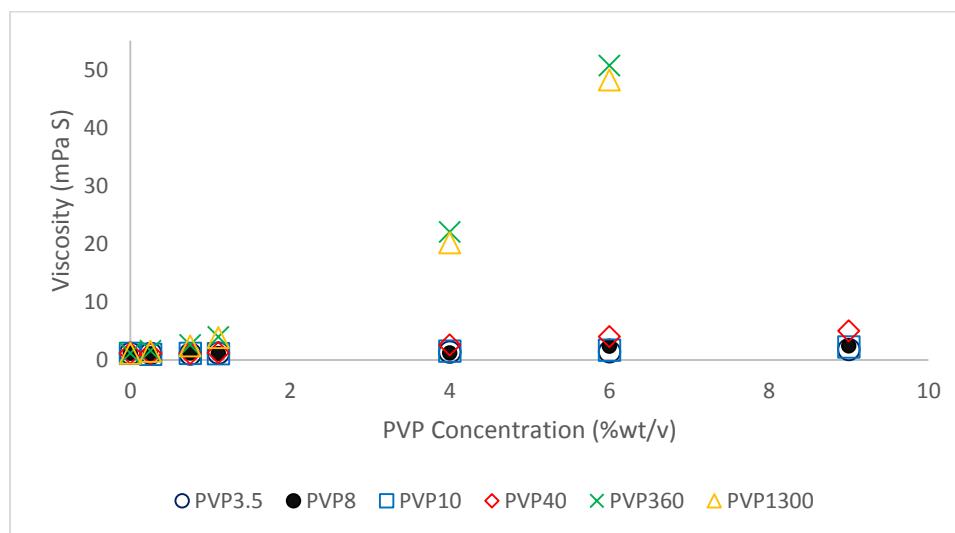


Figure S 5: Dynamic viscosity of the CTAB+PVP system at a CTAB concentration of 0.1 %wt/v and different PVP concentrations and molecular weights.

The results show that, as expected, the increase in polymer concentration results in increased viscosity. The viscosity of the PVP360 and PVP1300 systems increased at a much higher rate than the other polymers. The dynamic viscosity of CTAB was also measured to be approximately 1.149 mPa S. It's important to note as well that at all concentrations, the addition of CTAB did not significantly shift the viscosity contributed by the PVP therefore the changes in viscosity come from the polymer itself.

Surface Area Tables

Concentration [% wt/v]	PVP3.5	PVP8	PVP10	PVP40	PVP360	PVP1300
0.25	1.955E+18	1.558E+18	1.526E+18	1.206E+18	1.852E+18	1.285E+18
0.75	1.104E+18	2.145E+18	2.115E+18	1.384E+18	1.639E+18	1.494E+18
1.1	1.348E+18	1.655E+18	2.172E+18	1.966E+18	1.901E+18	1.664E+18
4	2.204E+18	1.842E+18	2.896E+18	3.203E+18	2.810E+18	3.062E+18
6	1.987E+18	2.427E+18	3.836E+18	3.781E+18	5.450E+18	4.989E+18
9	2.569E+18	2.610E+18	4.370E+18	5.050E+18	7.420E+18	7.682E+18

Table S 3: Total amount of surface area on nanotube

Concentration [% wt/v]	PVP3.5	PVP8	PVP10	PVP40	PVP360	PVP1300
0.25	2.449E+22	2.214E+22	1.972E+22	2.291E+22	3.083E+22	3.242E+22
0.75	7.347E+22	6.642E+22	5.917E+22	6.872E+22	9.250E+22	9.725E+22
1.1	1.078E+23	9.741E+22	8.679E+22	1.008E+23	1.357E+23	1.426E+23
4	3.919E+23	3.542E+23	3.156E+23	3.665E+23	4.933E+23	5.186E+23

6	5.878E+23	5.313E+23	4.734E+23	5.497E+23	7.400E+23	7.780E+23
9	8.817E+23	7.970E+23	7.101E+23	8.246E+23	1.110E+24	1.167E+24

Table S 4: Total amount of surface area provided by projected polymer molecule

Table S 3 and Table S 4 list the total surface area of the nanotube and polymers respectively at the final concentrations determined in the samples prepared. As can be seen, the surface area available for nanotubes increases with increasing concentration and molecular weight used. This is expected as with higher molecular weight polymer, there is also an increase in the viscosity and chain entanglement leading to more nanotubes being retained. The total amount of surface area of the polymer projection (assuming rigidity) also increases in the same manner expectedly due to the larger PVPs having a larger hydrodynamic radius therefore resulting in a larger area value calculated.

Electrophoretic Mobility

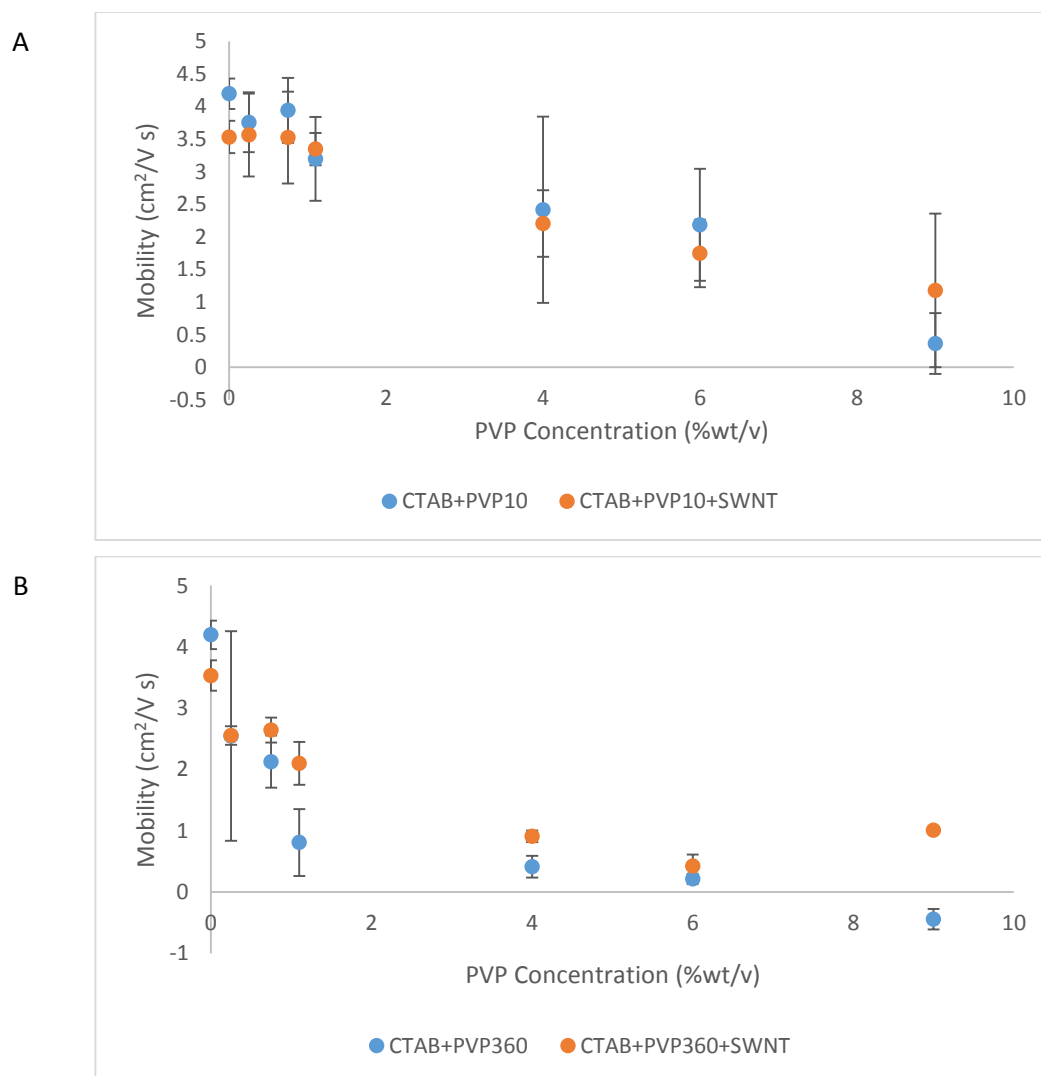


Figure S 6: Electrophoretic mobility measurements of solutions containing A) PVP10 and B)PVP360 with and without nanotubes

According to the figures above, it appears the mobility of CTAB in general decreases linearly with increasing polymer concentration. This is unsurprising as higher concentrations of PVP would lead to higher polymer entanglement. Using a higher molecular weight also leads to a greater decrease in mobility more readily as observed by the slope of Figure S 6A compared to that of Figure S 6B. Perhaps the most significant observation though is the effect of nanotubes. With the use of a lower polymer weight such as PVP10, it is observed that the electrophoretic mobility is unaffected by the presence of nanotubes however there is a noticeable increase in the overall mobility with samples containing a heavier molecular weight polymer and nanotubes. The “constraint release” hypothesis could be used here as nanotubes can disrupt the entanglement of polymer allowing CTAB to move more prominently.

Permissions



RightsLink®

Home Account Info Help



ACS Publications
MOST TRUSTED. MOST CITED. MOST READ.

Title: Adsorption of Polyvinylpyrrolidone onto Polystyrene Latexes and the Effect on Colloid Stability
Author: J. N. Smith, J. Meadows, and, and P. A. Williams*
Publication: Langmuir
Publisher: American Chemical Society
Date: Jan 1, 1996
Copyright © 1996, American Chemical Society

Logged in as:
Tennison Yu

LOGOUT

PERMISSION/LICENSE IS GRANTED FOR YOUR ORDER AT NO CHARGE

This type of permission/license, instead of the standard Terms & Conditions, is sent to you because no fee is being charged for your order. Please note the following:

- Permission is granted for your request in both print and electronic formats, and translations.
- If figures and/or tables were requested, they may be adapted or used in part.
- Please print this page for your records and send a copy of it to your publisher/graduate school.
- Appropriate credit for the requested material should be given as follows: "Reprinted (adapted) with permission from (COMPLETE REFERENCE CITATION). Copyright (YEAR) American Chemical Society." Insert appropriate information in place of the capitalized words.
- One-time permission is granted only for the use specified in your request. No additional uses are granted (such as derivative works or other editions). For any other uses, please submit a new request.

If credit is given to another source for the material you requested, permission must be obtained from that source.

BACK

CLOSE WINDOW

Copyright © 2014 Copyright Clearance Center, Inc. All Rights Reserved. [Privacy statement](#). Comments? We would like to hear from you. E-mail us at customer-care@copyright.com



RightsLink®

Home Account Info Help



ACS Publications
Most Trusted. Most Cited. Most Read.

Title: Physical Adsorption of Block Copolymers to SWNT and MWNT: A Nonwrapping Mechanism
Author: Einat Nativ-Roth et al.
Publication: Macromolecules
Publisher: American Chemical Society
Date: May 1, 2007
Copyright © 2007, American Chemical Society

Logged in as:
Tennison Yu

LOGOUT

PERMISSION/LICENSE IS GRANTED FOR YOUR ORDER AT NO CHARGE

This type of permission/license, instead of the standard Terms & Conditions, is sent to you because no fee is being charged for your order. Please note the following:

- Permission is granted for your request in both print and electronic formats, and translations.
- If figures and/or tables were requested, they may be adapted or used in part.
- Please print this page for your records and send a copy of it to your publisher/graduate school.
- Appropriate credit for the requested material should be given as follows: "Reprinted (adapted) with permission from (COMPLETE REFERENCE CITATION). Copyright (YEAR) American Chemical Society." Insert appropriate information in place of the capitalized words.
- One-time permission is granted only for the use specified in your request. No additional uses are granted (such as derivative works or other editions). For any other uses, please submit a new request.

If credit is given to another source for the material you requested, permission must be obtained from that source.

BACK

CLOSE WINDOW

Copyright © 2014 Copyright Clearance Center, Inc. All Rights Reserved. [Privacy statement](#). Comments? We would like to hear from you. E-mail us at customer-care@copyright.com

8/18/2014

Rightlink Printable License

**NATURE PUBLISHING GROUP LICENSE
TERMS AND CONDITIONS**

Aug 18, 2014

This is a License Agreement between Temison Yu ("You") and Nature Publishing Group ("Nature Publishing Group") provided by Copyright Clearance Center ("CCC"). The license consists of your order details, the terms and conditions provided by Nature Publishing Group, and the payment terms and conditions.

All payments must be made in full to CCC. For payment instructions, please see information listed at the bottom of this form.

License Number	3434240560875
License date	Jul 22, 2014
Licensed content publisher	Nature Publishing Group
Licensed content publication	Nature
Licensed content title	Helical microtubules of graphitic carbon
Licensed content author	Sumio Iijima
Licensed content date	Nov 7, 1991
Volume number	354
Issue number	6348
Type of Use	reuse in a dissertation / thesis
Requestor type	academic/educational
Format	electronic
Portion	figures/tables/illustrations
Number of figures/tables/illustrations	1
Figures	Figure 1
Author of this NPG article	no
Your reference number	None
Title of your thesis / dissertation	"Surfactant assisted dispersion of single walled carbon nanotubes in polyvinylpyrrolidone solutions"
Expected completion date	Aug 2014
Estimated size (number of pages)	105
Total	0.00 USD
Terms and Conditions	Terms and Conditions for Permissions

<https://100.copyright.com/CustomerAdminPLF.jsp?ref=c5f18f69-0eeb-4deb-bac9-b0245e8279d5>

1/3

8/18/2014

Rightlink Printable License

Nature Publishing Group hereby grants you a non-exclusive license to reproduce this material for this purpose, and for no other use, subject to the conditions below:

1. NPG warrants that it has, to the best of its knowledge, the rights to license reuse of this material. However, you should ensure that the material you are requesting is original to Nature Publishing Group and does not carry the copyright of another entity (as credited in the published version). If the credit line on any part of the material you have requested indicates that it was reprinted or adapted by NPG with permission from another source, then you should also seek permission from that source to reuse the material.
2. Permission granted free of charge for material in print is also usually granted for any electronic version of that work, provided that the material is incidental to the work as a whole and that the electronic version is essentially equivalent to, or substitutes for, the print version. Where print permission has been granted for a fee, separate permission must be obtained for any additional, electronic re-use (unless, as in the case of a full paper, this has already been accounted for during your initial request in the calculation of a print run). NB: In all cases, web-based use of full-text articles must be authorized separately through the 'Use on a Web Site' option when requesting permission.
3. Permission granted for a first edition does not apply to second and subsequent editions and for editions in other languages (except for signatories to the STM Permissions Guidelines, or where the first edition permission was granted for free).
4. Nature Publishing Group's permission must be acknowledged next to the figure, table or abstract in print. In electronic form, this acknowledgement must be visible at the same time as the figure/table/abstract, and must be hyperlinked to the journal's homepage.
5. The credit line should read:
Reprinted by permission from Macmillan Publishers Ltd: [JOURNAL NAME] (reference citation), copyright (year of publication)
For AOP papers, the credit line should read:
Reprinted by permission from Macmillan Publishers Ltd: [JOURNAL NAME], advance online publication, day month year (doi: 10.1038/sj.[JOURNAL ACRONYM].XXXXX)

Note: For republication from the *British Journal of Cancer*, the following credit lines apply.

Reprinted by permission from Macmillan Publishers Ltd on behalf of Cancer Research UK: [JOURNAL NAME] (reference citation), copyright (year of publication) For AOP papers, the credit line should read:
Reprinted by permission from Macmillan Publishers Ltd on behalf of Cancer Research UK: [JOURNAL NAME], advance online publication, day month year (doi: 10.1038/sj.[JOURNAL ACRONYM].XXXXX)

6. Adaptations of single figures do not require NPG approval. However, the adaptation should be credited as follows:

Adapted by permission from Macmillan Publishers Ltd: [JOURNAL NAME] (reference citation), copyright (year of publication)

Note: For adaptation from the *British Journal of Cancer*, the following credit line applies.
Adapted by permission from Macmillan Publishers Ltd on behalf of Cancer Research UK: [JOURNAL NAME] (reference citation), copyright (year of publication)
7. Translations of 401 words up to a whole article require NPG approval. Please visit <http://www.macmillanmedicalcommunications.com> for more information. Translations of up to a 400 words do not require NPG approval. The translation should be credited as follows:

Translated by permission from Macmillan Publishers Ltd: [JOURNAL NAME] (reference citation), copyright (year of publication).

<https://100.copyright.com/CustomerAdminPLF.jsp?ref=c5f18f69-0eeb-4deb-bac9-b0245e8279d5>

2/3

8/18/2014

Rightslink Printable License

Note: For translation from the *British Journal of Cancer*, the following credit line applies.

Translated by permission from Macmillan Publishers Ltd on behalf of Cancer Research UK: [JOURNAL NAME] (reference citation), copyright (year of publication)

We are certain that all parties will benefit from this agreement and wish you the best in the use of this material. Thank you.

Special Terms:

v1.1

You will be invoiced within 48 hours of this transaction date. You may pay your invoice by credit card upon receipt of the invoice for this transaction. Please follow instructions provided at that time.

To pay for this transaction now; please remit a copy of this document along with your payment. Payment should be in the form of a check or money order referencing your account number and this invoice number RLNK501358145.

Make payments to "COPYRIGHT CLEARANCE CENTER" and send to:

Copyright Clearance Center

Dept 001

P.O. Box 843006

Boston, MA 02284-3006

Please disregard electronic and mailed copies if you remit payment in advance.

Questions? customer@copyright.com or +1-855-239-3415 (toll free in the US) or +1-978-646-2777.

Gratis licenses (referencing \$0 in the Total field) are free. Please retain this printable license for your reference. No payment is required.

<https://100.copyright.com/CustomerAdmin/PLF.jsp?ref=c5f196a-0aab-42ab-bac9-b045e279d5>

3/3

8/18/2014

Rightslink Printable License

ROYAL SOCIETY OF CHEMISTRY LICENSE TERMS AND CONDITIONS

Aug 18, 2014

This is a License Agreement between Temison Yu ("You") and Royal Society of Chemistry ("Royal Society of Chemistry") provided by Copyright Clearance Center ("CCC"). The license consists of your order details, the terms and conditions provided by Royal Society of Chemistry, and the payment terms and conditions.

All payments must be made in full to CCC. For payment instructions, please see information listed at the bottom of this form.

License Number	3433990590906
License date	Jul 21, 2014
Licensed content publisher	Royal Society of Chemistry
Licensed content publication	Soft Matter
Licensed content title	Colloid-polymer mixtures in the protein limit
Licensed content author	Kevin J. Mutch, Jeroen S. van Duijneveldt, Julian Eastoe
Licensed content date	Nov 16, 2006
Volume number	3
Issue number	2
Type of Use	Thesis/Dissertation
Requestor type	academic/educational
Portion	figures/tables/images
Number of figures/tables/images	1
Format	electronic
Distribution quantity	4
Will you be translating?	no
Order reference number	None
Title of the thesis/dissertation	"Surfactant assisted dispersion of single walled carbon nanotubes in polyvinylpyrrolidone solutions"
Expected completion date	Aug 2014
Estimated size	105
Total	0.00 USD

Terms and Conditions

This License Agreement is between {Requestor Name} ("You") and The Royal Society of Chemistry ("RSC") provided by the Copyright Clearance Center ("CCC"). The license consists of your order details, the terms and conditions provided by the Royal Society of Chemistry, and the payment terms and conditions.

<https://100.copyright.com/CustomerAdmin/PLF.jsp?ref=6bc9ab5b-7d37-441e-ada8-c65e3e6488>

1/5

RSC / TERMS AND CONDITIONS

INTRODUCTION

The publisher for this copyrighted material is The Royal Society of Chemistry. By clicking "accept" in connection with completing this licensing transaction, you agree that the following terms and conditions apply to this transaction (along with the Billing and Payment terms and conditions established by CCC, at the time that you opened your RightsLink account and that are available at any time at .

LICENSE GRANTED

The RSC hereby grants you a non-exclusive license to use the aforementioned material anywhere in the world subject to the terms and conditions indicated herein. Reproduction of the material is confined to the purpose and/or media for which permission is hereby given.

RESERVATION OF RIGHTS

The RSC reserves all rights not specifically granted in the combination of (i) the license details provided by you and accepted in the course of this licensing transaction; (ii) these terms and conditions; and (iii) CCC's Billing and Payment terms and conditions.

REVOCATION

The RSC reserves the right to revoke this license for any reason, including, but not limited to, advertising and promotional uses of RSC content, third party usage, and incorrect source figure attribution.

THIRD-PARTY MATERIAL DISCLAIMER

If part of the material to be used (for example, a figure) has appeared in the RSC publication with credit to another source, permission must also be sought from that source. If the other source is another RSC publication these details should be included in your RightsLink request. If the other source is a third party, permission must be obtained from the third party. The RSC disclaims any responsibility for the reproduction you make of items owned by a third party.

PAYMENT OF FEE

If the permission fee for the requested material is waived in this instance, please be advised that any future requests for the reproduction of RSC materials may attract a fee.

ACKNOWLEDGEMENT

The reproduction of the licensed material must be accompanied by the following acknowledgement:

Reproduced ("Adapted" or "in part") from (Reference Citation) (or RefXX) with permission of The Royal Society of Chemistry.

If the licensed material is being reproduced from New Journal of Chemistry (NJC), Photochemical & Photobiological Sciences (PPS) or Physical Chemistry Chemical Physics (PCCP) you must include one of the following acknowledgements:

For figures originally published in NJC:

Reproduced ("Adapted" or "in part") from (Reference Citation) (or RefXX) with permission of

The Royal Society of Chemistry (RSC) on behalf of the European Society for Photobiology, the European Photochemistry Association and the RSC.

For figures originally published in PPS:

Reproduced ("Adapted" or "in part") from (Reference Citation) (or RefXX) with permission of The Royal Society of Chemistry (RSC) on behalf of the Centre National de la Recherche Scientifique (CNRS) and the RSC.

For figures originally published in PCCP:

Reproduced ("Adapted" or "in part") from (Reference Citation) (or RefXX) with permission of the PCCP Owner Societies.

HYPERTEXT LINKS

With any material which is being reproduced in electronic form, you must include a hypertext link to the original RSC article on the RSC's website. The recommended form for the hyperlink is <http://dx.doi.org/10.1039/DOI suffix>, for example in the link <http://dx.doi.org/10.1039/b110420a> the DOI suffix is 'b110420a'. To find the relevant DOI suffix for the RSC article in question, go to the Journals section of the website and locate the article in the list of papers for the volume and issue of your specific journal. You will find the DOI suffix quoted there.

LICENSE CONTINGENT ON PAYMENT

While you may exercise the rights licensed immediately upon issuance of the license at the end of the licensing process for the transaction, provided that you have disclosed complete and accurate details of your proposed use, no license is finally effective unless and until full payment is received from you (by CCC) as provided in CCC's Billing and Payment terms and conditions. If full payment is not received on a timely basis, then any license preliminarily granted shall be deemed automatically revoked and shall be void as if never granted. Further, in the event that you breach any of these terms and conditions or any of CCC's Billing and Payment terms and conditions, the license is automatically revoked and shall be void as if never granted. Use of materials as described in a revoked license, as well as any use of the materials beyond the scope of an unrevoked license, may constitute copyright infringement and the RSC reserves the right to take any and all action to protect its copyright in the materials.

WARRANTIES

The RSC makes no representations or warranties with respect to the licensed material.

INDEMNITY

You hereby indemnify and agree to hold harmless the RSC and the CCC, and their respective officers, directors, trustees, employees and agents, from and against any and all claims arising out of your use of the licensed material other than as specifically authorized pursuant to this license.

NO TRANSFER OF LICENSE

This license is personal to you or your publisher and may not be sublicensed, assigned, or transferred by you to any other person without the RSC's written permission.

8/16/2014

Rightlink Printable License

NO AMENDMENT EXCEPT IN WRITING

This license may not be amended except in a writing signed by both parties (or, in the case of "Other Conditions, v1.2", by CCC on the RSC's behalf).

OBJECTION TO CONTRARY TERMS

You hereby acknowledge and agree that these terms and conditions, together with CCC's Billing and Payment terms and conditions (which are incorporated herein), comprise the entire agreement between you and the RSC (and CCC) concerning this licensing transaction, to the exclusion of all other terms and conditions, written or verbal, express or implied (including any terms contained in any purchase order, acknowledgment, check endorsement or other writing prepared by you). In the event of any conflict between your obligations established by these terms and conditions and those established by CCC's Billing and Payment terms and conditions, these terms and conditions shall control.

JURISDICTION

This license transaction shall be governed by and construed in accordance with the laws of the District of Columbia. You hereby agree to submit to the jurisdiction of the courts located in the District of Columbia for purposes of resolving any disputes that may arise in connection with this licensing transaction.

LIMITED LICENSE

The following terms and conditions apply to specific license types:

Translation

This permission is granted for non-exclusive world English rights only unless your license was granted for translation rights. If you licensed translation rights you may only translate this content into the languages you requested. A professional translator must perform all translations and reproduce the content word for word preserving the integrity of the article.

Intranet

If the licensed material is being posted on an Intranet, the Intranet is to be password-protected and made available only to bona fide students or employees only. All content posted to the Intranet must maintain the copyright information line on the bottom of each image. You must also fully reference the material and include a hypertext link as specified above.

Copies of Whole Articles

All copies of whole articles must maintain, if available, the copyright information line on the bottom of each page.

Other Conditions

v1.2

Gratis licenses (referencing \$0 in the Total field) are free. Please retain this printable license for your reference. No payment is required.

If you would like to pay for this license now, please remit this license along with your payment made payable to "COPYRIGHT CLEARANCE CENTER" otherwise you will be invoiced within 48

<https://100.copyright.com/CustomerAdmin/PLF.jsp?ref=0bc8ab5b-7d37-441e-aded-c155e3e5498>

45

8/16/2014

Rightlink Printable License

hours of the license date. Payment should be in the form of a check or money order referencing your account number and this invoice number (Invoice Number).

Once you receive your invoice for this order, you may pay your invoice by credit card.

Please follow instructions provided at that time.

Make Payment To:

Copyright Clearance Center
Dept 001
P.O. Box 843006
Boston, MA 02284-3006

For suggestions or comments regarding this order, contact Rightlink Customer Support: customer@copyright.com or +1-877-622-5543 (toll free in the US) or +1-978-646-2777.

You will be invoiced within 48 hours of this transaction date. You may pay your invoice by credit card upon receipt of the invoice for this transaction. Please follow instructions provided at that time.

To pay for this transaction now; please remit a copy of this document along with your payment. Payment should be in the form of a check or money order referencing your account number and this invoice number RLNK501357605.

Make payments to "COPYRIGHT CLEARANCE CENTER" and send to:

Copyright Clearance Center

Dept 001
P.O. Box 843006
Boston, MA 02284-3006
Please disregard electronic and mailed copies if you remit payment in advance.
Questions? customer@copyright.com or +1-855-239-3415 (toll free in the US) or +1-978-646-2777.

Gratis licenses (referencing \$0 in the Total field) are free. Please retain this printable license for your reference. No payment is required.

<https://100.copyright.com/CustomerAdmin/PLF.jsp?ref=0bc8ab5b-7d37-441e-aded-c155e3e5498>

55

8/18/2014

Rightslink Printable License

**ELSEVIER LICENSE
TERMS AND CONDITIONS**

Aug 18, 2014

This is a License Agreement between Tennison Yu ("You") and Elsevier ("Elsevier") provided by Copyright Clearance Center ("CCC"). The license consists of your order details, the terms and conditions provided by Elsevier, and the payment terms and conditions.

All payments must be made in full to CCC. For payment instructions, please see information listed at the bottom of this form.

Supplier	Elsevier Limited The Boulevard, Langford Lane Kidlington, Oxford, OX5 1GB, UK
Registered Company Number	1982084
Customer name	Tennison Yu
Customer address	[REDACTED]
License number	3433990233948
License date	Jul 21, 2014
Licensed content publisher	Elsevier
Licensed content publication	Carbon
Licensed content title	Physics of carbon nanotubes
Licensed content author	M.S. Dresselhaus, G. Dresselhaus, R. Saito
Licensed content date	1995
Licensed content volume number	33
Licensed content issue number	7
Number of pages	9
Start Page	883
End Page	891
Type of Use	reuse in a thesis/dissertation
Intended publisher of new work	other
Portion	figures/tables/illustrations
Number of figures/tables/illustrations	2
Format	electronic
Are you the author of this	No

<https://www.copyright.com/CustomerAdmin/PLF.jsp?ref=1a8f7c3c-0402-4348-41a0-02ac5391820>

1/7

8/18/2014

Rightslink Printable License

Elsevier article?	
Will you be translating?	No
Title of your thesis/dissertation	"Surfactant assisted dispersion of single walled carbon nanotubes in polyvinylpyrrolidone solutions"
Expected completion date	Aug 2014
Estimated size (number of pages)	105
Elsevier VAT number	GB 494 6272 12
Permissions price	0.00 USD
VAT/Local Sales Tax	0.00 USD / 0.00 GBP
Total	0.00 USD
Terms and Conditions	

INTRODUCTION

1. The publisher for this copyrighted material is Elsevier. By clicking "accept" in connection with completing this licensing transaction, you agree that the following terms and conditions apply to this transaction (along with the Billing and Payment terms and conditions established by Copyright Clearance Center, Inc. ("CCC"), at the time that you opened your Rightslink account and that are available at any time at <http://www.copyright.com>).

GENERAL TERMS

2. Elsevier hereby grants you permission to reproduce the aforementioned material subject to the terms and conditions indicated.
3. Acknowledgement: If any part of the material to be used (for example, figures) has appeared in our publication with credit or acknowledgement to another source, permission must also be sought from that source. If such permission is not obtained then that material may not be included in your publication/copies. Suitable acknowledgement to the source must be made, either as a footnote or in a reference list at the end of your publication, as follows:
- "Reprinted from Publication title, Vol./edition number, Author(s), Title of article / title of chapter, Pages No., Copyright (Year), with permission from Elsevier [OR APPLICABLE SOCIETY COPYRIGHT OWNER]." Also Lancet special credit - "Reprinted from The Lancet, Vol. number, Author(s), Title of article, Pages No., Copyright (Year), with permission from Elsevier."
4. Reproduction of this material is confined to the purpose and/or media for which permission is hereby given.
5. Altering/Modifying Material: Not Permitted. However figures and illustrations may be altered/adapted minimally to serve your work. Any other abbreviations, additions, deletions and/or any other alterations shall be made only with prior written authorization of Elsevier Ltd. (Please contact Elsevier at permissions@elsevier.com)
6. If the permission fee for the requested use of our material is waived in this instance, please be advised that your future requests for Elsevier materials may attract a fee.

<https://www.copyright.com/CustomerAdmin/PLF.jsp?ref=1a8f7c3c-0402-4348-41a0-02ac5391820>

2/7

7. **Reservation of Rights:** Publisher reserves all rights not specifically granted in the combination of (i) the license details provided by you and accepted in the course of this licensing transaction, (ii) these terms and conditions and (iii) CCC's Billing and Payment terms and conditions.
8. **License Contingent Upon Payment:** While you may exercise the rights licensed immediately upon issuance of the license at the end of the licensing process for the transaction, provided that you have disclosed complete and accurate details of your proposed use, no license is finally effective unless and until full payment is received from you (either by publisher or by CCC) as provided in CCC's Billing and Payment terms and conditions. If full payment is not received on a timely basis, then any license preliminarily granted shall be deemed automatically revoked and shall be void as if never granted. Further, in the event that you breach any of these terms and conditions or any of CCC's Billing and Payment terms and conditions, the license is automatically revoked and shall be void as if never granted. Use of materials as described in a revoked license, as well as any use of the materials beyond the scope of an unrevoked license, may constitute copyright infringement and publisher reserves the right to take any and all action to protect its copyright in the materials.
9. **Warranties:** Publisher makes no representations or warranties with respect to the licensed material.
10. **Indemnity:** You hereby indemnify and agree to hold harmless publisher and CCC, and their respective officers, directors, employees and agents, from and against any and all claims arising out of your use of the licensed material other than as specifically authorized pursuant to this license.
11. **No Transfer of License:** This license is personal to you and may not be sublicensed, assigned, or transferred by you to any other person without publisher's written permission.
12. **No Amendment Except in Writing:** This license may not be amended except in a writing signed by both parties (or, in the case of publisher, by CCC on publisher's behalf).
13. **Objection to Contrary Terms:** Publisher hereby objects to any terms contained in any purchase order, acknowledgment, check endorsement or other writing prepared by you, which terms are inconsistent with these terms and conditions or CCC's Billing and Payment terms and conditions. These terms and conditions, together with CCC's Billing and Payment terms and conditions (which are incorporated herein), comprise the entire agreement between you and publisher (and CCC) concerning this licensing transaction. In the event of any conflict between your obligations established by these terms and conditions and those established by CCC's Billing and Payment terms and conditions, these terms and conditions shall control.
14. **Revocation:** Elsevier or Copyright Clearance Center may deny the permissions described in this License at their sole discretion, for any reason or no reason, with a full refund payable to you. Notice of such denial will be made using the contact information provided by you. Failure to receive such notice will not alter or invalidate the denial. In no event will Elsevier or Copyright Clearance Center be responsible or liable for any costs, expenses or damage incurred by you as a result of a denial of your permission request, other than a refund of the amount(s) paid by you to Elsevier and/or Copyright Clearance Center for denied permissions.

LIMITED LICENSE

The following terms and conditions apply only to specific license types:

15. **Translation:** This permission is granted for non-exclusive world English rights only unless your license was granted for translation rights. If you licensed translation rights you may only translate this content into the languages you requested. A professional translator must perform all translations and reproduce the content word for word preserving the integrity of the article. If this license is to re-use 1 or 2 figures then permission is granted for non-exclusive world rights in all languages.
16. **Posting licensed content on any Website:** The following terms and conditions apply as follows: Licensing material from an Elsevier journal: All content posted to the web site must maintain the copyright information line on the bottom of each image. A hyper-text must be included to the Homepage of the journal from which you are licensing at <http://www.sciencedirect.com/science/journal/xxxxx> or the Elsevier homepage for books at <http://www.elsevier.com>; Central Storage: This license does not include permission for a scanned version of the material to be stored in a central repository such as that provided by Heron/XanEdu.
- Licensing material from an Elsevier book: A hyper-text link must be included to the Elsevier homepage at <http://www.elsevier.com>. All content posted to the web site must maintain the copyright information line on the bottom of each image.
- Posting licensed content on Electronic reserve:** In addition to the above the following clauses are applicable: The web site must be password-protected and made available only to bona fide students registered on a relevant course. This permission is granted for 1 year only. You may obtain a new license for future website posting.
- For journal authors:** the following clauses are applicable in addition to the above: Permission granted is limited to the author accepted manuscript version* of your paper.
- *Accepted Author Manuscript (AAM) Definition:** An accepted author manuscript (AAM) is the author's version of the manuscript of an article that has been accepted for publication and which may include any author-incorporated changes suggested through the processes of submission processing, peer review, and editor-author communications. AAMs do not include other publisher value-added contributions such as copy-editing, formatting, technical enhancements and (if relevant) pagination.
- You are not allowed to download and post the published journal article (whether PDF or HTML, proof or final version), nor may you scan the printed edition to create an electronic version. A hyper-text must be included to the Homepage of the journal from which you are licensing at <http://www.sciencedirect.com/science/journal/xxxxx>. As part of our normal production process, you will receive an e-mail notice when your article appears on Elsevier's online service ScienceDirect (www.sciencedirect.com). That e-mail will include the article's Digital Object Identifier (DOI). This number provides the electronic link to the published article and should be included in the posting of your personal version. We ask that you wait until you receive this e-mail and have the DOI to do any posting.
- Posting to a repository:** Authors may post their AAM immediately to their employer's

8/16/2014

Rightlink Printable License

institutional repository for internal use only and may make their manuscript publicly available after the journal-specific embargo period has ended.

Please also refer to [Elsevier's Article Posting Policy](#) for further information.

18. **For book authors** the following clauses are applicable in addition to the above: Authors are permitted to place a brief summary of their work online only. You are not allowed to download and post the published electronic version of your chapter, nor may you scan the printed edition to create an electronic version. **Posting to a repository:** Authors are permitted to post a summary of their chapter only in their institution's repository.

20. **Thesis/Dissertation:** If your license is for use in a thesis/dissertation your thesis may be submitted to your institution in either print or electronic form. Should your thesis be published commercially, please reapply for permission. These requirements include permission for the Library and Archives of Canada to supply single copies, on demand, of the complete thesis and include permission for UMI to supply single copies, on demand, of the complete thesis. Should your thesis be published commercially, please reapply for permission.

Elsevier Open Access Terms and Conditions

Elsevier publishes Open Access articles in both its Open Access journals and via its Open Access articles option in subscription journals.

Authors publishing in an Open Access journal or who choose to make their article Open Access in an Elsevier subscription journal select one of the following Creative Commons user licenses, which define how a reader may reuse their work: Creative Commons Attribution License (CC BY), Creative Commons Attribution – Non Commercial - ShareAlike (CC BY NC SA) and Creative Commons Attribution – Non Commercial – No Derivatives (CC BY NC ND)

Terms & Conditions applicable to all Elsevier Open Access articles:

Any reuse of the article must not represent the author as endorsing the adaptation of the article nor should the article be modified in such a way as to damage the author's honour or reputation.

The author(s) must be appropriately credited.

If any part of the material to be used (for example, figures) has appeared in our publication with credit or acknowledgement to another source it is the responsibility of the user to ensure their reuse complies with the terms and conditions determined by the rights holder.

Additional Terms & Conditions applicable to each Creative Commons user license:

CC BY: You may distribute and copy the article, create extracts, abstracts, and other revised versions, adaptations or derivative works of or from an article (such as a translation), to include in a collective work (such as an anthology), to text or data mine the article, including for commercial purposes without permission from Elsevier

<http://dx.doi.org/10.1016/j.copyright.2014.08.001>

5/7

8/16/2014

Rightlink Printable License

CC BY NC SA: For non-commercial purposes you may distribute and copy the article, create extracts, abstracts and other revised versions, adaptations or derivative works of or from an article (such as a translation), to include in a collective work (such as an anthology), to text and data mine the article and license new adaptations or creations under identical terms without permission from Elsevier

CC BY NC ND: For non-commercial purposes you may distribute and copy the article and include it in a collective work (such as an anthology), provided you do not alter or modify the article, without permission from Elsevier

Any commercial reuse of Open Access articles published with a CC BY NC SA or CC BY NC ND license requires permission from Elsevier and will be subject to a fee.

Commercial reuse includes:

- Promotional purposes (advertising or marketing)
- Commercial exploitation (e.g. a product for sale or loan)
- Systematic distribution (for a fee or free of charge)

Please refer to [Elsevier's Open Access Policy](#) for further information.

21. Other Conditions:

v1.6

You will be invoiced within 48 hours of this transaction date. You may pay your invoice by credit card upon receipt of the invoice for this transaction. Please follow instructions provided at that time.

To pay for this transaction now, please remit a copy of this document along with your payment. Payment should be in the form of a check or money order referencing your account number and this invoice number RLNK501357604. Make payments to "COPY RIGHT CLEARANCE CENTER" and send to:

Copyright Clearance Center

Dept 001
P.O. Box 843006
Boston, MA 02284-3006

Please disregard electronic and mailed copies if you remit payment in advance. Questions? customer@copyright.com or +1-855-239-3415 (toll free in the US) or +1-978-646-2777.

Gratis licenses (referencing \$0 in the Total field) are free. Please retain this printable license for your reference. No payment is required.

<http://dx.doi.org/10.1016/j.copyright.2014.08.001>

6/7

8/18/2014

Rightlink Printable License

**ELSEVIER LICENSE
TERMS AND CONDITIONS**

Aug 18, 2014

This is a License Agreement between Tennison Yu ("You") and Elsevier ("Elsevier") provided by Copyright Clearance Center ("CCC"). The license consists of your order details, the terms and conditions provided by Elsevier, and the payment terms and conditions.

All payments must be made in full to CCC. For payment instructions, please see information listed at the bottom of this form.

Supplier	Elsevier Limited The Boulevard, Langford Lane Kidlington, Oxford, OX5 1GB, UK
Registered Company Number	1982084
Customer name	Tennison Yu
Customer address	
License number	3433990075480
License date	Jul 21, 2014
Licensed content publisher	Elsevier
Licensed content publication	Composites Science and Technology
Licensed content title	Sensors and actuators based on carbon nanotubes and their composites: A review
Licensed content author	Chunyu Li, Erik T. Thostenson, Tsu-Wei Chou
Licensed content date	May 2008
Licensed content volume number	68
Licensed content issue number	6
Number of pages	23
Start Page	1227
End Page	1249
Type of Use	reuse in a thesis/dissertation
Intended publisher of new work	other
Portion	figures/tables/illustrations
Number of figures/tables/illustrations	1
Format	electronic

<https://www.copyright.com/CustomerAdminPLF.jsp?ref=a900303-8523-4b1b-baed-d7e2d47ba3a>

1/7

8/18/2014

Rightlink Printable License

Are you the author of this Elsevier article?	No
Will you be translating?	No
Title of your thesis/dissertation	"Surfactant assisted dispersion of single walled carbon nanotubes in polyvinylpyrrolidone solutions"
Expected completion date	Aug 2014
Estimated size (number of pages)	105
Elsevier VAT number	GB 494 6272 12
Permissions price	0.00 USD
VAT/Local Sales Tax	0.00 USD / 0.00 GBP
Total	0.00 USD
Terms and Conditions	

INTRODUCTION

1. The publisher for this copyrighted material is Elsevier. By clicking "accept" in connection with completing this licensing transaction, you agree that the following terms and conditions apply to this transaction (along with the Billing and Payment terms and conditions established by Copyright Clearance Center, Inc. ("CCC"), at the time that you opened your Rightslink account and that are available at any time at <http://myaccount.copyright.com>).

GENERAL TERMS

- Elsevier hereby grants you permission to reproduce the aforementioned material subject to the terms and conditions indicated.
- Acknowledgement:** If any part of the material to be used (for example, figures) has appeared in our publication with credit or acknowledgement to another source, permission must also be sought from that source. If such permission is not obtained then that material may not be included in your publication/copies. Suitable acknowledgement to the source must be made, either as a footnote or in a reference list at the end of your publication, as follows:

"Reprinted from Publication title, Vol /edition number, Author(s), Title of article / title of chapter, Pages No., Copyright (Year), with permission from Elsevier [OR APPLICABLE SOCIETY COPYRIGHT OWNER]." Also Lancet special credit - "Reprinted from The Lancet, Vol number, Author(s), Title of article, Pages No., Copyright (Year), with permission from Elsevier."
- Reproduction of this material is confined to the purpose and/or media for which permission is hereby given.
- Altering/Modifying Material:** Not Permitted. However figures and illustrations may be altered/adapted minimally to serve your work. Any other abbreviations, additions, deletions and/or any other alterations shall be made only with prior written authorization of Elsevier Ltd. (Please contact Elsevier at permissions@elsevier.com)
- If the permission fee for the requested use of our material is waived in this instance, please be

<https://www.copyright.com/CustomerAdminPLF.jsp?ref=a900303-8523-4b1b-baed-d7e2d47ba3a>

2/7

advised that your future requests for Elsevier materials may attract a fee.

7. **Reservation of Rights:** Publisher reserves all rights not specifically granted in the combination of (i) the license details provided by you and accepted in the course of this licensing transaction, (ii) these terms and conditions and (iii) CCC's Billing and Payment terms and conditions.

8. **License Contingent Upon Payment:** While you may exercise the rights licensed immediately upon issuance of the license at the end of the licensing process for the transaction, provided that you have disclosed complete and accurate details of your proposed use, no license is finally effective unless and until full payment is received from you (either by publisher or by CCC) as provided in CCC's Billing and Payment terms and conditions. If full payment is not received on a timely basis, then any license preliminarily granted shall be deemed automatically revoked and shall be void as if never granted. Further, in the event that you breach any of these terms and conditions or any of CCC's Billing and Payment terms and conditions, the license is automatically revoked and shall be void as if never granted. Use of materials as described in a revoked license, as well as any use of the materials beyond the scope of an unrevoked license, may constitute copyright infringement and publisher reserves the right to take any and all action to protect its copyright in the materials.

9. **Warranties:** Publisher makes no representations or warranties with respect to the licensed material.

10. **Indemnity:** You hereby indemnify and agree to hold harmless publisher and CCC, and their respective officers, directors, employees and agents, from and against any and all claims arising out of your use of the licensed material other than as specifically authorized pursuant to this license.

11. **No Transfer of License:** This license is personal to you and may not be sublicensed, assigned, or transferred by you to any other person without publisher's written permission.

12. **No Amendment Except in Writing:** This license may not be amended except in a writing signed by both parties (or, in the case of publisher, by CCC on publisher's behalf).

13. **Objection to Contrary Terms:** Publisher hereby objects to any terms contained in any purchase order, acknowledgment, check endorsement or other writing prepared by you, which terms are inconsistent with these terms and conditions or CCC's Billing and Payment terms and conditions. These terms and conditions, together with CCC's Billing and Payment terms and conditions (which are incorporated herein), comprise the entire agreement between you and publisher (and CCC) concerning this licensing transaction. In the event of any conflict between your obligations established by these terms and conditions and those established by CCC's Billing and Payment terms and conditions, these terms and conditions shall control.

14. **Revocation:** Elsevier or Copyright Clearance Center may deny the permissions described in this License at their sole discretion, for any reason or no reason, with a full refund payable to you. Notice of such denial will be made using the contact information provided by you. Failure to receive such notice will not alter or invalidate the denial. In no event will Elsevier or Copyright Clearance Center be responsible or liable for any costs, expenses or damage incurred by you as a result of a denial of your permission request, other than a refund of the amount(s) paid by you to Elsevier and/or Copyright Clearance Center for denied permissions.

LIMITED LICENSE

The following terms and conditions apply only to specific license types:

15. **Translation:** This permission is granted for non-exclusive world **English** rights only unless your license was granted for translation rights. If you licensed translation rights you may only translate this content into the languages you requested. A professional translator must perform all translations and reproduce the content word for word preserving the integrity of the article. If this license is to re-use 1 or 2 figures then permission is granted for non-exclusive world rights in all languages.

16. **Posting licensed content on any Website:** The following terms and conditions apply as follows: Licensing material from an Elsevier journal: All content posted to the web site must maintain the copyright information line on the bottom of each image; A hyper-text must be included to the Homepage of the journal from which you are licensing at <http://www.sciencedirect.com/science/journal/xxxxx> or the Elsevier homepage for books at <http://www.elsevier.com>; Central Storage: This license does not include permission for a scanned version of the material to be stored in a central repository such as that provided by Heron/XanEdu

Licensing material from an Elsevier book: A hyper-text link must be included to the Elsevier homepage at <http://www.elsevier.com>. All content posted to the web site must maintain the copyright information line on the bottom of each image.

Posting licensed content on Electronic reserve: In addition to the above the following clauses are applicable: The web site must be password-protected and made available only to bona fide students registered on a relevant course. This permission is granted for 1 year only. You may obtain a new license for future website posting.

For journal authors: the following clauses are applicable in addition to the above: Permission granted is limited to the author accepted manuscript version* of your paper.

***Accepted Author Manuscript (AAM) Definition:** An accepted author manuscript (AAM) is the author's version of the manuscript of an article that has been accepted for publication and which may include any author-incorporated changes suggested through the processes of submission processing, peer review, and editor-author communications. AAMs do not include other publisher value-added contributions such as copy-editing, formatting, technical enhancements and (if relevant) pagination.

You are not allowed to download and post the published journal article (whether PDF or HTML, proof or final version), nor may you scan the printed edition to create an electronic version. A hyper-text must be included to the Homepage of the journal from which you are licensing at <http://www.sciencedirect.com/science/journal/xxxxx>. As part of our normal production process, you will receive an e-mail notice when your article appears on Elsevier's online service ScienceDirect (www.sciencedirect.com). That e-mail will include the article's Digital Object Identifier (DOI). This number provides the electronic link to the published article and should be included in the posting of your personal version. We ask that you wait until you receive this e-mail and have the DOI to do any posting.

Posting to a repository: Authors may post their AAM immediately to their employer's institutional repository for internal use only and may make their manuscript publicly available after the journal-specific embargo period has ended.

Please also refer to [Elsevier's Article Posting Policy](#) for further information.

18. **For book authors** the following clauses are applicable in addition to the above: Authors are permitted to place a brief summary of their work online only. You are not allowed to download and post the published electronic version of your chapter, nor may you scan the printed edition to create an electronic version. **Posting to a repository:** Authors are permitted to post a summary of their chapter only in their institution's repository.

20. **Thesis/Dissertation:** If your license is for use in a thesis/dissertation your thesis may be submitted to your institution in either print or electronic form. Should your thesis be published commercially, please reapply for permission. These requirements include permission for the Library and Archives of Canada to supply single copies, on demand, of the complete thesis and include permission for UMI to supply single copies, on demand, of the complete thesis. Should your thesis be published commercially, please reapply for permission.

Elsevier Open Access Terms and Conditions

Elsevier publishes Open Access articles in both its Open Access journals and via its Open Access articles option in subscription journals.

Authors publishing in an Open Access journal or who choose to make their article Open Access in an Elsevier subscription journal select one of the following Creative Commons user licenses, which define how a reader may reuse their work: Creative Commons Attribution License (CC BY), Creative Commons Attribution – Non Commercial - ShareAlike (CC BYNC SA) and Creative Commons Attribution – Non Commercial – No Derivatives (CC BYNC ND)

Terms & Conditions applicable to all Elsevier Open Access articles:

Any reuse of the article must not represent the author as endorsing the adaptation of the article nor should the article be modified in such a way as to damage the author's honour or reputation.

The author(s) must be appropriately credited.

If any part of the material to be used (for example, figures) has appeared in our publication with credit or acknowledgement to another source it is the responsibility of the user to ensure their reuse complies with the terms and conditions determined by the rights holder.

Additional Terms & Conditions applicable to each Creative Commons user license:

CC BY: You may distribute and copy the article, create extracts, abstracts, and other revised versions, adaptations or derivative works of or from an article (such as a translation), to include in a collective work (such as an anthology), to text or data mine the article, including for commercial

purposes without permission from Elsevier

CC BYNC SA: For non-commercial purposes you may distribute and copy the article, create extracts, abstracts and other revised versions, adaptations or derivative works of or from an article (such as a translation), to include in a collective work (such as an anthology), to text and data mine the article and license new adaptations or creations under identical terms without permission from Elsevier

CC BYNC ND: For non-commercial purposes you may distribute and copy the article and include it in a collective work (such as an anthology), provided you do not alter or modify the article, without permission from Elsevier

Any commercial reuse of Open Access articles published with a CC BYNC SA or CC BYNC ND license requires permission from Elsevier and will be subject to a fee.

Commercial reuse includes:

- Promotional purposes (advertising or marketing)
- Commercial exploitation (e.g. a product for sale or loan)
- Systematic distribution (for a fee or free of charge)

Please refer to [Elsevier's Open Access Policy](#) for further information.

21. Other Conditions:

v1.6

You will be invoiced within 48 hours of this transaction date. You may pay your invoice by credit card upon receipt of the invoice for this transaction. Please follow instructions provided at that time.

To pay for this transaction now, please remit a copy of this document along with your payment. Payment should be in the form of a check or money order referencing your account number and this invoice number RLNKS01357601. Make payments to "COPY RIGHT CLEARANCE CENTER" and send to:

**Copyright Clearance Center
Dept 001
P.O. Box 843006
Boston, MA 02284-3006**

Please disregard electronic and mailed copies if you remit payment in advance. Questions? customerscare@copyright.com or +1-855-239-3415 (toll free in the US) or +1-978-646-2777.

Gratis licenses (referencing \$0 in the Total field) are free. Please retain this printable license for your reference. No payment is required.

8182014

Rightslink Printable License

**JOHN WILEY AND SONS LICENSE
TERMS AND CONDITIONS**

Aug 18, 2014

This is a License Agreement between Temison Yu ("You") and John Wiley and Sons ("John Wiley and Sons") provided by Copyright Clearance Center ("CCC"). The license consists of your order details, the terms and conditions provided by John Wiley and Sons, and the payment terms and conditions.

All payments must be made in full to CCC. For payment instructions, please see information listed at the bottom of this form.

License Number	3433980865046
License date	Jul 21, 2014
Licensed content publisher	John Wiley and Sons
Licensed content publication	Advanced Materials
Licensed content title	Evaporation-Induced Self-Assembly: Nanostructures Made Easy
Licensed copyright line	© 1999 WILEY-VCH Verlag GmbH, Weinheim, Fed. Rep. of Germany
Licensed content author	C. Jeffrey Brinker, Yunfeng Lu, Alan Sellinger, Hongyou Fan
Licensed content date	May 6, 1999
Start page	579
End page	585
Type of use	Dissertation/Thesis
Requestor type	University/Academic
Format	Electronic
Portion	Figure/table
Number of figures/tables	1
Original Wiley figure/table number(s)	Figure 1
Will you be translating?	No
Title of your thesis / dissertation	"Surfactant assisted dispersion of single walled carbon nanotubes in polyvinylpyrrolidone solutions"
Expected completion date	Aug 2014
Expected size (number of pages)	105
Total	0.00 USD
Terms and Conditions	

TERMS AND CONDITIONS

<https://wiley.com/CustomerAdmin/PLF.jsp?ref=for12075-8d-43ee-425e-180af9e68972>

1/7

8182014

Rightslink Printable License

This copyrighted material is owned by or exclusively licensed to John Wiley & Sons, Inc. or one of its group companies (each a "Wiley Company") or handled on behalf of a society with which a Wiley Company has exclusive publishing rights in relation to a particular work (collectively "WILEY"). By clicking  in connection with completing this licensing transaction, you agree that the following terms and conditions apply to this transaction (along with the billing and payment terms and conditions established by the Copyright Clearance Center Inc., ("CCC's Billing and Payment terms and conditions"), at the time that you opened your Rightslink account (these are available at any time at <http://waccount.copyright.com>).

Terms and Conditions

- The materials you have requested permission to reproduce or reuse (the "Wiley Materials") are protected by copyright.
- You are hereby granted a personal, non-exclusive, non-sub licensable (on a stand-alone basis), non-transferable, worldwide, limited license to reproduce the Wiley Materials for the purpose specified in the licensing process. This license is for a one-time use only and limited to any maximum distribution number specified in the license. The first instance of republication or reuse granted by this license must be completed within two years of the date of the grant of this license (although copies prepared before the end date may be distributed thereafter). The Wiley Materials shall not be used in any other manner or for any other purpose, beyond what is granted in the license. Permission is granted subject to an appropriate acknowledgement given to the author, title of the material/book/journal and the publisher. You shall also duplicate the copyright notice that appears in the Wiley publication in your use of the Wiley Material. Permission is also granted on the understanding that nowhere in the text is a previously published source acknowledged for all or part of this Wiley Material. Any third party content is expressly excluded from this permission.
- With respect to the Wiley Materials, all rights are reserved. Except as expressly granted by the terms of the license, no part of the Wiley Materials may be copied, modified, adapted (except for minor reformatting required by the new Publication), translated, reproduced, transferred or distributed, in any form or by any means, and no derivative works may be made based on the Wiley Materials without the prior permission of the respective copyright owner. You may not alter, remove or suppress in any manner any copyright, trademark or other notices displayed by the Wiley Materials. You may not license, rent, sell, loan, lease, pledge, offer as security, transfer or assign the Wiley Materials on a stand-alone basis, or any of the rights granted to you hereunder to any other person.
- The Wiley Materials and all of the intellectual property rights therein shall at all times remain the exclusive property of John Wiley & Sons Inc, the Wiley Companies, or their respective licensors, and your interest therein is only that of having possession of and the right to reproduce the Wiley Materials pursuant to Section 2 herein during the continuance of this Agreement. You agree that you own no right, title or interest in or to the Wiley Materials or any of the intellectual property rights therein. You shall have no rights hereunder other than the license as provided for above in Section 2. No right, license or interest to any trademark,

<https://wiley.com/CustomerAdmin/PLF.jsp?ref=for12075-8d-43ee-425e-180af9e68972>

2/7

8182014

Rightlink Printable License

trade name, service mark or other branding ("Marks") of WILEY or its licensors is granted hereunder, and you agree that you shall not assert any such right, license or interest with respect thereto.

- NEITHER WILEY NOR ITS LICENSORS MAKES ANY WARRANTY OR REPRESENTATION OF ANY KIND TO YOU OR ANY THIRD PARTY, EXPRESS, IMPLIED OR STATUTORY, WITH RESPECT TO THE MATERIALS OR THE ACCURACY OF ANY INFORMATION CONTAINED IN THE MATERIALS, INCLUDING, WITHOUT LIMITATION, ANY IMPLIED WARRANTY OF MERCHANTABILITY, ACCURACY, SATISFACTORY QUALITY, FITNESS FOR A PARTICULAR PURPOSE, USABILITY, INTEGRATION OR NON-INFRINGEMENT AND ALL SUCH WARRANTIES ARE HEREBY EXCLUDED BY WILEY AND ITS LICENSORS AND WAIVED BY YOU
- WILEY shall have the right to terminate this Agreement immediately upon breach of this Agreement by you.
- You shall indemnify, defend and hold harmless WILEY, its Licensors and their respective directors, officers, agents and employees, from and against any actual or threatened claims, demands, causes of action or proceedings arising from any breach of this Agreement by you.
- IN NO EVENT SHALL WILEY OR ITS LICENSORS BE LIABLE TO YOU OR ANY OTHER PARTY OR ANY OTHER PERSON OR ENTITY FOR ANY SPECIAL, CONSEQUENTIAL, INCIDENTAL, INDIRECT, EXEMPLARY OR PUNITIVE DAMAGES, HOWEVER CAUSED, ARISING OUT OF OR IN CONNECTION WITH THE DOWNLOADING, PROVISIONING, VIEWING OR USE OF THE MATERIALS REGARDLESS OF THE FORM OF ACTION, WHETHER FOR BREACH OF CONTRACT, BREACH OF WARRANTY, TORT, NEGLIGENCE, INFRINGEMENT OR OTHERWISE (INCLUDING, WITHOUT LIMITATION, DAMAGES BASED ON LOSS OF PROFITS, DATA, FILES, USE, BUSINESS OPPORTUNITY OR CLAIMS OF THIRD PARTIES), AND WHETHER OR NOT THE PARTY HAS BEEN ADVISED OF THE POSSIBILITY OF SUCH DAMAGES. THIS LIMITATION SHALL APPLY NOTWITHSTANDING ANY FAILURE OF ESSENTIAL PURPOSE OF ANY LIMITED REMEDY PROVIDED HEREIN.
- Should any provision of this Agreement be held by a court of competent jurisdiction to be illegal, invalid, or unenforceable, that provision shall be deemed amended to achieve as nearly as possible the same economic effect as the original provision, and the legality, validity and enforceability of the remaining provisions of this Agreement shall not be affected or impaired thereby.
- The failure of either party to enforce any term or condition of this Agreement shall not constitute a waiver of either party's right to enforce each and every term and condition of this Agreement. No breach under this agreement shall be deemed waived or excused by either party unless such waiver or consent is in writing signed by the party granting such waiver or consent. The waiver by or consent of a party to a breach of any provision of this Agreement

<https://onlinelibrary.wiley.com/CustomerAdmin/PLF.jsp?ref=for12075-83d-43ee-425e-180af9b68072>

37

8182014

Rightlink Printable License

shall not operate or be construed as a waiver of or consent to any other or subsequent breach by such other party.

- This Agreement may not be assigned (including by operation of law or otherwise) by you without WILEY's prior written consent.
- Any fee required for this permission shall be non-refundable after thirty (30) days from receipt by the CCC.
- These terms and conditions together with CCC's Billing and Payment terms and conditions (which are incorporated herein) form the entire agreement between you and WILEY concerning this licensing transaction and (in the absence of fraud) supersedes all prior agreements and representations of the parties, oral or written. This Agreement may not be amended except in writing signed by both parties. This Agreement shall be binding upon and inure to the benefit of the parties' successors, legal representatives, and authorized assigns.
- In the event of any conflict between your obligations established by these terms and conditions and those established by CCC's Billing and Payment terms and conditions, these terms and conditions shall prevail.
- WILEY expressly reserves all rights not specifically granted in the combination of (i) the license details provided by you and accepted in the course of this licensing transaction, (ii) these terms and conditions and (iii) CCC's Billing and Payment terms and conditions.
- This Agreement will be void if the Type of Use, Format, Circulation, or Requestor Type was misrepresented during the licensing process.
- This Agreement shall be governed by and construed in accordance with the laws of the State of New York, USA, without regards to such state's conflict of law rules. Any legal action, suit or proceeding arising out of or relating to these Terms and Conditions or the breach thereof shall be instituted in a court of competent jurisdiction in New York County in the State of New York in the United States of America and each party hereby consents and submits to the personal jurisdiction of such court, waives any objection to venue in such court and consents to service of process by registered or certified mail, return receipt requested, at the last known address of such party.

WILEY OPEN ACCESS TERMS AND CONDITIONS

Wiley Publishes Open Access Articles in fully Open Access Journals and in Subscription journals offering Online Open. Although most of the fully Open Access journals publish open access articles under the terms of the Creative Commons Attribution (CC BY) License only, the subscription journals and a few of the Open Access Journals offer a choice of Creative Commons Licenses: Creative Commons Attribution (CC-BY) license [Creative Commons Attribution Non-Commercial \(CC-BY-NC\) license](#) and [Creative Commons Attribution Non-Commercial-NoDerivs \(CC-BY-NC-ND\) License](#). The license type is clearly identified on the article.

<https://onlinelibrary.wiley.com/CustomerAdmin/PLF.jsp?ref=for12075-83d-43ee-425e-180af9b68072>

47

Copyright in any research article in a journal published as Open Access under a Creative Commons License is retained by the author(s). Authors grant Wiley a license to publish the article and identify itself as the original publisher. Authors also grant any third party the right to use the article freely as long as its integrity is maintained and its original authors, citation details and publisher are identified as follows: [Title of Article/Author/Journal Title and Volume/Issue]. Copyright (c) [year] [copyright owner as specified in the Journal]. Links to the final article on Wiley's website are encouraged where applicable.

The Creative Commons Attribution License

The [Creative Commons Attribution License \(CC-BY\)](#) allows users to copy, distribute and transmit an article, adapt the article and make commercial use of the article. The CC-BY license permits commercial and non-commercial re-use of an open access article, as long as the author is properly attributed.

The Creative Commons Attribution License does not affect the moral rights of authors, including without limitation the right not to have their work subjected to derogatory treatment. It also does not affect any other rights held by authors or third parties in the article, including without limitation the rights of privacy and publicity. Use of the article must not assert or imply, whether implicitly or explicitly, any connection with, endorsement or sponsorship of such use by the author, publisher or any other party associated with the article.

For any reuse or distribution, users must include the copyright notice and make clear to others that the article is made available under a Creative Commons Attribution license, linking to the relevant Creative Commons web page.

To the fullest extent permitted by applicable law, the article is made available as is and without representation or warranties of any kind whether express, implied, statutory or otherwise and including, without limitation, warranties of title, merchantability, fitness for a particular purpose, non-infringement, absence of defects, accuracy, or the presence or absence of errors.

Creative Commons Attribution Non-Commercial License

The [Creative Commons Attribution Non-Commercial \(CC-BY-NC\) License](#) permits use, distribution and reproduction in any medium, provided the original work is properly cited and is not used for commercial purposes.(see below)

Creative Commons Attribution-Non-Commercial-NoDerivs License

The [Creative Commons Attribution Non-Commercial-NoDerivs License \(CC-BY-NC-ND\)](#) permits use, distribution and reproduction in any medium, provided the original work is properly cited, is not used for commercial purposes and no modifications or adaptations are made. (see below)

Use by non-commercial users

For non-commercial and non-promotional purposes, individual users may access, download, copy, display and redistribute to colleagues Wiley Open Access articles, as well as adapt, translate, text-

and data-mine the content subject to the following conditions:

- The authors' moral rights are not compromised. These rights include the right of "paternity" (also known as "attribution" - the right for the author to be identified as such) and "integrity" (the right for the author not to have the work altered in such a way that the author's reputation or integrity may be impugned).
- Where content in the article is identified as belonging to a third party, it is the obligation of the user to ensure that any reuse complies with the copyright policies of the owner of that content.
- If article content is copied, downloaded or otherwise reused for non-commercial research and education purposes, a link to the appropriate bibliographic citation (authors, journal, article title, volume, issue, page numbers, DOI and the link to the definitive published version on [Wiley Online Library](#)) should be maintained. Copyright notices and disclaimers must not be deleted.
- Any translations, for which a prior translation agreement with Wiley has not been agreed, must prominently display the statement: "This is an unofficial translation of an article that appeared in a Wiley publication. The publisher has not endorsed this translation."

Use by commercial "for-profit" organisations

Use of Wiley Open Access articles for commercial, promotional, or marketing purposes requires further explicit permission from Wiley and will be subject to a fee. Commercial purposes include:

- Copying or downloading of articles, or linking to such articles for further redistribution, sale or licensing;
- Copying, downloading or posting by a site or service that incorporates advertising with such content;
- The inclusion or incorporation of article content in other works or services (other than normal quotations with an appropriate citation) that is then available for sale or licensing, for a fee (for example, a compilation produced for marketing purposes, inclusion in a sales pack)
- Use of article content (other than normal quotations with appropriate citation) by for-profit organisations for promotional purposes
- Linking to article content in e-mails redistributed for promotional, marketing or educational purposes;
- Use for the purposes of monetary reward by means of sale, resale, licence, loan, transfer or other form of commercial exploitation such as marketing products

8/18/2014

Rightlink Printable License

- Print reprints of Wiley Open Access articles can be purchased from corporatesales@wiley.com

Further details can be found on Wiley Online Library
<http://olabout.wiley.com/WileyCDA/Section/id-410895.html>

Other Terms and Conditions:

v1.9

You will be invoiced within 48 hours of this transaction date. You may pay your invoice by credit card upon receipt of the invoice for this transaction. Please follow instructions provided at that time.

To pay for this transaction now, please remit a copy of this document along with your payment. Payment should be in the form of a check or money order referencing your account number and this invoice number RLNK501357597. Make payments to "COPY RIGHT CLEARANCE CENTER" and send to:

Copyright Clearance Center
 Dept 001
 P.O. Box 843006
 Boston, MA 02284-3006

Please disregard electronic and mailed copies if you remit payment in advance. Questions? customer@copyright.com or +1-855-239-3415 (toll free in the US) or +1-978-646-2777.

Gratis licenses (referencing \$0 in the Total field) are free. Please retain this printable license for your reference. No payment is required.

<http://100.copyright.com/CustomerAdminPLF.jsp?ref=1ca12075-8d0-43ee-a05a-80a9e868072>

7/7

8/18/2014

Rightlink Printable License

SPRINGER LICENSE TERMS AND CONDITIONS

Aug 18, 2014

This is a License Agreement between Ternison Yu ("You") and Springer ("Springer") provided by Copyright Clearance Center ("CCC"). The license consists of your order details, the terms and conditions provided by Springer, and the payment terms and conditions.

All payments must be made in full to CCC. For payment instructions, please see information listed at the bottom of this form.

License Number	3433980593316
License date	Jul 21, 2014
Licensed content publisher	Springer
Licensed content publication	Russian Journal of Physical Chemistry
Licensed content title	Acid-base interactions and complex formation while recovering copper(II) ions from aqueous solutions using cellulose adsorbent in the presence of polyvinylpyrrolidone
Licensed content author	T. E. Nikiforova
Licensed content date	Jan 1, 2012
Volume number	86
Issue number	12
Type of Use	Thesis/Dissertation
Portion	Figures
Author of this Springer article	No
Country of republication	other
Order reference number	None
Original figure numbers	Molecular Structures on page 1838
Title of your thesis / dissertation	"Surfactant assisted dispersion of single walled carbon nanotubes in polyvinylpyrrolidone solutions"
Expected completion date	Aug 2014
Estimated size(pages)	105
Total	0.00 CAD

Terms and Conditions

Introduction

The publisher for this copyrighted material is Springer Science + Business Media. By clicking "accept" in connection with completing this licensing transaction, you agree that the following terms and conditions apply to this transaction (along with the Billing and Payment terms and conditions established by Copyright Clearance Center, Inc. ("CCC"), at the time that you opened your

<http://100.copyright.com/CustomerAdminPLF.jsp?ref=882603fb-42a8-4460-bf0c-ae0358eacc16>

14/4

Rightslink account and that are available at any time at lmsaaccount.copyright.com.

Limited License

With reference to your request to reprint in your thesis material on which Springer Science and Business Media control the copyright, permission is granted, free of charge, for the use indicated in your enquiry.

Licenses are for one-time use only with a maximum distribution equal to the number that you identified in the licensing process.

This License includes use in an electronic form, provided its password protected or on the university's intranet or repository, including UMI (according to the definition at the Sherpa website: <http://www.sherpa.ac.uk/romeo/>). For any other electronic use, please contact Springer at (permissions.dordrecht@springer.com or permissions.heidelberg@springer.com).

The material can only be used for the purpose of defending your thesis limited to university-use only. If the thesis is going to be published, permission needs to be re-obtained (selecting "book/textbook" as the type of use).

Although Springer holds copyright to the material and is entitled to negotiate on rights, this license is only valid, subject to a courtesy information to the author (address is given with the article/chapter) and provided it concerns original material which does not carry references to other sources (if material in question appears with credit to another source, authorization from that source is required as well).

Permission free of charge on this occasion does not prejudice any rights we might have to charge for reproduction of our copyrighted material in the future.

Altering/Modifying Material: Not Permitted

You may not alter or modify the material in any manner. Abbreviations, additions, deletions and/or any other alterations shall be made only with prior written authorization of the author(s) and/or Springer Science + Business Media. (Please contact Springer at (permissions.dordrecht@springer.com or permissions.heidelberg@springer.com))

Reservation of Rights

Springer Science + Business Media reserves all rights not specifically granted in the combination of (i) the license details provided by you and accepted in the course of this licensing transaction, (ii) these terms and conditions and (iii) CCC's Billing and Payment terms and conditions.

Copyright Notice Disclaimer

You must include the following copyright and permission notice in connection with any reproduction of the licensed material: "Springer and the original publisher /journal title, volume, year of publication, page, chapter/article title, name(s) of author(s), figure number(s), original copyright notice) is given to the publication in which the material was originally published, by adding, with kind permission from Springer Science and Business Media"

Warranties: None

Example 1: Springer Science + Business Media makes no representations or warranties with respect to the licensed material.

Example 2: Springer Science + Business Media makes no representations or warranties with respect to the licensed material and adopts on its own behalf the limitations and disclaimers established by CCC on its behalf in its Billing and Payment terms and conditions for this licensing transaction.

Indemnity

You hereby indemnify and agree to hold harmless Springer Science + Business Media and CCC, and their respective officers, directors, employees and agents, from and against any and all claims arising out of your use of the licensed material other than as specifically authorized pursuant to this license.

No Transfer of License

This license is personal to you and may not be sublicensed, assigned, or transferred by you to any other person without Springer Science + Business Media's written permission.

No Amendment Except in Writing

This license may not be amended except in a writing signed by both parties (or, in the case of Springer Science + Business Media, by CCC on Springer Science + Business Media's behalf).

Objection to Contrary Terms

Springer Science + Business Media hereby objects to any terms contained in any purchase order, acknowledgment, check endorsement or other writing prepared by you, which terms are inconsistent with these terms and conditions or CCC's Billing and Payment terms and conditions. These terms and conditions, together with CCC's Billing and Payment terms and conditions (which are incorporated herein), comprise the entire agreement between you and Springer Science + Business Media (and CCC) concerning this licensing transaction. In the event of any conflict between your obligations established by these terms and conditions and those established by CCC's Billing and Payment terms and conditions, these terms and conditions shall control.

Jurisdiction

All disputes that may arise in connection with this present License, or the breach thereof, shall be settled exclusively by arbitration, to be held in The Netherlands, in accordance with Dutch law, and to be conducted under the Rules of the 'Netherlands Arbitrage Instituut' (Netherlands Institute of Arbitration). OR:

All disputes that may arise in connection with this present License, or the breach thereof, shall be settled exclusively by arbitration, to be held in the Federal Republic of Germany, in accordance with German law.

Other terms and conditions:

v1.3

You will be invoiced within 48 hours of this transaction date. You may pay your invoice by credit card upon receipt of the invoice for this transaction. Please follow instructions

8/15/2014

RightsLink Printable License

provided at that time.

To pay for this transaction now, please remit a copy of this document along with your payment. Payment should be in the form of a check or money order referencing your account number and this invoice number RLNK501357593.

Make payments to "COPYRIGHT CLEARANCE CENTER" and send to:

Copyright Clearance Center
Dept 001
P.O. Box 843006

Boston, MA 02284-3006

Please disregard electronic and mailed copies if you remit payment in advance.

Questions? customercare@copyright.com or +1-855-239-3415 (toll free in the US) or +1-978-646-2777.

Gratis licenses (referencing \$0 in the Total field) are free. Please retain this printable license for your reference. No payment is required.



ACS Publications
MOST TRUSTED. MOST CITED. MOST READ.

RightsLink®

[Home](#)
[Account Info](#)
[Help](#)

Logged in as:
Tennison Yu

[LOGOUT](#)

Title: Dynamic Light Scattering and Optical Absorption in Biological Nanofluids of Gold Nanoparticles in Poly(vinyl pyrrolidone) Molecules

Author: A. Mishra, S. Ram, and G. Ghosh

Publication: The Journal of Physical Chemistry C

Publisher: American Chemical Society

Date: Apr 1, 2009

Copyright © 2009, American Chemical Society

PERMISSION/LICENSE IS GRANTED FOR YOUR ORDER AT NO CHARGE

This type of permission/license, instead of the standard Terms & Conditions, is sent to you because no fee is being charged for your order. Please note the following:

- Permission is granted for your request in both print and electronic formats, and translations.
- If figures and/or tables were requested, they may be adapted or used in part.
- Please print this page for your records and send a copy of it to your publisher/graduate school.
- Appropriate credit for the requested material should be given as follows: "Reprinted (adapted) with permission from (COMPLETE REFERENCE CITATION). Copyright (YEAR) American Chemical Society." Insert appropriate information in place of the capitalized words.
- One-time permission is granted only for the use specified in your request. No additional uses are granted (such as derivative works or other editions). For any other uses, please submit a new request.

If credit is given to another source for the material you requested, permission must be obtained from that source.

[BACK](#)
[CLOSE WINDOW](#)

Copyright © 2014 [Copyright Clearance Center, Inc.](#) All Rights Reserved. [Privacy statement.](#) Comments? We would like to hear from you. E-mail us at customercare@copyright.com



RightsLink®

Home Account Info Help



ACS Publications
Most Trusted. Most Cited. Most Read.

Title: Dependence of Optical Transition Energies on Structure for Single-Walled Carbon Nanotubes in Aqueous Suspension: An Empirical Kataura Plot
Author: R. Bruce Weisman* and and Sergei M. Bachilo
Publication: Nano Letters
Publisher: American Chemical Society
Date: Sep 1, 2003
Copyright © 2003, American Chemical Society

Logged in as:
Tennison Yu

LOGOUT

PERMISSION/LICENSE IS GRANTED FOR YOUR ORDER AT NO CHARGE

This type of permission/license, instead of the standard Terms & Conditions, is sent to you because no fee is being charged for your order. Please note the following:

- Permission is granted for your request in both print and electronic formats, and translations.
- If figures and/or tables were requested, they may be adapted or used in part.
- Please print this page for your records and send a copy of it to your publisher/graduate school.
- Appropriate credit for the requested material should be given as follows: "Reprinted (adapted) with permission from (COMPLETE REFERENCE CITATION). Copyright (YEAR) American Chemical Society." Insert appropriate information in place of the capitalized words.
- One-time permission is granted only for the use specified in your request. No additional uses are granted (such as derivative works or other editions). For any other uses, please submit a new request.

If credit is given to another source for the material you requested, permission must be obtained from that source.

BACK

CLOSE WINDOW



RightsLink®

Home Account Info Help



ACS Publications
Most Trusted. Most Cited. Most Read.

Title: Dispersion of Single-Walled Carbon Nanotubes of Narrow Diameter Distribution
Author: Yongqiang Tan and and Daniel E. Resasco*
Publication: The Journal of Physical Chemistry B
Publisher: American Chemical Society
Date: Aug 1, 2005
Copyright © 2005, American Chemical Society

Logged in as:
Tennison Yu

LOGOUT

PERMISSION/LICENSE IS GRANTED FOR YOUR ORDER AT NO CHARGE

This type of permission/license, instead of the standard Terms & Conditions, is sent to you because no fee is being charged for your order. Please note the following:

- Permission is granted for your request in both print and electronic formats, and translations.
- If figures and/or tables were requested, they may be adapted or used in part.
- Please print this page for your records and send a copy of it to your publisher/graduate school.
- Appropriate credit for the requested material should be given as follows: "Reprinted (adapted) with permission from (COMPLETE REFERENCE CITATION). Copyright (YEAR) American Chemical Society." Insert appropriate information in place of the capitalized words.
- One-time permission is granted only for the use specified in your request. No additional uses are granted (such as derivative works or other editions). For any other uses, please submit a new request.

If credit is given to another source for the material you requested, permission must be obtained from that source.

BACK

CLOSE WINDOW

Copyright © 2014 Copyright Clearance Center, Inc. All Rights Reserved. [Privacy statement](#). Comments? We would like to hear from you. E-mail us at customercare@copyright.com

Curriculum Vitae

Name: Tennison Yu

Post-secondary Education and Degrees: McMaster University
Hamilton, Ontario, Canada
2007-2012 B.Sc.

University of Western Ontario
London, Ontario, Canada
2012-2014, M.E.Sc

Honours and Awards: Western Graduate Research Award Fund
2012-2013

Seminar Presentation Award
2014

Dean's Honour List
McMaster University
2009, 2011

NSERC Industrial Undergraduate Student Research Award [URSA]
Amorfix Life Sciences Ltd.
2010

Related Work Experience Teaching Assistant
University of Western Ontario
2012-2014